Electrostatic Fuel Conditioning of Internal Combustion Engines

by

Phillip I. Gold

Department of Mechanical Engineering

California State University, Los Angeles

June 15, 1982

This research was conducted with the sponsorship of the National Aeronautics and Space Administration under Grant No. NAG 3-73.

Electrostatic Fuel Conditioning of Internal Combustion Engines

by

Phillip I. Gold

Department of Mechanical Engineering

California State University, Los Angeles

June 15, 1982

This research was conducted with
the sponsorship of the National
Aeronautics and Space Administration
under Grant No. NAG 3-73.

Abstract

Tests were conducted to determine if the performance of diesel engines could be influenced by the presence of electrostatic and magnetic fields. Field forces were applied in a variety of configurations including pretreatment of the fuel and air, however, no affect on engine performance was observed.

ACKNOWLEDGEMENTS

The author wishes to thank Mr. Albert J. Kovacs for his efforts in the behalf of this project.

TABLE OF CONTENTS

INTRODUCTION

The objective of this research was to investigate the influence of magnetic and electrostatic fields on the operation and performance of diesel engines. This concept derived from the work of Yukichi Asakawa at the High Voltage Laboratory of Nihon University, Tokyo. Over a period of many years, Asakawa published a series of papers (1-5)* describing his work on the affect of magnetic and electrostatic fields on combustion and vaporization rates of gaseous and liquid fuels.

Asakawa concluded that the presence of magnetic and electrostatic fields can have the effect of accelerating vaporization and combustion rates of liquid and gaseous fuels. This concept has met with success in industrial applications such as electrostatic precipitation in power generating stations, the printing industry and in electrostatic coating processes.

Equipment used in electrostatic spraying of organic coatings is capable of producing electrostatic charges up to 100 KV, resulting in an extremely fine dispersion of atomized liquid. The homogeneity of the dispersion is excellent due to like-charges on the liquid droplets which repel one another in the spray. The application of these fields requires only currents in the micro amp range resulting in very little power consumption.

It is clear that this effect has potentially attractive applications to internal combustion engines. Indeed, Asakawa (6) claimed to have achieved a substantial improvement in the performance of a small 2 cycle engine in an experiment which is discussed in some detail later.

TECHNICAL APPROACH AND RESULTS

The initial effort in this program was directed toward the installation and baselining of the two diesel engine/dynamometer combinations chosen for this project. These systems, which are described in detail in Appendix I, included an Onan, water-cooled marine-generator type engine and a Petter, air-cooled type AA1 engine. Both engines are single-cylinder, direct-injection types.

*Numbers in parenthesis refer to references at the end of this report. Several references not widely available in english translation are included in the appendix.

Since both engines were to be used in tests involving high-voltage electrostatic fields, care was taken to ensure that they were electrostatically isolated from ground. This problem proved to be substantially more difficult than anticipated, as exhaust systems and other necessary connections become insidiously effective electrical grounds.

After the engines were in place and tested, system operating manuals, test procedures, and data sheets were developed. These are described in Appendix II.

In order to evaluate the influence of electrostatic and magnetic fields on engine performance, a number of specific tests were devised. These tests were differentiated primarily by the manner in which the presence of charge or field was interjected into the experiment and are described below.

Test A Affect of electrostatic fields on diesel engine performance

Tests were conducted to verify Asakawa's claim, described above, of improved engine performance in the presence of an electrostatic field. Asakawa claimed to have observed a substantial increase in combustion efficiency in the presence of an electrostatic field. In his experiments, one terminal from the high-voltage side of a 200 W transformer was applied to the cylinder cover of an air-cooled, 90 cc, two-cycle engine which was electrically isolated from ground.

While the engine was running, output and engine rpm were observed with a fan brake dynamometer and an electric tachometer. Asakawa reported that beginning with the original 2300 rpm throttle setting, a 4 KV electric field charge was induced resulting in an increase of engine speed to 3200 rpm. Field charges up to 7.2 KV showed nearly identical results, while below 4 KV, only negligible changes in rpm were observed. Although not specifically stated by Asakawa, it is presumed that throttle settings and loads were held constant during the tests. Simultaneous measurements of fuel consumption revealed a spontaneous increase in the rate of fuel consumption when the field was applied. It was Asakawa's specific contention that the combustion process was enhanced by the presence of an electrostatic field, in this case within the cylinder of the engine, caused by electifying the engine block.

Test A was conducted in an effort to replicate Asakawa's experiments with one major change, that is, the use of a diesel rather than a spark ignition engine. One other modification was effected in the manner in which the electrostatic charge was applied. Indeed, according to Gauss' law, when a static electric charge is placed on a conductor, the excess charge is confined entirely to the surface of the conductor and the field within the conductor must be zero. Thus, in the experiment described by Asakawa, no electrostatic field could have existed within the combustion chamber to influence the combustion process!

TEST A1

This test was an attempt to replicate Asakawa's experiment using the Petter diesel. An adjustable voltage transformer was used in conjunction with a gaseous tube-type transformer to provide output voltages up to 15000 volts on the secondary of the gaseous tube transformer. This transformer produces 7500 volts between each secondary outlet and ground, or a total of 15000 volts across the secondary winding with a primary input of 115 volts. One side of the secondary was applied to the cylinder head of the engine, while the other side of the secondary was grounded. With the engine electrically isolated from ground, a maximum of 15000 volts could be produced between the engine and ground.

The engine was mounted on a 3/4 inch table which was electrically isolated from the steel support frame. The exhaust line was electrically isolated using mica board hangers. To provide complete electrical isolation, the hydraulic dynamometer/tachometer was disconnected from the engine. A stroboscope was used to measure engine rpm.

The engine was warmed-up for 25 minutes to obtain a steady-state oil temperature of 170 F. Fuel consumption readings were taken at 60 second intervals of steady-state operation. The test was repeated three times as follows: Fuel consumption was recorded with the electrostatic device off. Immediately thereafter, the electrostatic device was activated and the fuel consumption recorded once more. The dynamometer was disconnected to ensure electrical isolation. The results of this test are shown in Table 1.

Table 1

Engine Uncharged		Engine Charged	
Speed (RPM)	Fuel Consumption (cc/min)	Speed (RPM)	Fuel Consumption (cc/min)
2210	3.3	2200	3.2
2280	3.3	2280	3.2
2445	3.4	2450	3.4

Literally no change in fuel consumption was observed as a result of application of the electrostatic charge to the engine block.

Test A2

In this test, the fuel was subjected to a 15000 volt electrostatic field outside of the engine block near the fuel inlet. A simple parallel electrode device (see Figure 1) was placed near the fuel inlet where the fuel passing to the engine was subjected to the electrostatic field. No potential was placed on the engine which was isolated from ground. Both positive and negative leads of the transformer were connected to the device, and the full 15000 volts applied without current flow. Testing was started after the engine was warmed for 25 minutes to obtain an oil temperature of 170 F. The engine was partially loaded and fuel consumption recorded at 60 second intervals of steady-state operation. Readings with and without the electrostatic field in place were repeated four times. The results of this test are shown in Table 2.

Figure 1

Test Electrode

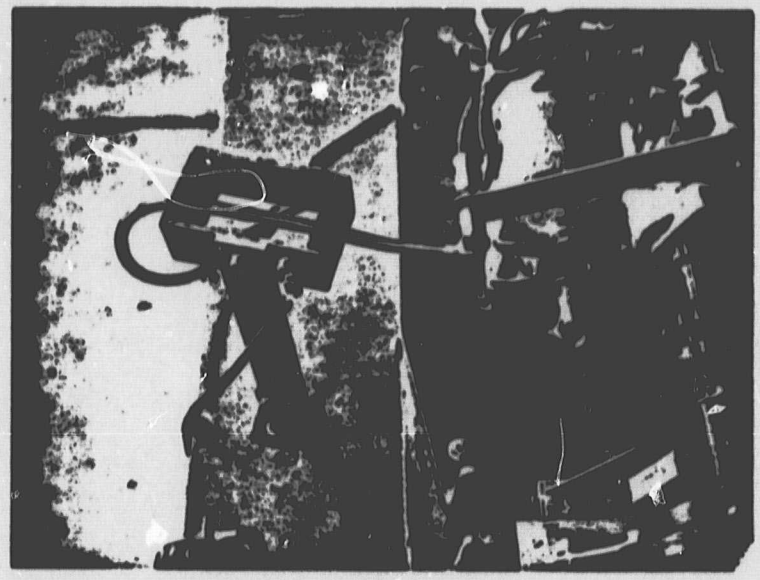

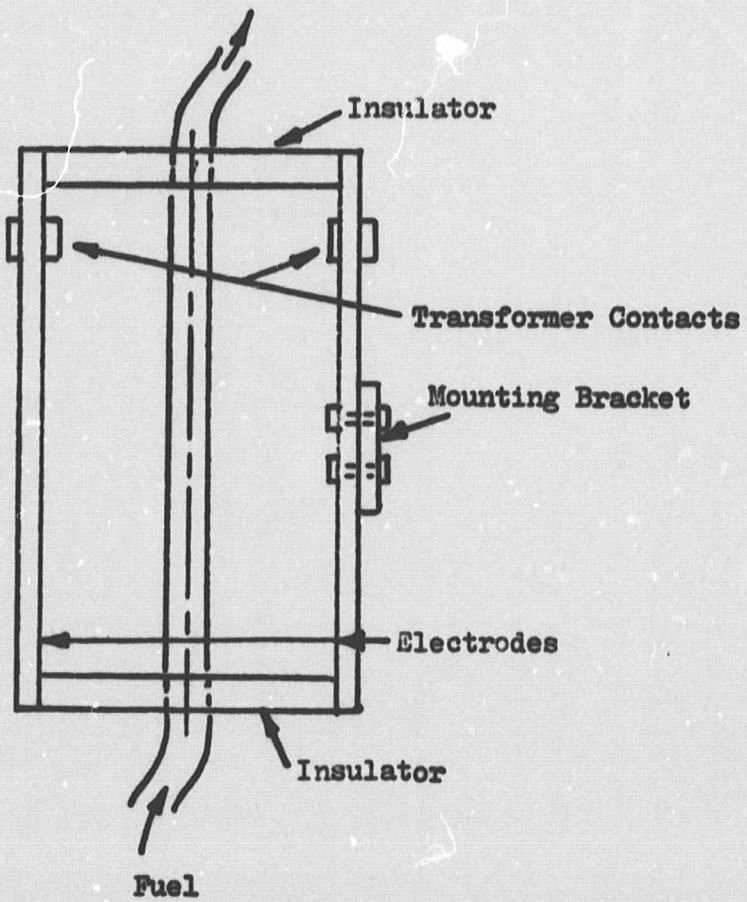

Table 2

Fuel Consumption (cc/min)

Speed (RPM)	Load (ft-lbf)	Charged	Uncharged
2300	1.4	6.7	6.6
2300	1.2	6.2	6.2
2300	1.2	6.2	6.2
2300	0.9	6.0	6.0

Once again, the electrostatic treatment produced no detectable effect.

Test A3

In the final test of this series, the fuel was again subjected to a 15000 volt field outside the engine block near the fuel inlet. A flat-plate electrode was placed near the fuel inlet (see Figure 2). The engine was electrically isolated from ground and connected to the negative side of the transformer. The flat-plate electrode was connected to the positive side of the transformer. 15000 volts was applied without current flow. Testing was started after the engine oil temperature reached 170 F. The engine was partially loaded, and fuel consumption was recorded at 60 second intervals of steady-state operation. Readings with and without the electrostatic field in place were repeated four times. The results of this test are shown in Table 3.

Table 3

Fuel Consumption (cc/min)

Speed (RPM)	Load (ft-lbf)	Charged	Uncharged
2300	2.2	7.6	7.6
2300	2.2	7.6	7.6
2300	2.2	7.6	7.6
2300	2.2	7.6	7.6

No detectable affect on engine performance was produced by the field.

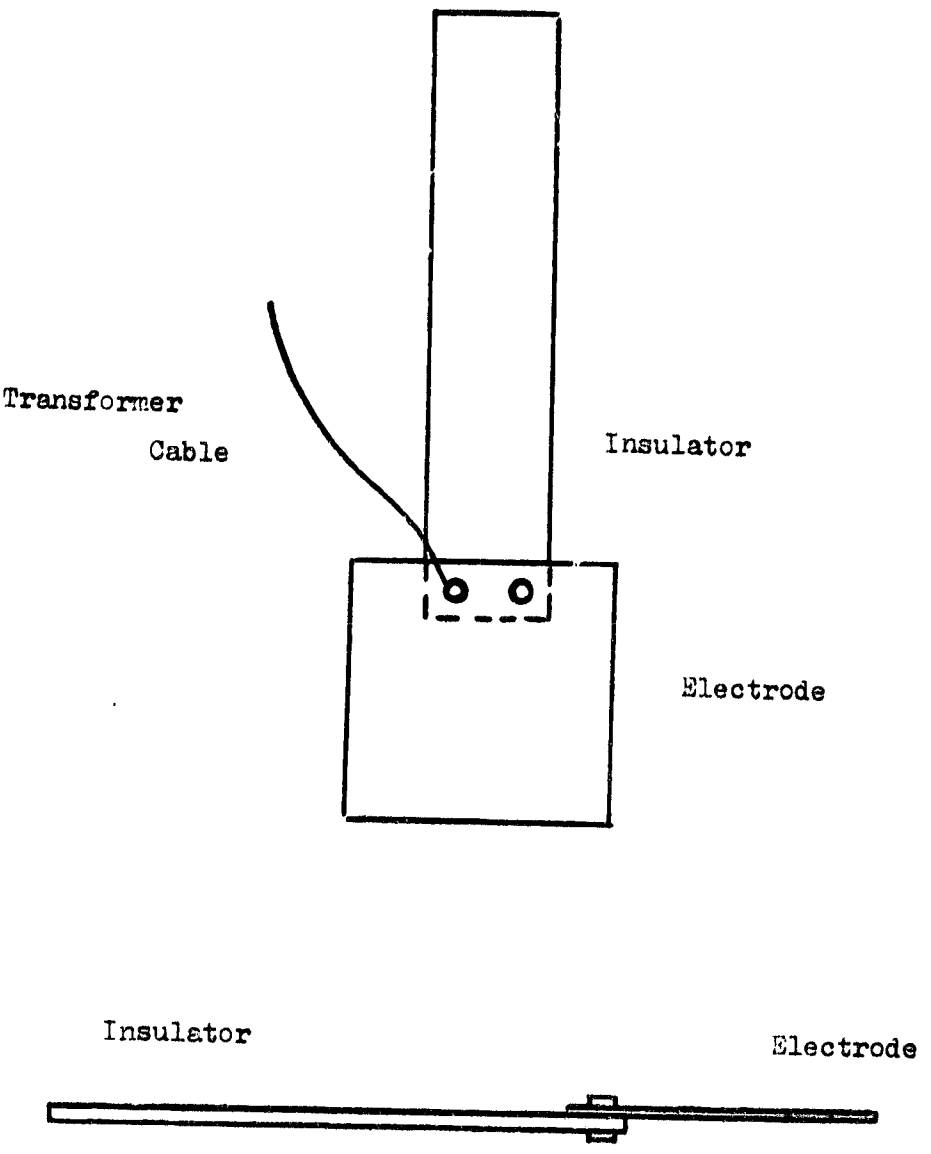

Figure 2

Test Electrode

Test B Affect of electrostatically charged combustion air on diesel engine performance

The principle of electrogasdynamics has been successfully applied to electrostatic coating processes. In an electrogasdynamic spray system, a minute quantity of conditioning fluid (such as isopropyl alcohol) is introduced into the stream of atomizing air going to the spray nozzle or injector. The air stream passes through an ionic discharge zone where it is saturated with negatively charged ions. The presence of the vaporized conditioning fluid in the air stream allows these ions to be swept forward with the air to the tip of the spray nozzle, building up to a high potential field. In spray operations, the charge is transmitted to the liquid to be sprayed through the metal tip of the nozzle which acts as a high voltage electrode. Voltages vary from 60 to over 100 KV D.C. (see Figure 3).

Figure 3 EGD High Voltage Generator

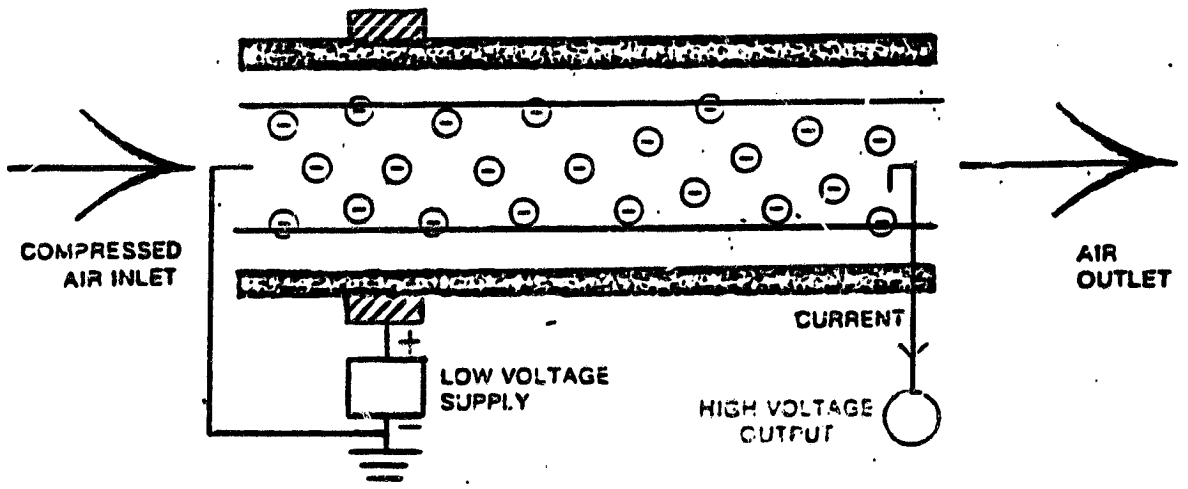

The objective of Test B was to determine the affect of introducing electrostatically charged air into the cylinder of the Onan diesel engine during the intake stroke of the cycle. An EGD SPEEFLO Electrostatic manual spray coating system was obtained for this test. The air intake manifold of the engine was modified so that the EGD injector unit could be attached directly to the engine and the charged air mixed with the naturally aspirated. (see Appendix I).

In this test, the engine was run alternatively, for 60 seconds with air injection only, with the atomized carrier fluid in air (but without electrostatic charging), and with the fully charged carrier fluid in air. This sequence was chosen to highlight any specific influence of the electrostatically charged particle as distinct from any supercharging effect of the relatively small quantity of air used, as well as the combustion of the minute quantities of isopropyl alcohol carrier fluid. The results of the test sequence are summarized in Table 4.

Table 4

EGD Test B

(Isopropyl alcohol carrier fluid)

Test No.	Engine Torque (ft/lbf)	RPM	Air	Carrier Fluid	Charge	Fuel Consumption (ml/min)
1	no load	1400	yes	yes	no	1.3
2	no load	1450	yes	no	no	1.25
3	no load	1450	yes	yes	yes	1.25
4	2.5	2350	yes	yes	no	8.2
5	2.5	2390	yes	no	no	7.4
6	2.4	2390	yes	yes	yes	7.6
7	2.4	2350	yes	no	no	7.4
8	2.4	2350	yes	yes	yes	7.4
9	3.6	2650	yes	no	no	10.3
10	3.4	2700	yes	no	no	9.2
11	3.4	2700	yes	yes	yes	9.2
12	3.4	2700	yes	no	no	9.2
13	3.5	2700	yes	yes	yes	7.8
14	3.5	2700	yes	no	no	8.2
15	3.5	2700	yes	yes	yes	9.0
16	3.5	2700	yes	no	no	7.4
17	3.5	2650	yes	yes	yes	9.0
18	2.75	2050	yes	yes	no	7.2
19	2.75	2050	yes	yes	no	7.2
20	2.75	2100	yes	no	no	6.8
21	2.75	2100	yes	no	no	6.8
22	2.7	2100	yes	no	no	6.6
23	2.75	2100	yes	yes	yes	6.8
24	2.75	2100	yes	yes	yes	6.8
25	2.75	2100	yes	no	no	6.8

Although some variations in fuel consumption rate were observed, they appeared to be random and could not be connected with the presence or absence of the charged carrier fluid in the injected air.

Test C Magnetic Fuel Treatment

Recent interest has developed in the use of so-called magnetic fuel treatment to improve the performance of internal combustion engines. Manufacturers claim increased fuel economy, improved overall performance and reduced emissions. Although the specific configuration varies from manufacturer to manufacturer, magnetic fuel treatment devices generally involve passing the fuel through an intense magnetic field before it is aspirated or injected into the engine. (see Figure 4, for example)

Figure 4

Azaka Co. Polarion-X
Magnetic Fuel Conditioning Device

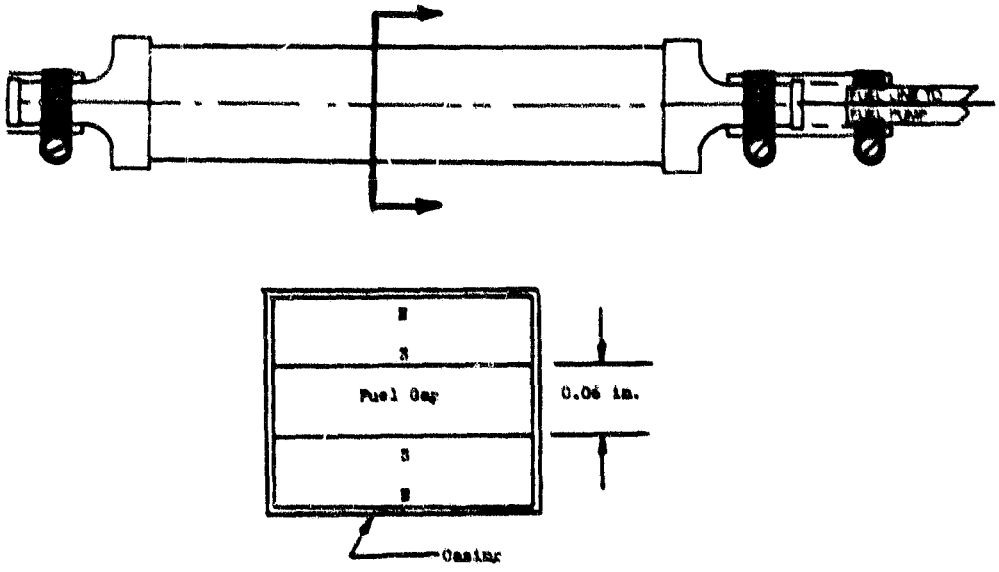

The use of electrostatic fields to affect injector spray patterns and drop size distributions is a well known phenomenon based on the essentially electrostatic nature of surface tension forces and their role in droplet formation. The influence of magnetic fields in this process is somewhat obscure in view of the essentially non-magnetic character of typical hydrocarbon fuels.

It might be argued that the transfer of fuel from refinery to the tank of an automobile introduces trace quantities of contaminants from handling, storage and pumping operations. Rust particles and magnetic microfines, as well as quantities of polar or ionic contaminants are usually found in fuel supplies.

The interaction of this melange of fuel and contaminants with the magnetic field as it passes through the fuel treatment device en route to the engine is unclear. Certainly any magnetic substance will interact with the magnetic field within the device, but having exited from the magnetic field, no residual magnetization would be expected to persist long enough for the fuel to be atomized in a carburator or injector.

It was the objective of this test to evaluate the effectiveness of the Azaka Co. Polarion - X magnetic fuel conditioning unit. The unit, shown in Figure 4, produces a 2500 (maximum) gauss field in a 0.6 in. gap through which the fuel flows. The poles of the permanent ceramic magnets are oriented so as to produce a continuous polarizing effect on the fuel which contacts only the magnetic south pole.

The test was conducted using the Onan engine. This engine, having been recently rebuilt was first thoroughly run-in. A base-line was then developed by operating the engine for eight hours over a period of several days. The engine was started and run at 1,000 rpm with no load for 10 minutes, then for 5 minutes at the test conditions (1,500 rpm at a load of 17 ft-lbf). At this point the run was commenced. Fuel consumption was observed while maintaining the engine operating speed and torque at nominal values.

This test was repeated using the Polarion - X unit placed in the fuel line after the fuel pump. This procedure was subjected to a blind control by which tests were performed with the device and with a unit which does not contain magnets, but which is in every other manner identical. Test personnel were not aware of the distinction between the units, but were simply instructed to test them in turn. The results of this test are shown in Table 5.

It is clear that no significant charge in fuel consumption rate resulted from the magnetic fuel treatment.

Table 5

Magnetic Fuel Treatment Test*

Test	Running Time (min)	Fuel Consumption (ml/min)	Mean Fuel Consumption (ml/min)
Baseline	80	16.0	
	120	15.9	16.1
	120	16.2	
	120	16.2	
Unit #1 (dummy)	100	15.8	
	120	15.7	15.8
	120	15.7	
	120	15.9	
Baseline	120	15.5	15.8
	120	16.0	
Unit #2 (Polarion-X)	120	15.9	
	120	15.7	15.8
	120	15.8	
	120	15.8	

*All tests were performed at 1500 rpm and 17 ft-lbf. Fuel consumption during each test period was steady and showed less fluctuation than the test-to-test variations.

CONCLUSIONS AND RECOMMENDATIONS

The tests conducted during the course of this project failed to detect any apparent relationship between the presence of electrostatic or magnetic fields and diesel engine performance. This complete lack of any positive response is strangely at odds with the very overt results claimed by Asakawa in a wide variety of applications. Some of these are described in english translations of several of Asakawa's papers included in Appendix III.

A definitive conclusion regarding the use of electrostatic or magnetic fields in internal combustion engine applications must include a plausible explanation of the interaction between the field and the combustion process.

In the case of magnetic fields, this appears to be totally lacking at present. Hydrocarbon fuels are almost devoid of magnetic materials-except for possible impurities. Furthermore, unless the fuel were to contain impurites whose magnetization persisted after leaving the influence of a magnetic field, no residual effect would be observed. Thus, a flow-through device, such as the Polarion-X would not be expected to produce any magnetization of the impurities in the fuel which could persist after the fuel left the device.

Any possible effect would require that the atomization and/or combustion processes themselves take place in the magnetic field. In this context, it seems more likely that the use of an electrostatic field is more likely to prove effective in affecting the combustion process. Spray formation, drop size distribution, and homogeneity are surface tension dependent. Surface tension is the macroscopic manifestation of essentially electrostatic forces and is strongly affected by external electrostatic fields. It seems likely, therefore, that electrostatic fields applied at the tip of a conventional type injector could be made to produce a more uniform spray drop size distribution leading, perhaps, to more complete combustion.

Another possible avenue of approach is to investigate the influence of electrostatic fields on the combustion process itself. Asakawa observed reaction rates in homogeneous gas phase combustion taking place within an electrostatic field and reported increased reaction rates. Although he did not accompany his observations with a theory to explain them, it seems reasonable that the combustion process, involving a variety of chain reactions and ionic free radicals, can be altered by the presence of an electrostatic field. It may be possible, therefore, to apply this concept to improving combustion efficiency.

REFERENCES

*1. Asakawa, Y., "Combustion Improvement of Internal Combustion Engines," JSME, 1st Symp. Engines, July, 1970.

2. _____, "Promotion and of Vaporization by Means of The Application of an Electric Field," JSME, Semi-Annual Symp., Sept., 1967.

3. _____, Promotion and Retardation of Heat Transfer by Electric Fields," Nature, 261, 220-221 (1976).

4. _____, "New Method for the Promotion of Vaporization, JSME, General Meeting No. 623, pp 137-155, 1965.

5. _____, and S. Tomita, "Improvement of Combustion in Internal Combustion Engines by Application of an Electrical Field," JSME Shimizu Meeting, No. 700-9, pp 25-32, 1977.

6. _____, "Physical Methods for Improving Combustion," 6th Combustion Symp., pp 923-929, Aug., 1956.

*References 1, 2, 4 and 5 are not generally available in the english translation and are, therefore, included in Appendix III for the interested reader. References 4 and 5 were made available by the Bendix Engineering Development Center.

Appendix I: Test Engines and Equipment

System 1 -	Engine:	Onan 4 cycle; vertical single cylinder (marine generator type); 3 1/2" bore; 3 1/2" stroke; 33.7 cubic inch displacement; 18.5 to 1 compression ratio; 5.5 hp at 1800 rpm.
	Dynamometer:	Westinghouse type SKH
System 2	Engine:	Petter type AA1 4 cycle; vertical single cylinder; 2 3/4" bore; 2 1/4" stroke; 13.4 cubic inch displacement; 17 to 1 compression ratio; 3.5 hp at 3600 rpm (1.8 hp at 1800 rpm).
	Dynamometer:	Go-Power type DY-7D

Figure 1

Petter Unit

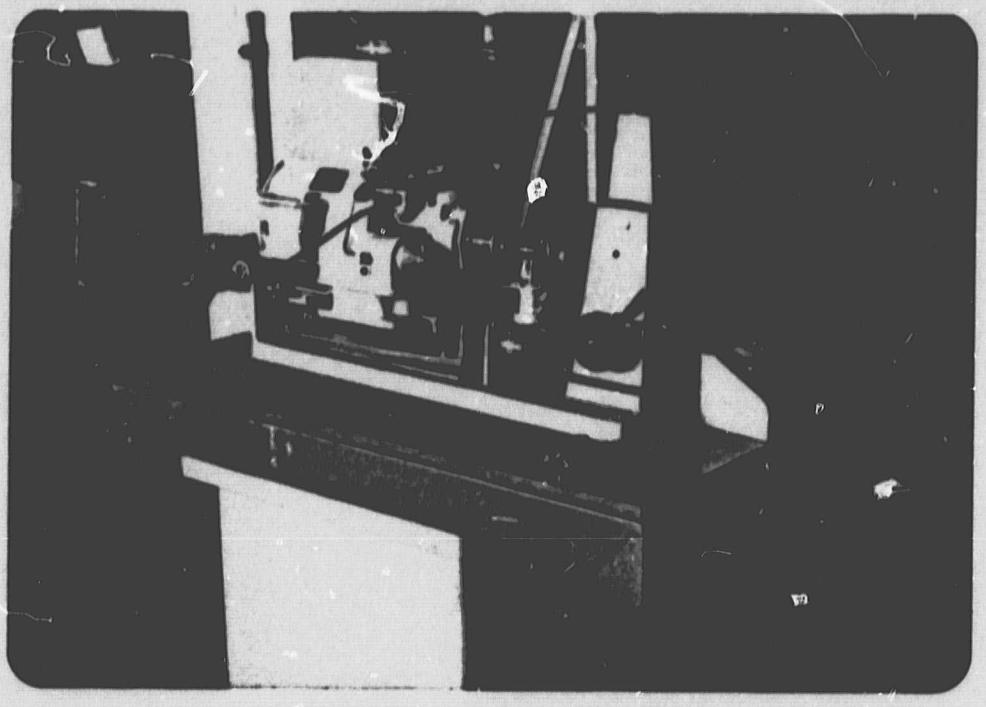

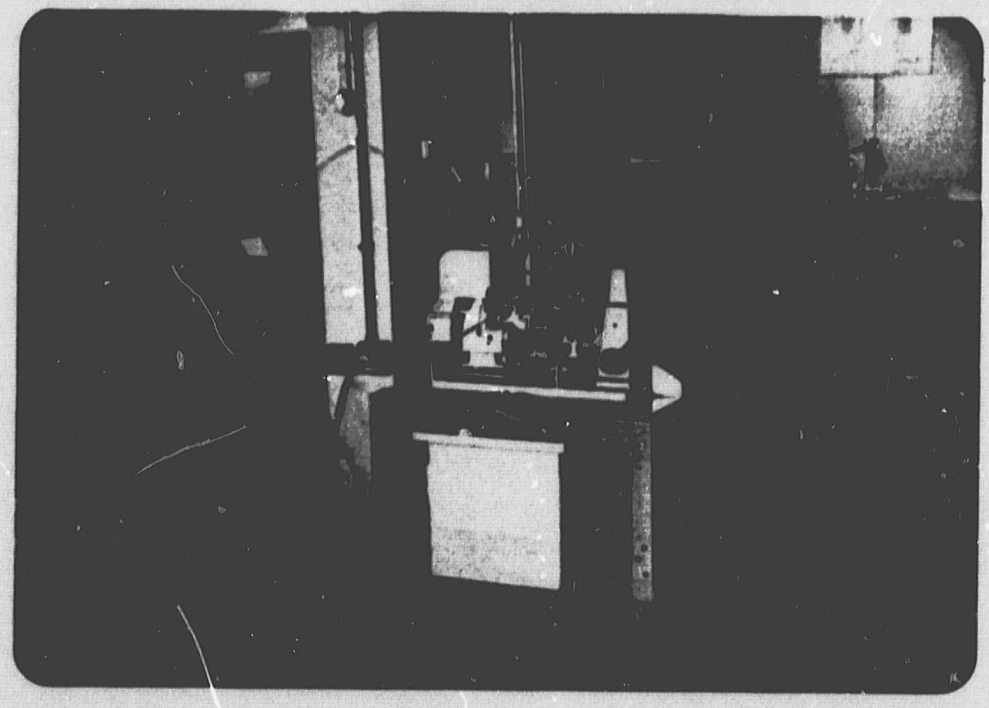

Figure 2

Onan Unit

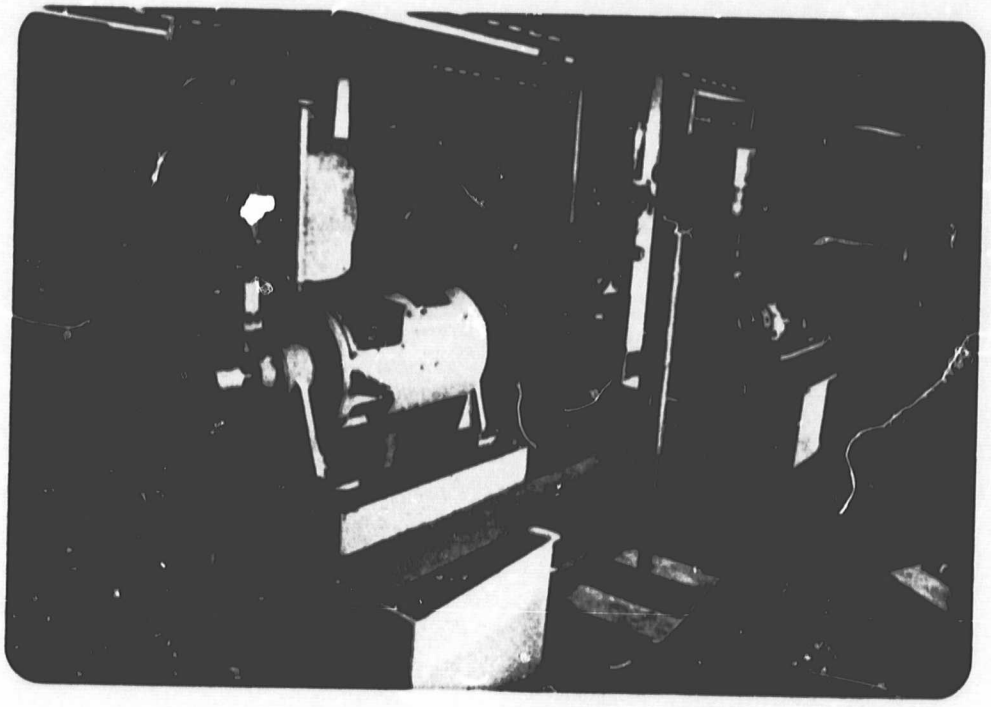

Note bracket for EGD unit injector gun below air cleaner.

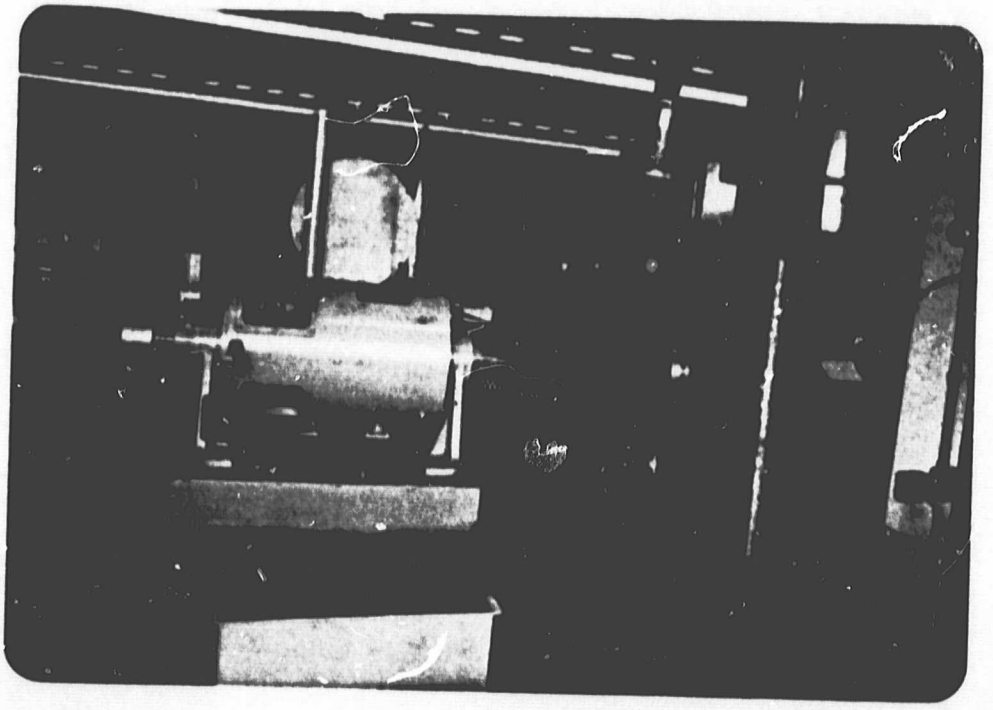

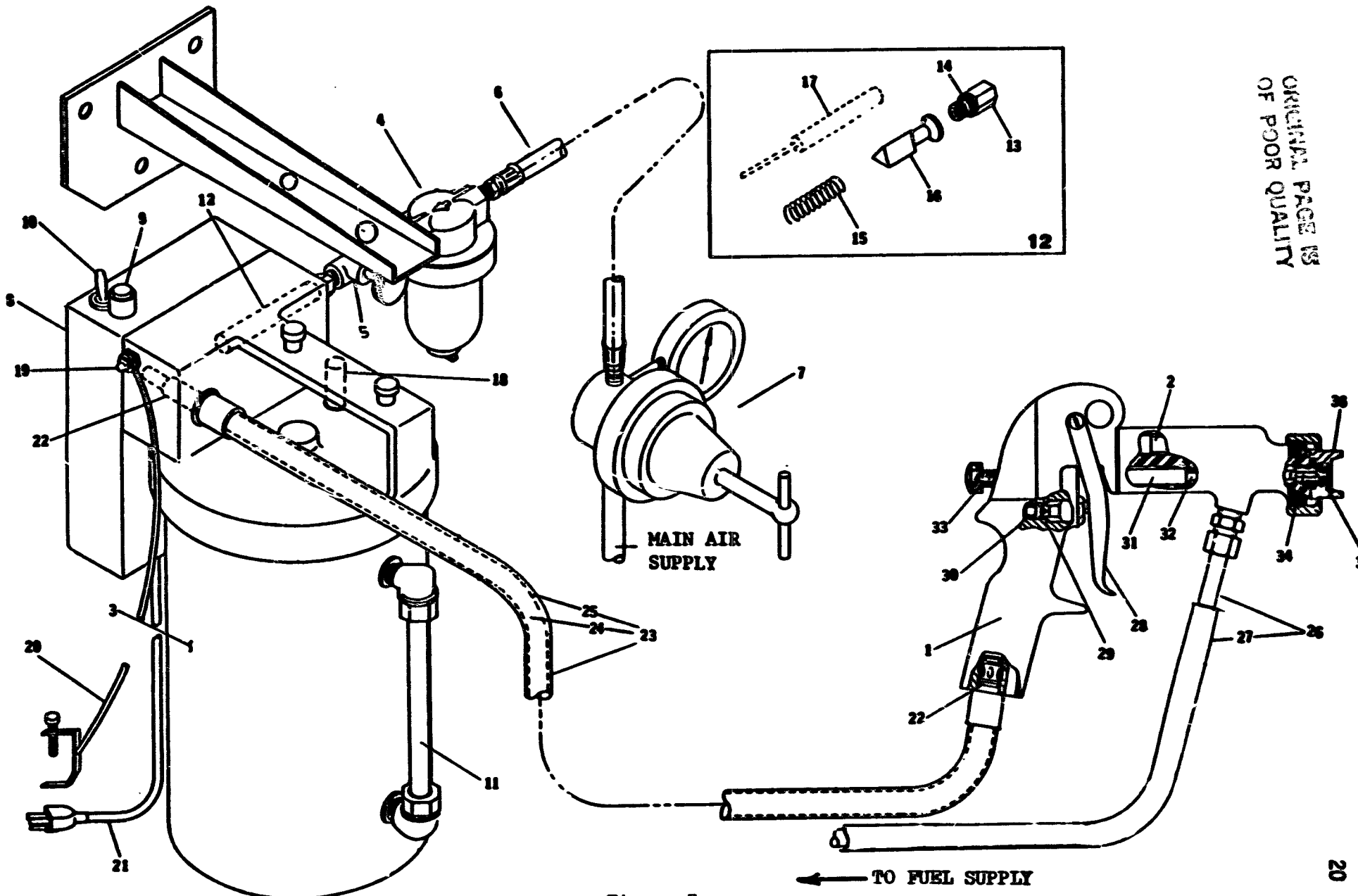

Figure 3

EGD Injector Gun and Conditioning Fluid Unit Hook-up

Figure 3 (Continued)

Parts Breakdown

Item No.	Description
1	Hand Gun Assembly
2	Generator Assembly
3	Conditioning Unit Assembly
4	Oil-Moisture Separator
5	Valve
6	Air Hook-up Hose
7	Regulator and Air Pressure Gauge
8	Power Supply - 110 V
9	Pilot Light
10	Toggle Switch
11	Sight Glass
12	Flow Switch Assembly
13	Retainer, Flow Switch
14	"O" Ring, Flow Switch
15	Spring, Flow Switch
16	Piston, Flow Switch
17	Magnetic Reed Switch
18	Fill Plug
19	Ground Post Assembly
20	Ground Wire Assembly
21	Line Cord
22	Connector Assembly,
23	Atomizing Air Hose
24	Exciter Wire
25	Ground Wire
26	Fluid Hose Assembly
27	Jacket, Fluid Hose, 24 Ft.
28	Trigger
29	Air Valve Assembly
30	Compression Spring, Air Valve
31	Front Fluid Shaft Insulator
32	Front Fluid Shaft
33	Compression Spring, Fluid Adjustment Screw
34	Fluid Needle
35	Fluid Tip
36	Air Cap

Figure 3 (Continued)

Explanation of Electrical and Air Hook-up

Clean dry atomizing air is provided to the Conditioning Unit Assembly (3) through the Air Hook-up Hose (6) and Oil-Moisture Separator (4). The air is regulated by the Regulator (7). The system pressure is set by adjusting the Regulator (7) and slowly opening Valve (5) to avoid air surges.

When the Trigger (28) is pulled back, the following occurs:

The Air Valve (29) in the gun handle is opened allowing the atomizing air to flow through the system. The atomizing air passes by the air-operated Flow Switch (12) in the conditioning unit and into the conditioning unit fluid container where it mixes with the conditioning fluid vapor. The treated atomizing air leaves the conditioning unit and is routed to the spray gun through the Atomizing Air Hose (23). The atomizing air enters the Hand Gun Assembly (1) through the handle where it is routed to the Generator (2) and through the air passages in the barrel of the gun to the Air Cap (36) where it is used to atomize the fuel supply. The fuel supply line will be plugged in the ionized air tests.

The atomizing air passing the Flow Switch Assembly (12) pushes the Flow Switch Piston (16) into a recess provided in the conditioning unit. The piston is magnetic and its movement activates the Magnetic Reed Switch (17) which establishes electrical contact with the line voltage. With the Toggle Switch (10) in the ON position, the Pilot Light (9) and Power Supply (8) are activated. The low voltage charge provided by the Power Supply (8) is transmitted to the Hand Gun Assembly (1) through the Exciter Wire (24) located in the Atomizing Air Hose (23). The exciter voltage is fed to the Generator (2) through the Gun Connector Assembly (22) and the connector wire (not shown).

The treated atomizing air passing through the generator is excited to a high electrostatic charge. The charge s transmitted to an electrical contact before the atomizing air leaves the generator, which feeds the charge to the Fluid Tip (35). The atomizing air is routed to the Air Cap (36)

After the Air Valve (29) is opened, the Trigger (28) engages the Front Fluid Shaft Insulator (31) and pulls it back. This retracts the Front Fluid Shaft (32) which unseats the Fluid Needle (34) from the Fluid Tip (35). The fluid is then simultaneously atomized and electrostatically charged. As indicated earlier, the fluid line will be plugged for these tests.

When the gun Trigger is released, the following occurs:

Figure 3 (Continued)

Explanation of Electrical and Air Hook-up

The Front Fluid Shaft Insulator (31) is released and pushed forward by the Fluid Adjustment Compression Spring (33). This, in turn, pushes the Front Fluid Shaft (32) forward and the Fluid Needle (34) is reseated in the Fluid Tip (35) cutting off the flow of fluid.

Then the Air Valve (29) is closed by the Air Valve Compression Spring (30) and the flow of atomizing air is stopped. Without the air flow, the Flow Switch Spring (15) moves the Flow Switch Piston (16) back to its original position. The Magnetic Reed Switch (17) is deactivated and contact with line voltage is disrupted. The Pilot Light (9) and Power Supply (8) are shut off thereby discontinuing the exciter voltage to the Generator (2). Without the exciter voltage and the flow of air, the Generator (2) cannot provide an electrostatic charge to the Fluid Tip (35). It should be noted that the electrostatic charge is transmitted to the Fluid Tip (35) only when both the atomizing air is flowing and the Power Supply (8) is activated. The Pilot Light (9) is lit only when air is passing through the system and the Toggle Switch (10) is in the "ON" position. The light indicates that the system is operating.

The Ground Wire (25) is routed to the gun through the Atomizing Air Hose (23) to provide a grounded handle for the operator.

Appendix II: Engine Operating Manuals, Test Procedures and Data Sheets

A

Onan Test Procedures

PERFORMANCE TEST OF A DIESEL ENGINE USING AN ELECTRIC DC DYNAMOMETER

1. OBJECTIVE.

The objective of this test is to obtain sufficient data to establish the power output, efficiency, and performance characteristics of a diesel engine operating at constant speed and fixed throttle conditions.

2. TEST CONDITIONS.

Test runs should not be made until the engine has been thoroughly warmed up.

3. FUEL CONSUMPTION.

Fuel consumption is measured simultaneously with brake horsepower. The fuel consumption measurement must not be started until the engine is stabilized. A measuring interval of not less than sixty (60) seconds should be observed. All specific fuel consumption shall be based upon observed brake power.

4. EQUIPMENT.

4.1 ENGINE DESCRIPTION.

The test engine is an Onan 4 cycle, vertical single cylinder (marine generator type); $3\frac{1}{2}$ in. bore; $3\frac{1}{2}$ in. stroke; 33.7 cubic inch displacement; 18.5:1 compression ratio; 5.5 hp at 1800 rpm. Locate and identify the following engine components.

4.1.1 Throttle.

4.1.2 Decompression release solenoid and plunger.

4.1.3 Fuel tank.

4.1.4 Air flow meter.

4.1.5 Cooling system.

4.2 MOTOR-GENERATOR.

The motor-generator used in this test is a Westinghouse 5 kW, 125 volt, 40 amp dynamometer. Its operating speed is 1150 to 3600 rpm. Identify the following motor-generator components.

4.2.1 Torque arm.

4.2.2 Dynamometer housing lock.

4.2.3 Spring scale.

4.3 FUEL PANEL.

It is possible with proper use of the fuel panel to measure the fuel flow into the engine. This is done by measuring the volume of fuel used over a specified time period. The draft gage is used to measure air flow into the engine. Identify the following components.

4.3.1 Fuel burrette.

4.3.2 Fuel selector valve.

4.3.3 Draft gage.

4.3.4 Fuel tank.

4.4 CONTROL PANEL.

The control panel monitors and controls the power into and out of the motor-generator. Identify the following components.

4.4.1 Set-up switch.

4.4.2 Armature rheostat.

4.4.3 Field rheostat.

4.4.4 Voltmeter.

4.4.5 Ammeter.

4.4.6 Revolution counter.

4.4.7 Timing clock.

4.5 POWER SUPPLY.

This unit supplies power to the control panel. It has a simple on/off switch. Do not adjust the voltage; it has been preset. Identify the on/off switch.

5. OPERATIONAL PROCEDURES.

5.1 ENGINE PREPARATIONS.

5.1.1 Connect the fuel panel.

5.1.2 Connect the instrumentation.

5.1.3 Check the cooling water.

5.1.4 Check the oil level.

5.1.5 Check the throttle.

5.1.6 Examine the controls so that the engine and dynamometer can be stopped in an emergency. When the dynamometer is motoring the engine, the emergency stop is made by opening the line switch. When the engine is driving the generator, opening the decompression release plunger is the fastest stopping procedure.

5.1.7 Make sure the fuel selector valve is closed.

5.1.8 Locate the nearest CO_2 fire extinguisher.

5.2 ENGINE STARTING PROCEDURE.

5.2.1 Lock the dynamometer.

5.2.2 Press the STOP switch.

5.2.3 Set the grid resistance to provide maximum armature circuit resistance, thereby limiting starting current surge. This is the extreme counter-clockwise position, with the handle at "eight o'clock".

5.2.4 Turn the field rheostats to provide maximum field current for starting. This is the extreme counter-clockwise position, and field resistance is lowest.

5.2.5 Set the SET-UP switch at Fast Motoring and press the START switch.

5.2.6 Allow the engine to turn over a few seconds then push the plunger on the decompression solenoid and turn the knurled knob until the pin is locked in place.

5.2.7 Open the throttle sufficiently to return the ammeter reading to zero.

5.2.8 Open the line switch by pressing the STOP button, thus disconnecting the dynamometer from the power line. The engine is now idling, and its speed is controlled by the throttle.

5.3 ENGINE LOADING PROCEDURE.

5.3.1 Put the armature rheostat at the extreme counter-clockwise position.

5.3.2 Put the field rheostat at the extreme clockwise position.

5.3.3 Put the SET-UP switch at "Res".

5.3.4 Unlock the dynamometer.

5.3.5 Set the throttle to the maximum obtainable without exceeding a current reading of 40 amps on the supply unit ammeter or an engine speed of 1700 rpm.

5.3.6 Press the START button. To obtain any combination of loads and speeds, adjust the field rheostats as required.

5.3.7 Watch the ammeter on the supply unit and do not exceed 40 amps.

5.3.8 Turn on the power supply to the electric speed counter.

NOTE: The power requirement may rise with no increase in speed. Watch the ammeter when load changes are made to be sure the dc power supply unit is not overloaded.

DECOMPRESSION RELEASE SOLENOID.

The decompression release solenoid operates the decompression release. The decompression release may also be operated by hand. To operate the decompression release manually, simply push the plunger while the engine is rotating and turn the knurled knob until the pin is locked in place. To stop the engine, turn the knob until it is free and pull it out as far as it will go.

6. CONSTANT-SPEED TEST.

A test covering the full range of torque loads at a constant rpm will serve to identify the general characteristics of the test engine. Such parameters as BRAKE TORQUE, BRAKE MEAN EFFECTIVE PRESSURE, BRAKE POWER, BRAKE SPECIFIC FUEL CONSUMPTION, BRAKE SPECIFIC AIR CONSUMPTION, AND BRAKE THERMAL EFFICIENCY will provide an evaluation of its performance.

The number of test runs to determine a curve depends on the nature of the curve and the accuracy of the test, but runs at no-load, and at 20, 40, 60, 80, and 100 percent of maximum brake power are usually required.

6.1 CONSTANT-SPEED TEST PROCEDURE.

6.1.1 Check the dynamometer control panel to get an understanding of the location and purpose of each of the controls and gages.

6.1.2 Check the fuel supply.

6.1.3 Connect the control panel to the 110v ac wall outlet.

6.1.4 Turn on the cooling water pump. The switch is located near the throttle. The red light should now be on.

6.1.5 Start the engine as described in paragraph 5.2.

6.1.6 Load the engine as described in paragraph 5.3.

6.1.7 Before commencing the test, practice adjusting both the load load control and throttle control to obtain the desired operating points. For this test, keep the speed at 1700 rpm.

6.1.8 Adjust the load and throttle settings to give maximum output, while maintaining the speed constant at 1700 rpm. Record all system parameters on the data sheet.

6.1.9 Adjust the load and throttle settings to give, successively, 80, 60, 40, and 20% (as possible) of the maximum output, while maintaining the speed at 1700 rpm. Each time, wait for steady state before recording the system parameters.

6.1.10 Shut down the engine by releasing the decompression plunger and turning off the control panel and power supply. Let the cooling water pump run for a few minutes before turning it off.

7. FIXED-THROTTLE TEST.

The peak BRAKE POWER, peak BRAKE TORQUE, and minimum BRAKE SPECIFIC FUEL CONSUMPTION are commonly used to describe or rate an engine.[1] These are readily determined from the usual SAE dynamometer test, in which the runs are made at full-throttle over the entire range of engine speeds and then repeated at part-throttle settings which will produce selected fractions of the full-throttle load. The SAE code specifies tests at no-load, 20, 40, 60, 80, and 100 percent load at each speed. A more thorough investigation of performance also includes measuring the friction power of the engine over the speed range and then determining the indicated performance of the engine.

For valid friction measurements, operating conditions must be as close as possible to the conditions existing when the engine is delivering power. In particular, the engine coolant and oil temperatures must be maintained. There are several acceptable methods for determining friction. Motoring, or driving the engine with the dynamometer is the preferred method.

7.1 FIXED-THROTTLE TEST PROCEDURE.

Steps 1-6 of the Constant-Speed Test are repeated essentially without change.

7.1.7 Increase the throttle setting gradually to full-throttle (100 percent) while increasing the load to control the engine speed to approximately 1700 rpm. Record the load and other system parameters. By adjusting the load, measure the system parameters at the other desired test speeds. Do not change the throttle setting. Wait for steady state to obtain after changing the load.

7.1.8 To conserve time, conduct a partial-throttle test at 60 percent of

---

1. The SAE Code defines maximum brake power as the highest developed at a given speed and peak power as the highest power developed.

full-throttle load only. Adjust the throttle and load settings to control the engine speed to about 1700 rpm and a load of about 60 percent of that observed at full throttle at 1700 rpm. Wait for steady state and record all system parameters. By adjusting the load, measure the system parameters at the other desired test speeds. Do not change the throttle setting.

7.1.9 Shut down the engine as described in step 6.1.10.

8. ANALYSIS.

8.1 CALCULATIONS.

8.1.1 Symbols and Units.

A/F (Air-Fuel Ratio)	
E (Barometric Pressure)	in. Hg
BHP (Brake Horsepower)	hp
BHP_c (Corrected Brake Horsepower)	hp
BMEP (Brake Mean Effective Pressure)	lbf/in^2
BTE (Brake Thermal Efficiency)	%
E (Atmospheric Water Vapor Pressure)	in. Hg
FEP (Fuel Equivalent Power)	hp
FHP (Friction Horsepower)	hp
IHP (Indicated Horsepower)	hp
m_A (Air Flow Rate)	lbm/hr
ME (Mechanical Efficiency)	%
m_F (Fuel Flow Rate)	lbm/min
RPM (Engine Speed)	rpm
SAC (Specific Air Consumption)	lbm/hp-hr
SFC (Specific Fuel Consumption)	lbm/hp-hr
T (Inlet Air Temperature)	F
TORQUE (Torque)	ft-lbf
V_d (Engine Displacement)	in^3

VE (Volumetric Efficiency) %

ρ_A (Inlet Air Density) lbm/ft^3

8.1.2 Brake Power (BHP).

(1) BHP = TORQUE x RPM/5250

8.1.3 Indicated Power (IHP).

The determination of IHP requires the separate measurement of Friction Power, FHP, and the calculation of Corrected Brake Power, BHP_c.

(2) IHP = FHP + BHP_c

8.1.4 Corrected Brake Power (BHP_c).

Engine performance is affected by barometric pressure, temperature, and humidity. In order to provide a common basis of comparison it is customary to correct BHP calculations to conditions of dry air at 29.00 in. hg and 85 F. The following formula is specified by the SAE Test Code for the correction.

(3) $BHP_c = [BHP + FHP][(B - E)/29.00][(460 + T)/545]^{\frac{1}{2}} - FHP$

A psychrometric chart for the determination of water vapor pressure, E, is provided in Figure 1. If FHP is unknown, it may be omitted from the equation.

8.1.5 Fuel Flow Rate (m_F).

The fuel flow in lbm/min is given by:

(4) m_F = FUEL CONSUMPTION (cm^3/min) x FUEL DENSITY (lbm/ft^3)/2831

8.1.6 Specific Fuel Consumption (SFC).

The Specific Fuel Consumption is a measure of efficiency that indicates the amount of fuel an engine consumes per unit of power produced. The SFC is generally around 0.5 lbm/hp-hr for diesels. The SFC will change at different speeds and throttle settings. The lower the SFC, the more efficient the engine.

(5) SFC = 60 x m_F/BHP_c or 60 x m_F/IHP

8.1.7 Fuel Equivalent Power (FEP).

This represents the energy available in the fuel consumed.

(6) FEP = 778 x HHV x m_F/33000

where HHV is the Higher Heating Value of the fuel in Btu/lbm.

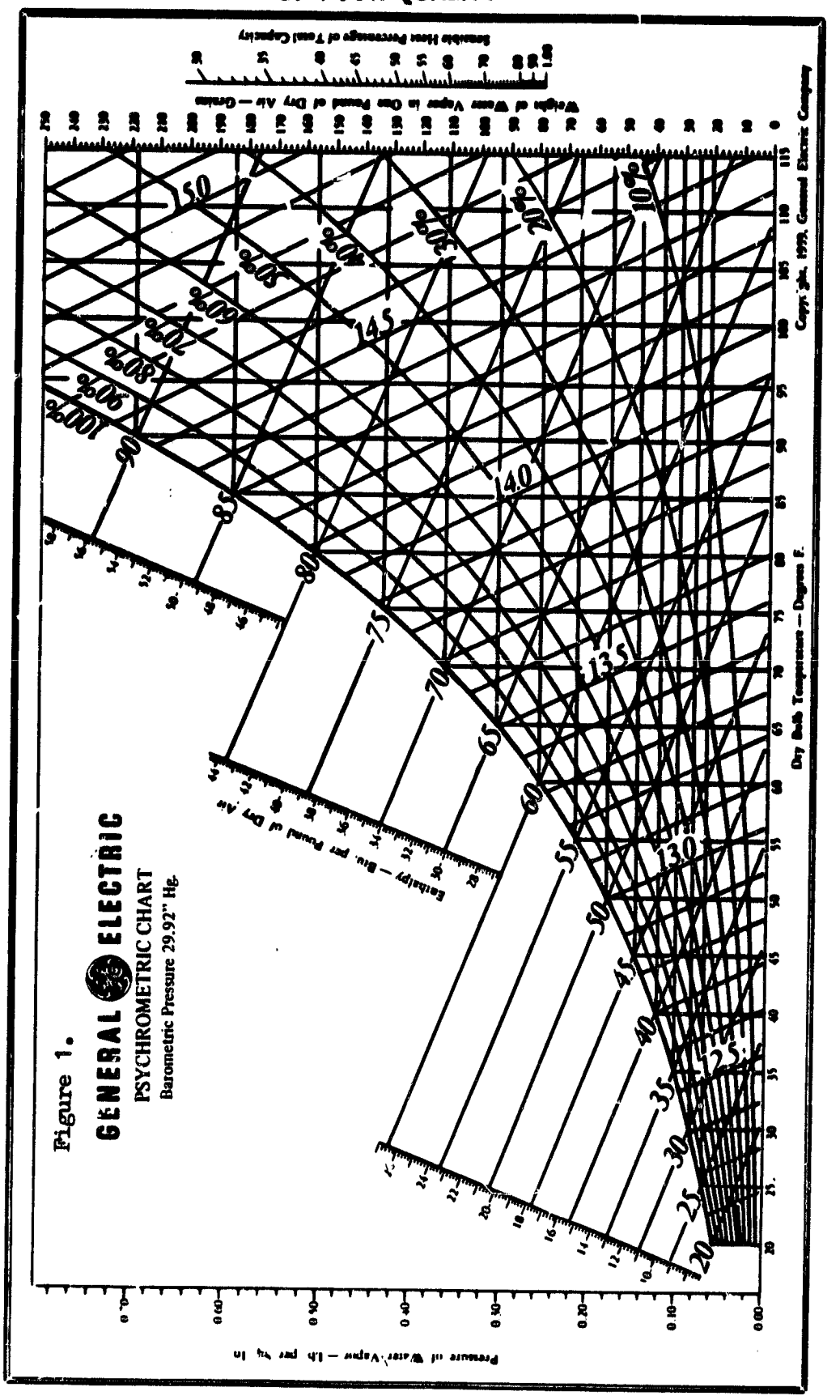

Figure 1.

8.1.8 Mechanical Efficiency (ME).

(7) $ME = 100 \times BHP_c/IHP$

8.1.9 Brake Thermal Efficiency (BTE).

The Brake Thermal Efficiency is the ratio of the power delivered at the crankshaft to the power available in the fuel. The thermal efficiency of an engine changes with the engine speed and throttle setting.

(8) $BTE = 100 \times BHP_c/FEP$

8.1.10 Brake Mean Effective Pressure (BMEP).

The Brake Mean Effective Pressure is the pressure which acting constantly throughout a complete operating cycle would produce the measured power output. Included is the effect of the combustion gas pressure during the power stroke and the pressure used for pumping in the intake air, pushing out the exhaust gases, and to overcome the internal friction.

The BMEP is generally between 100 and 180 lbf/in^2 for automotive engines. The BMEP is an important point of comparison for engines because it indicates the efficiency of the cylinder head porting and design, and the BMEP is independent of the rpm or size of the engine

(9) $BMEP = 792000 \times BHP_c/RPM \times V_d$

8.1.11 Air Flow Rate (m_A).

The air flow in ft^3/min or lbm/hr is shown in Figure 2 as a function of the pressure drop across the flow nozzle. Note that the flow rate is plotted for conditions of dry air at 29.92 in. Hg and 60 F.

The air flow must be corrected to the conditions of temperature, pressure, and humidity observed during the test. The actual air flow rate is then

(10) $m_A = m_A(obs)[(B - E)/29.92][520/(460 + T)]^{\frac{1}{2}}$

8.1.12 Air-Fuel Ratio (A/F).

(11) $A/F = m_A/(60 \times m_F)$

8.1.13 Specific Air Consumption (SAC).

(12) $SAC = m_A/BHP_c$ or m_A/IHP

Figure 2

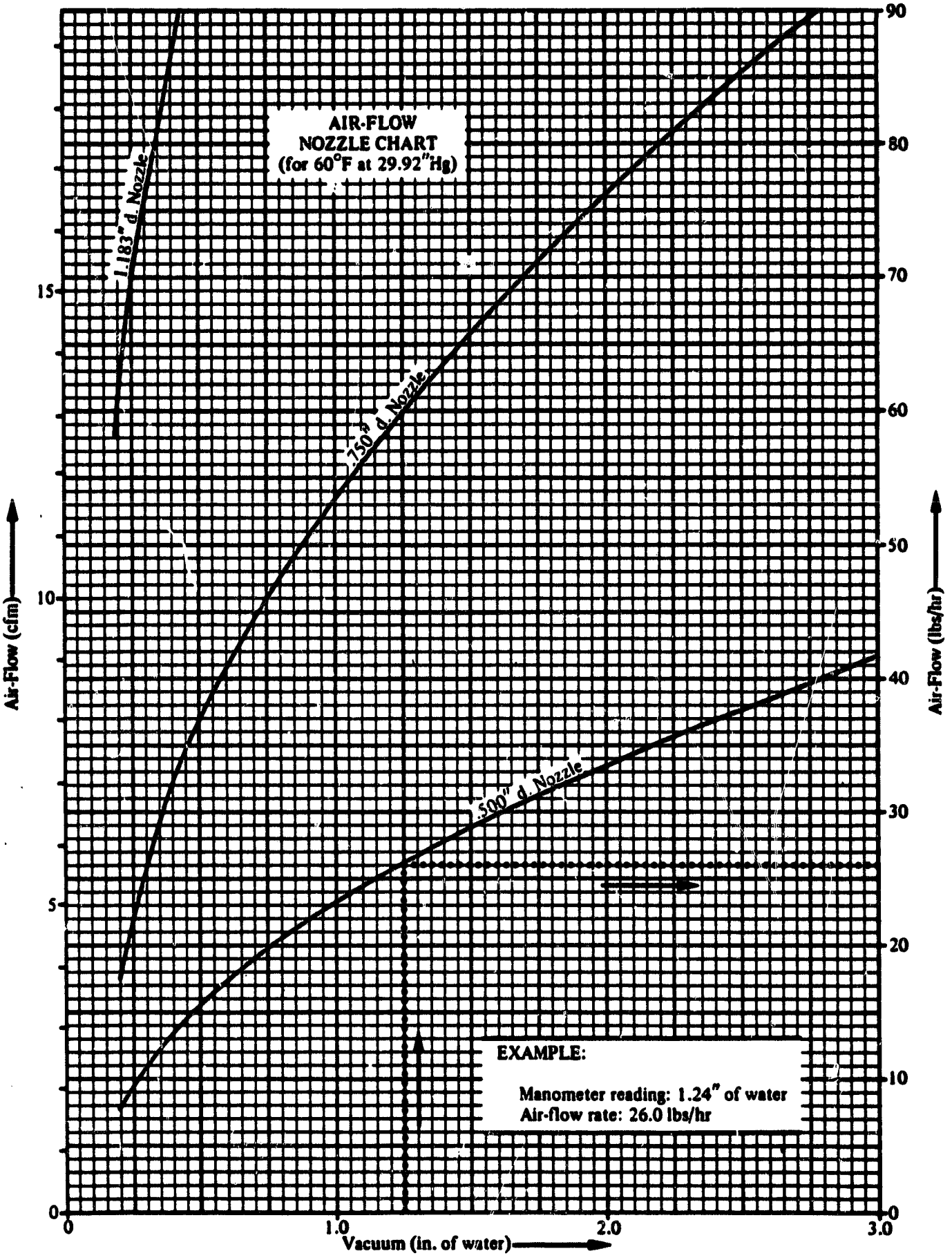

8.1.14 Volumetric Efficiency (VE).

The Volumetric Efficiency is the ratio of the air drawn into the engine cylinder to the maximum amount of air which could have been drawn into the cylinder. Because the engine runs at high speed, the cylinder seldom fills to its full capacity. The VE is generally between 60 percent and 80 percent for an unsupercharged engine.

The VE changes with engine speed.

(13) $VE = 5760 \times m_A/(RPM \times V_d \times \rho_A)$

CONSTANT-SPEED TEST ENGINE ANALYSIS

DATA SHEET

Date_____ Engine _____ Test No._____

Operator_____ Barometric Pressure_____ in. Hg

Fuel Type_____ Air Temperature, Dry Bulb_____ F

Specific Gravity_____ Air Temperature, Wet Bulb_____ F

1. Engine RPM	1700	1700	1700	1700	1700
2. Load	100%	80%	60%	40%	20%
3. Torque (ft-lbf)*					
4. Voltage (volts)					
5. Current (amps)					
6. Power (watts)**					
7. Air Flow (in. H_2O)					
8. Fuel Consumption (cm^3/min)					

* While the test is in progress, a curve of torque or power versus fuel consumption should be plotted. If the tests are accurate, a smooth curve will result.

** Generator output power.

Comments:

FIXED-THROTTLE TEST ENGINE ANALYSIS

DATA SHEET

Date_____ Engine_____ Test No._____

Operator_____ Barometric Pressure_____ in. Hg

Fuel Type_____ Air Temperature, Dry Bulb_____ F

Specific Gravity_____ Air Temperature, Wet Bulb_____ F

	Full-Throttle			Partial-Throttle*		
1. Engine RPM	1100	1400	1700	1100	1400	1700
2. Torque (ft-lbf)**						
3. Voltage (volts)						
4. Current (amps)						
5. Power (watts)***						
6. Air Flow (in. H_2O)						
7. Fuel Consumption (cm^3/min)						

* Adjust throttle and load settings to control the engine speed to approximately 1700 rpm and a load about 60 percent of that observed at full throttle at 1700 rpm. By adjusting the load, measure the system parameters at the other desired speeds. Do not change the throttle setting.

** While the test is in progress, a curve of torque or power versus fuel consumption should be plotted. If the tests are accurate, a smooth curve will result.

*** Generator output power.

Comments:

CONSTANT-SPEED TEST ANALYSIS

Test No._____ Engine_____

1. Engine RPM	1700	1700	1700	1700	1700
2. Load	100%	80%	60%	40%	20%
3. Torque (ft-lbf)					
4. Power (watts)					
5. BHP (hp)					
6. BHP_c (hp)					
7. m_A (obs) (lbm/hr)					
8. m_A (lbm/hr)					
9. m_F (lbm/hr)					
10. A/F					
11. SFC (lbm/hp-hr)					
12. SAC (lbm/hp-hr)					
13. BMEP (lbf/in^2)					
14. TE (%)					
15. VE (%)					

FIXED-THROTTLE TEST ANALYSIS

Test No._____ Engine_____

	Full-Throttle Test			Partial-Throttle (60%) Test		
1. Engine RPM	1100	1400	1700	1100	1400	1700
2. Torque (ft-lbf)						
3. Power (watts)						
4. BHP (hp)						
5. BHP_c (hp)						
6. m_A (obs) (lbm/hr)						
7. m_A (lbm/hr)						
8. m_F (lbm/min)						
9. A/F						
10. SFC (lbm/hp-hr)						
11. SAC (lbm/hp-hr)						
12. BMEP (lbf/in^2)						
13. TE (%)						
14. VE (%)						

B

Petter Test Procedures

PERFORMANCE TEST OF A DIESEL ENGINE USING A HYDRAULIC DYNAMOMETER

1. OBJECTIVE.

The objective of this test is to obtain sufficient data to establish the power output, efficiency, and performance characterisitcs of a diesel engine operating at constant speed and fixed throttle conditions.

2. TEST CONDITIONS.

Test runs should not be made until the engine has been thoroughly warmed up.

3. FUEL CONSUMPTION.

Fuel consumption is measured simultaneously with brake horsepower. The fuel consumption measurement must not be started until the engine is stabilized. A measuring interval of not less than sixty (60) seconds should be observed. All specific fuel consumption shall be based upon observed brake horsepower.

4. EQUIPMENT.

4.1 ENGINE DESCRIPTION.

The test engine is a Petter 4 cycle, vertical single cylinder; 2 3/4 in. bore; 2 1/4 in. stroke; 13.4 cubic inch displacement; 17:1 compression ratio; 3.5 hp at 3600 rpm (1.8 hp at 1800 rpm). Locate and identify the following engine components.

4.1.1 Variable speed control.

4.1.2 Decompression lever.

4.1.3 STOP/RUN lever.

4.1.4 Fuel tank, fuel line, and tank cock.

4.1.5 Fuel Injector.

4.1.6 Priming plinger.

4.1.7 Air flow meter.

4.1.8 Overload stop lever.

4.2 DYNAMOMETER

The dynamometer is a Go-Power hydraulic dynamometer. Identify the following dynamometer components.

4.2.1 Load gage.

4.2.2 Load control knob.

4.2.3 Tachometer.

4.2.4 Throttle control handle.

4.2.5 Throttle cable.

4.2.6 Power absorption unit.

4.2.7 Water in/out connections.

5. OPERATIONAL PROCEDURES.

5.1 ENGINE PREPARATIONS.

5.1.1 Connect the fuel panel.

5.1.2 Check the oil level.

5.1.3 Operate the dynamometer throttle several times to make sure it isn't sticking.

5.1.4 Make sure the tachometer drive coupling is properly aligned.

5.1.5 Rotate the dynamometer load control knob to the fully clockwise (closed) position.

5.1.6 Connect the inlet hose to the water supply. Turn on the water supply pump and check the hose connections for leaks.

5.1.7 Open the load control slowly (in direction of arrow on control knob face). This allows water to flow through the absorption unit.

5.1.8 Check the system for leaks.

5.1.9 If a leak is found, shut off the water, tighten all connections, and turn the water on again.

5.1.10 Close the load control valve by rotating the load knob fully clockwise to the stop. This stops water flow to the absorption unit. Do not attempt to start the engine at this point.

5.2 ENGINE STARTING PROCEDURE.

5.2.1 Set the throttle at 40 percent.

5.2.2 Move the STOP/RUN lever to the RUN position.

5.2.3 If the fuel tank has been allowed to run dry, it will be necessary to bleed air out of the fuel system. Proceed as follows:

1. Loosen the bleed screw about ¼ turn.

2. Open the throttle to 100%.

3. Place the knotted end of the starting rope in the notch of the starting pulley and wind the rope around the pulley in a clockwise direction.

4. Engage the decompressor lever by holding it back against the stop.

5. Pull the starting rope quickly and smoothly off the starting pulley. With the decompressor lever engaged, there will be little resistance to the pull.

6. Diesel fuel will leak past the loosened bleed screw. It will bubble during the first few pulls as air is forced from the fuel lines. Continue to operate the starter pulley until clear, bubble-free fuel leaks past the bleed screw, then tighten the screw.

5.2.4 Depress and release the overload stop lever.

5.2.5 Using both hands, turn the starting pulley in the direction opposite to the white arrow above the pulley until the resistance is encountered. Bounce the pulley against this resistance and listen for the squeak of the fuel injector as it sprays fuel into the cylinder. Continue until the injector has squeaked about ten times. This is equivalent to chocking a gasoline engine.

5.2.6 Place the end of the strating rope in the notch of the starting pulley and wind the rope clockwise around the pulley two and a half turns. Do not wrap the starter rope around the hand or wrist.

5.2.7 Make sure the decompressor lever is disengaged. It should be down against the cylinder head, well away from the stop.

5.2.8 Pull the starter rope quickly and smoothly to inwind it completely from the starting pulley.

5.2.9 If the engine fires and dies back, move the starting pulley back to the pressure resistance point, rewind the starting rope and pull aigain.

5.2.10 When the engine is operating satisfactorily, reduce the throttle setting until it is running smoothly.

5.3 ENGINE STOPPING PROCEDURE.

5.3.1 To stop the engine, remove the load by rotating the load control to its maximum clockwise position while reducing the throttle setting until the engine runs smoothly. Let the engine idle at no load for a minute or two.

5.3.2 Move the STOP/RUN lever to the STOP position. The engine will stop.

5.3.3 Shut off the water supply .

IMPORTANT DON'TS-

1. Don't stop the engine with the decompressor lever or the valve seats and cylinder head joint.

2. Don't operate the overload stop lever when the engine is running.

3. Don' remove or tamper with the setting of the overload stop.

4. Don't stop the engine by allowing it to run out of fuel. When the engine is allowed to run dry, air gets into the fuel lines making it necessary to bleed and prime the system.

5.4 ENGINE LOADING PROCEDURE.

5.4.1 Set the load control knob to minimum (fully clockwise).

5.4.2 Start the engine as in paragraph 5.2 and adjust the throttle to 2500 rpm. Allow for warm up.

5.4.3 Before commencing a test, practice adjusting both the throttle and load control knob to obtain the desired operating points. Notice that the dynamometer does not respond immediately to changes in the load control settings. The delayed response is due to the time required for water to flow into and out of the power absorption unit.

6. CONSTANT-SPEED TEST.

A test covering the full range of torque loads at a constant rpm will serve to identify the general characteristics of the test engine. Such parameters as BRAKE TORQUE, BRAKE MEAN EFFECTIVE PRESSURE, BRAKE POWER, BRAKE SPECIFIC FUEL CONSUMPTION, BRAKE SPECIFIC AIR CONSUMPTION, and BRAKE THERMAL EFFICIENCY will provide an evaluation of its performance.

The number of test runs to determine a curve depends on the nature of the curve and the accuracy of the test, but runs at no-load, and at 20, 40, 60, 80, and 100 percent of maximum brake power are usually required.

6.1 CONSTANT-SPEED TEST PROCEDURE.

6.1.1 Before starting the engine, review paragraph 5, OPERATIONAL PROCEDURES.

6.1.2 Connect all fuel, air, and water lines.

6.1.3 Start the engine as described in paragraph 5.2. Adjust the throttle for 2500 rpm. Allow time for warm up.

6.1.4 Slowly move the throttle to the wide open position (100%) while increasing the load to hold the speed at 2500 rpm. Record all system parameters.

6.1.5 Adust the load and throttle to give, successively, 80, 60, 40, and 20 percent (as possible) of the maximum output, while maintaining the speed at 2500 rpm. Each time, wait for steady state before recording the system parameters.

6.1.6 Shut down the engine as described in paragraph 5.3.

7. FIXED-THROTTLE TEST.

The peak BRAKE POWER, peak BRAKE TORQUE, and minimum BRAKE SPECIFIC FUEL CONSUMPTION are commonly used to describe or rate an engine.[1] These are readily determined from the usual SAE dynamometer test, in which the runs are made at full-throttle over the entire range of engine speeds and then repeated at part-throttle settings which will produce selected fractions of the full-throttle load. The SAE code specifies tests at no-load, 20, 40, 60, 80, and 100 percent load at each speed. A more thorough investigation of performance also includes measuring the friction power of the engine over the speed range and then determining the indicated performance of the engine.

For valid friction measurements, operating conditions must be as close as possible to the conditions existing when the engine is delivering power. In particular, the coolant and oil temperatures must be maintained. There are several acceptable methods for determining friction. Motoring, or driving the engine with the dynamometer is the preferred method. The hydraulic dynamometer, however, does not have this capability.

7.1 FIXED-THROTTLE TEST PROCEDURE.

7.1.1 Before starting the engine, review paragraph 5, OPERATIONAL PROCEDURES.

7.1.2 Connect all fuel, air, and water lines.

7.1.3 Start the engine as described in paragraph 5.2. Adjust the throttle for 2000 rpm. Allow time for warm up.

7.1.4 Slowly increase the throttle to the wide open position while increasing the load, as necessary, to limit the engine speed to 3200 rpm. Record all system parameters.

7.1.5 Using the load control, adjust the engine speed to each of the remaining engine speeds. Do not change the throttle setting. Wait for steady state after adjusting the load before recording the system parameters.

7.1.6 To conserve time, conduct a partial-throttle test at 60 percent of

1. The SAE code defines maximum brake power as the highest developed at a given speed and peak power as the highest power developed.

full-throttle load only. Adjust the throttle and load settings to control the engine speed to about 3200 rpm and a load of about 60 percent of that observed at full throttle at 3200 rpm. Wait for steady state and record all system parameters. By adjusting the load, measure the system parameters at the other desired test speeds. Do not change the throttle setting.

7.1.7 Shut down the engine as described in step 5.3.

8. ANALYSIS.

8.1 CALCULATIONS.

8.1.1 Symbols and Units.

A/F (Air-Fuel Ratio)	
E (Barometric Pressure)	in. Hg
BHP (Brake Horsepower)	hp
BHP_c (Corrected Brake Horsepower)	hp
BMEP (Brake Mean Effective Pressure)	lbf/in^2
BTE (Brake Thermal Efficiency)	%
E (Atmospheric Water Vapor Pressure)	in. Hg
FEP (Fuel Equivalent Power)	hp
FHP (Friction Horsepower)	hp
IHP (Indicated Horsepower)	hp
m_A (Air Flow Rate)	lbm/hr
ME (Mechanical Efficiency)	%
m_F (Fuel Flow Rate)	lbm/min
RPM (Engine Speed)	rpm
SAC (Specific Air Consumption)	lbm/hp-hr
SFC (Specific Fuel Consumption)	lbm/hp-hr
T (Inlet Air Temperature)	F
TORQUE (Torque)	ft-lbf
V_d (Engine Displacement)	in^3

VE (Volumetric Efficiency) %

ρ_A (Inlet Air Density) lbm/ft^3

8.1.2 Brake Power (BHP).

(1) BHP = TORQUE x RPM/5250

8.1.3 Indicated Power (IHP).

The determination of IHP requires the separate measurement of Friction Power, FHP, and the calculation of Corrected Brake Power, BHP_c.

(2) IHP = FHP + BHP_c

8.1.4 Corrected Brake Power (BHP_c).

Engine performance is affected by barometric pressure, temperature, and humidity. In order to provide a common basis of comparison it is customary to correct BHP calculations to conditions of dry air at 29.00 in. hg and 85 F. The following formula is specified by the SAE Test Code for the correction.

(3) $BHP_c = [BHP + FHP][(B - E)/29.00][(460 + T)/545]^{\frac{1}{2}} - FHP$

A psychrometric chart for the determination of water vapor pressure, E, is provided in Figure 1. If FHP is unknown, it may be omitted from the equation.

8.1.5 Fuel Flow Rate (m_F).

The fuel flow in lbm/min is given by:

(4) m_F = FUEL CONSUMPTION (cm^3/min) x FUEL DENSITY (lbm/ft^3)/2831

8.1.6 Specific Fuel Consumption (SFC).

The Specific Fuel Consumption is a measure of efficiency that indicates the amount of fuel an engine consumes per unit of power produced. The SFC is generally around 0.5 lbm/hp-hr for diesels. The SFC will change at different speeds and throttle settings. The lower the SFC, the more efficient the engine.

(5) SFC = 60 x m_F/BHP_c or 60 x m_F/IHP

8.1.7 Fuel Equivalent Power (FEP).

This represents the energy available in the fuel consumed.

(6) FEP = 778 x HHV x m_F/33000

where HHV is the Higher Heating Value of the fuel in Btu/lbm.

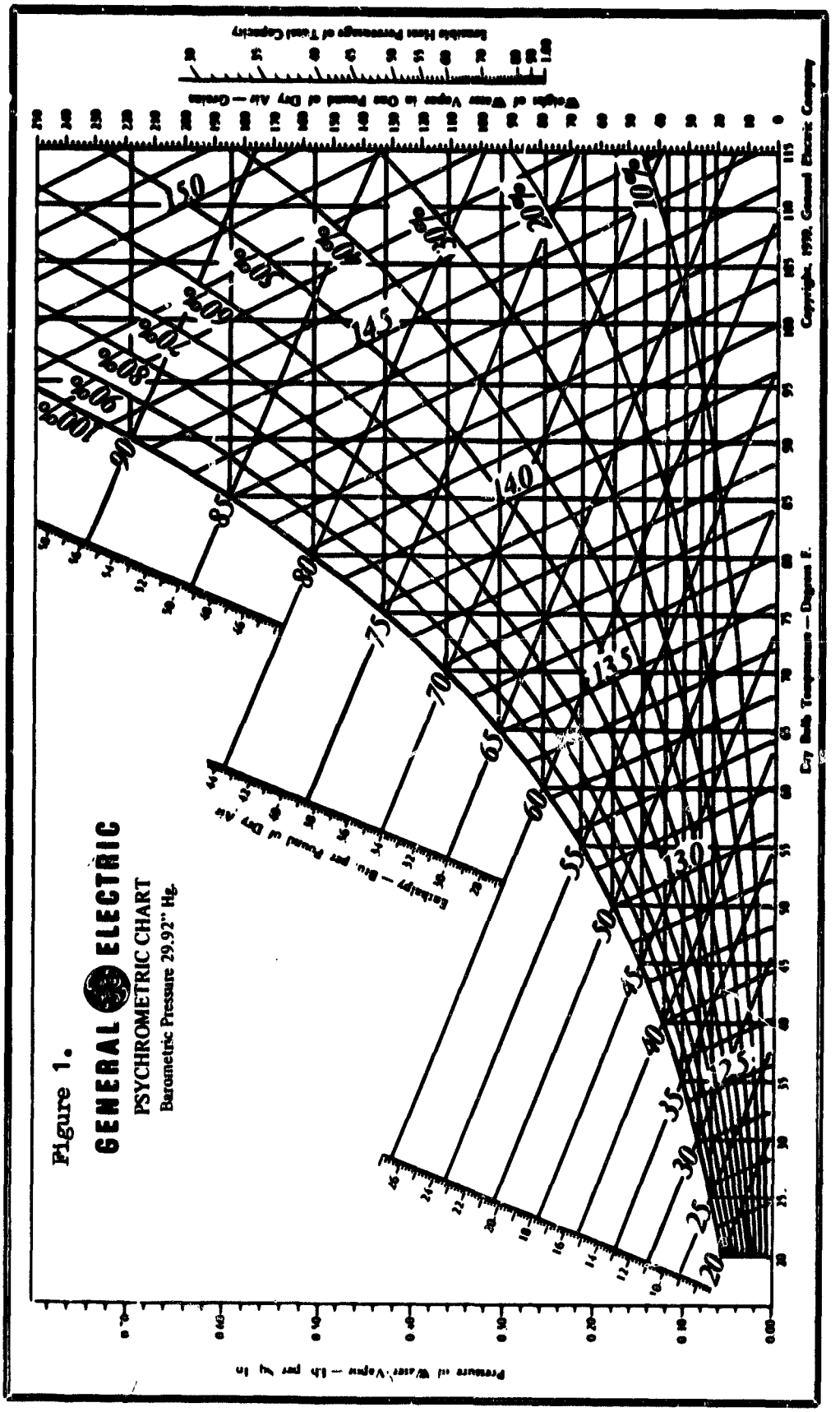

Figure 1.

8.1.8 Mechanical Efficiency (ME).

(7) $ME = 100 \times BHP_c/IHP$

8.1.9 Brake Thermal Efficiency (BTE).

The Brake Thermal Efficiency is the ratio of the power delivered at the crankshaft to the power available in the fuel. The thermal efficiency of an engine changes with the engine speed and throttle setting.

(8) $BTE = 100 \times BHP_c/FEP$

8.1.10 Brake Mean Effective Pressure (BMEP).

The Brake Mean Effective Pressure is the pressure which acting constantly throughout a complete operating cycle would produce the measured power output. Included is the effect of the combustion gas pressure during the power stroke and the pressure used for pumping in the intake air, pushing out the exhaust gases, and to overcome the internal friction.

The BMEP is generally between 100 and 180 lbf/in^2 for automotive engines. The BMEP is an important point of comparison for engines because it indicates the efficiency of the cylinder head porting and design, and the BMEP is independent of the rpm or size of the engine

(9) $BMEP = 792000 \times BHP_c/RPM \times V_d$

8.1.11 Air Flow Rate (m_A).

The air flow in ft^3/min or lbm/hr is shown in Figure 2 as a function of the pressure drop across the flow nozzle. Note that the flow rate is plotted for conditions of dry air at 29.92 in. Hg and 60 F.

The air flow must be corrected to the conditions of temperature, pressure, and humidity observed during the test. The actual air flow rate is then

(10) $m_A = m_A(obs)[(B - E)/29.92][520/(460 + T)]^{\frac{1}{2}}$

8.1.12 Air-Fuel Ratio (A/F).

(11) $A/F = m_A/(60 \times m_F)$

8.1.13 Specific Air Consumption (SAC).

(12) $SAC = m_A/BHP_c$ or m_A/IHP

Figure 2

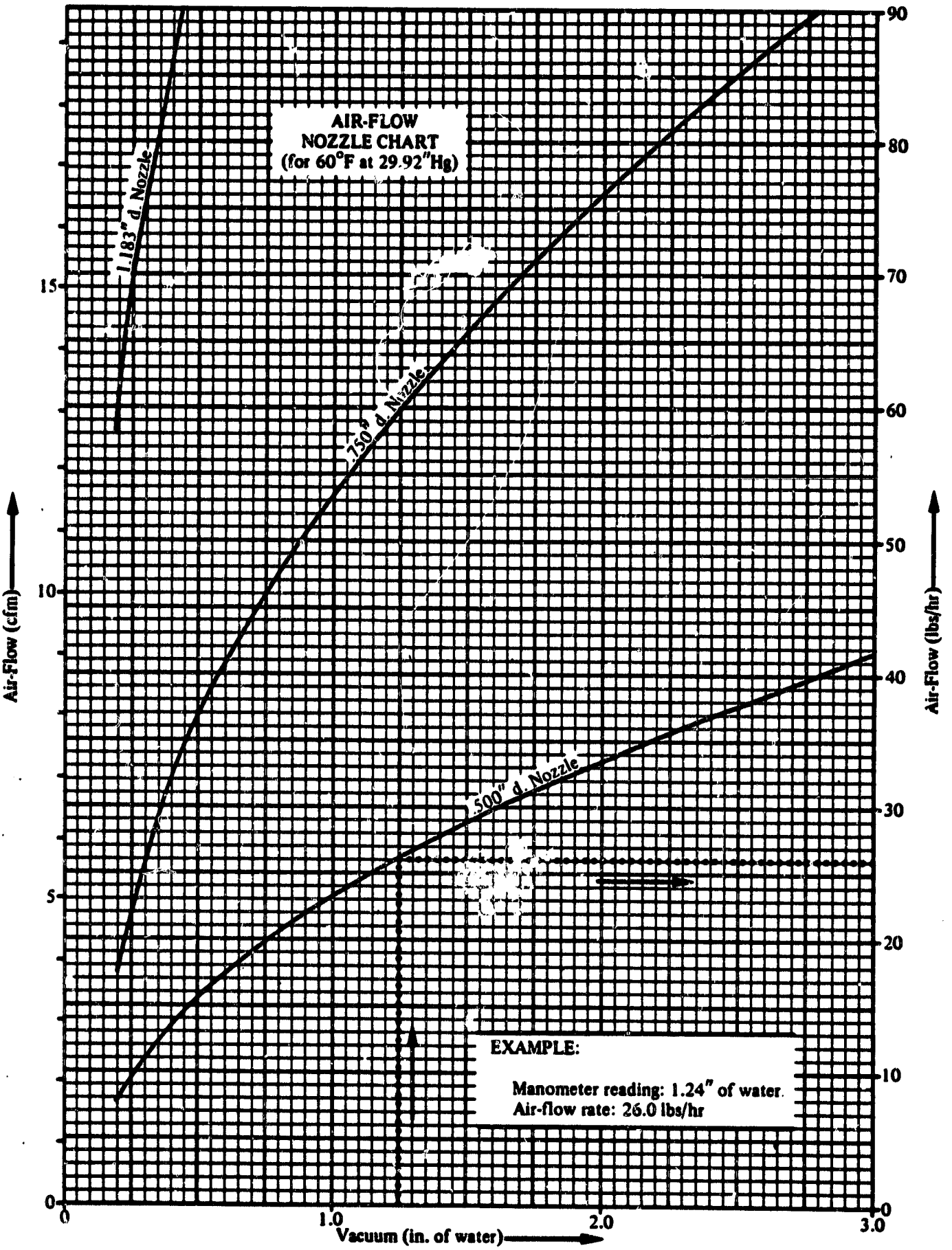

8.1.14 Volumetric Efficiency (VE).

The Volumetric Efficiency is the ratio of the air drawn into the engine cylinder to the maximum amount of air which could have been drawn into the cylinder. Because the engine runs at high speed, the cylinder seldom fills to its full capacity. The VE is generally between 60 percent and 80 percent for an unsupercharged engine.

The VE changes with engine speed.

(13) $VE = 5760 \times m_A/(RPM \times V_d \times \rho_A)$

CONSTANT-SPEED TEST ENGINE ANALYSIS

DATA SHEET

Date_____ Engine _____ Test No._____

Operator_____ Barometric Pressure_____ in. Hg

Fuel Type_____ Air Temperature, Dry Bulb_____ F

Specific Gravity_____ Air Temperature, Wet Bulb_____ F

1. Engine RPM	2500	2500	2500	2500	2500
2. Load	100%	80%	60%	40%	20%
3. Torque (ft-lbf)*					
4. Air Flow (in. H_2O)					
5. Fuel Consumption (cm^3/min)					

* While the test is in progress, a curve of torque or power versus fuel consumption should be plotted. If the tests are accurate, a smooth curve will result.

Comments:

FIXED-THROTTLE TEST ENGINE ANALYSIS

DATA SHEET

Date_____ Engine_____ Test No._____

Operator_____ Barometric Pressure_____ in. Hg

Fuel Type_____ Air Temperature, Dry Bulb_____ F

Specific Gravity_____ Air Temperature, Wet Bulb_____ F

	Full-Throttle Test					
1. Engine RPM	1200	1600	2000	2400	2800	3200
2. Torque (ft-lbf)*						
3. Air Flow (in. H_2O)						
4. Fuel Consumption (cm^3/min)						

* While the test is in progress, a curve of torque or power versus fuel consumption should be plotted. If the tests are accurate, a smooth curve will result.

Comments:

FIXED-THROTTLE TEST ENGINE ANALYSIS

DATA SHEET

Date_____ Engine_____ Test No._____

Operator_____ Barometric Pressure_____ in. Hg

Fuel Type_____ Air Temperature, Dry Bulb_____ F

Specific Gravity_____ Air Temperature, Wet Bulb_____ F

	Partial-Throttle Test (60%)*					
1. Engine RPM	1200	1600	2000	2400	2800	3200
2. Torque (ft-lbf)**						
3. Air Flow (in. H_2O)						
4. Fuel Consumption (cm^3/min)						

* Adjust throttle and load settings to control the engine speed to approximately 1700 rpm and a load about 60 percent of that observed at full throttle at 1700 rpm. By adjusting the load, measure the system parameters at the other desired speeds. Do not change the throttle setting.

** While the test is in progress, a curve of torque or power versus fuel consumption should be plotted. If the tests are accurate, a smooth curve will result.

Comments:

CONSTANT-SPEED TEST ANALYSIS

Test No._____ Engine_____

1. Engine RPM	2500	2500	2500	2500	2500
2. Load	100%	80%	60%	40%	20%
3. Torque (ft-lbf)					
4. BHP (hp)					
5. BHP_c (hp)					
6. m_A (obs) (lbm/hr)					
7. m_A (lbm/hr)					
8. m_F (lbm/hr)					
9. A/F					
10. SFC (lbm/hp-hr)					
11. SAC (lbm/hp-hr)					
12. BMEP (lbf/in^2)					
13. TE (%)					
14. VE (%)					

FIXED-THROTTLE TEST ANALYSIS

Test No._____ Engine_____

	Full-Throttle Test					
1. Engine RPM	1200	1600	2000	24000	2800	3200
2. Torque (ft-lbf)						
3. BHP (hp)						
4. BHP_c (hp)						
5. m_A (obs) (lbm/hr)						
6. m_A (lbm/hr)						
7. m_F (lbm/min)						
8. A/F						
9. SFC (lbm/hp-hr)						
10. SAC (lbm/hp-hr)						
11. BMEP (lbf/in^2)						
12. TE (%)						
13. VE (%)						

FIXED-THROTTLE TEST ANALYSIS

Test No._____ Engine_____

	Partial-Throttle Test (60%)*					
1. Engine RPM	1200	1600	2000	2400	2800	3200
2. Torque (ft-lbf)						
3. BHP (hp)						
4. BHP_c (hp)						
5. m_A (obs) (lbm/hr)						
6. m_A (lbm/hr)						
7. m_F (lbm/min)						
8. A/F						
9. SFC (lbm/hp-hr)						
10. SAC (lbm/hp-hr)						
11. BMEP (lbf/in^2)						
12. TE (%)						
13. VE (%)						

Appendix III: Selected Papers

No 73 - 1270-1 JSME 1ST SYMPOSIUM ENGINE

Combustion Improvement of Internal Combustion Engine

PROMOTION OF COMBUSTION

1. INTRODUCTION

In previously published papers we have stated that combustion velocity is greatly increased by the addition of an electric field to a combustion system. Moreover, we had also established that combustion velocity is affected and differs in each of the following methods subject to the following;

(1) how the electric field is produced ahd applied;

(2) the differences in characteristics of the applied A. C. and D. C. current; and

(3) the reactions produced by the A. C. cycles.

In this paper we will summarize below the experiments which were conducted for the promotion of combustion.

2. PROCEDURES FOR THE EXPERIMENTS

2.1 Combustion Taking Place at Atmospheric Pressure

There may be several arrangements for producing the electric field force to produce the effect on the combustion rate. Some typical arrangements are shown in Fig. 1.

The procedures used in this experiment were to ignite a Bunsen burner using methane gas as fuel shown in [Fig. 1 (A) (B)], and to ignite the surface of a flammable fluid placed in a burning dish [Fig. 1 (C)].

The procedure of the experiments to produce a electric field to the flames might be done in either of two ways. The first way is to place

the flame between high voltage terminals [Fig. 1 (A)]. The second way is to place one terminal (positive) in the flame and the other terminal to ground [Fig. 1 (B) (C)] .

In addition, we can consider a system that combines both systems as shown in Fig. 2, where the effects were remarkably increased; as shown below, compared to each single system. When a magnetic field was applied to the flame flux in the electric field, as in Fig. 3, the behavior of the flame flux was excited and the combustion rate increased.

As to the above mentioned, the consumption of electric power due to the applied electric field is caused by leakage current. Accordingly, even in the high electric fields of 20-30KV, the leakage current is only 100-150μA, i.e. the consumption of electric power is only a few watts.

2.2 Internal - Combustion Engine

Based on the results of the remarkable increase of combustion rate at atmospheric pressure due to the electric field charge, one of the poles of a high-voltage power supply was attached to the cylinder cover, and the changes of output and RPM were measured by a fan-brake dynamometer and an electric tachometer, respectively.

3. EXPERIMENTAL RESULTS

3.1 Combustion at Atmospheric Pressure

Previous experiments have used Fig. 1-A which is the most conventional system to apply an electric field. For such a system Professor Kinbara[2] concluded that the shortening of flame length due to the electric field results from the reduction of the evaporation rate.

On the other hand, Weinberg[3] pointed out that the flame in the electric field was pulled toward the outer electrode and also the soot-formation was reduced.

However, they did not refer to the phenomena on combustion and the difference of the velocity of combustion.

Using the systems with applied electric fields shown in Figures 1 - A, 2 and 3, we have investigated the electric field effects on the combustion phenomena such as the change of flame form and the increase of the velocity of combustion.

(a) Method For Positioning The Terminals Outside Of The Flame

When terminals are placed on the outside of the flame, the length of the flame is shortened and the width is increased horizontally, and it is pulled toward each terminal depending on the polarity. For instance, we will show the results of the influence of the terminals on a gas flame from a Bunsen burner in Fig. 4 & 5. At the beginning of this experiment, the flame was adjusted to be 260mm in length and placed between two terminals which were 60 x 110mm in size, these bars were a type of iron material. When an electric field was induced in the terminals the flame became short and wide. In fact there was not much difference in the length of the flame when the terminal distance was 100mm or 130mm; however, the width of the flame increased from 1.3 to 4.0 times. Particularly when the terminal distance was 100mm the flame was almost 2.0 times as wide as when the distance was 130mm. Thus the shape of the flame is influenced

by the distances of the terminals from the flame and shows that the size and shape are changed by the density of the electric field.

(b) Method for Positioning a Cylindrically Shaped Terminal on the Outside of a Flame

We used a 74mm dia. iron cylinder as a terminal and experimentally found that a longer cylinder changed the flame to a shorter and wider shape.

(c) One terminal is placed in the flame (no figure) and the second terminal is grounded. [Fig. 1 (b)] .

(c-1) Direct Current

When an electric field is placed on a flame which is adjusted at a 290mm length the flame is shortened as plotted along a logarithmic path as shown in Fig. 8. In addition it was noted that when the flame was originally adjusted for this experiment it was in a deoxidized state but changed into an oxidized flame and the deoxidized state disappeared completely when an electric field was induced above 6KV. This phenomena of flame length shortening and the deoxidized flame disappearance must mean that combustion velocity was accelerated by the presence of an electric field--i.e. an essential change of combustion.

(c-2) Alternating Current

In the same manner as outlined above we induced an AC electric field current to the flame. This time we observed a cyclic expansion and contraction movement of the flame. The cycles of expansion and

contraction were synchronous with the alternating current cycles. And also this time there appeared to be about a 10^{-4} Amp electric current in the flame. (In a natural burning flame 10^{-8} to 10^{-9} Amp electric current is normal.) Therefore this experiment shows us that it is worth inducing a second electric field outside of the flame to increase combustion velocity.

(c-3) The first terminal is in the flame. The second terminal is outside the flame. Fig. 11.

The measurements of the combustion velocity of light oil and kerosene were 0.15; 0.23 grams/min and increased to 0.52; 0.67 grams/min or approximately 3.5 and 2.9 times from the original combustion rates. Also the measurement of the combustion velocity of gasoline which was 0.45 grams/min originally increased to 2.25 grams/min or approximately 5.0 times.

At this time it became evident that there was approximately a 15 to 20% decrease in combustion velocity without an induced electric field at atmospheric pressure in the above procedures.

Thus it was confirmed that the combustion velocity can be greatly increased when an electric field is induced into a combustion system. In seeking a practical method of application for these series of experiments we found that the method in [Fig. 1 (c)] was most efficient.

(d) One terminal is placed in the flame and the other terminal is grounded.

(d-1) Direct Current Fig. 12 (Burning Normal Heptane)

The characteristics of flame combustion are completely different when the terminal placement in the flame is positive or negative. Generally, where the positive terminal is inside the flame, the flame appears to be repelled from the terminal and it becomes shorter. When the negative terminal is inside the flame, the flame appears to be attracted by the terminal and it becomes longer. These are shown in Fig. 13 & 14.

The fact that the shapes of the flames are changed depends on whether the terminal in the flame is positive or negative might tell us that the ion current which is generated in the natural combustion system repels or attracts the flame itself and this is due to the fact that the distribution of the ionizing current around the flame is mostly positive outside the flame periphery.

By considering the rate differences in the combustion process we measured the combustion amount per second. The results are shown in Fig. 12. The combustion amount/sec in the situation in which the flame tends to become short because of the positive pole increases in proportion to the voltage. However, the CA/sec in which the flame tends to become longer because of the negative pole does not increase or decrease. Such a phenomena can be explained since it takes a longer time for a specified amount of fuel to burn as a long flame. This may mean a decrease in the combustion velocity (or it may indicate a minimization of unburnt fuel); thus, it is possible to say this experiment may lead to a way as a

method to develop control techniques of the combustion velocity.

(d-2) Alternating Current (Fig. 1 (c) & Fig. 12).

The characteristics of this combustion system are completely different from that shown at Fig. 13 & 14. As the voltage increases the flame becomes longer and wider; the entire flame vibrates in synchronization with the phases of the AC current. Fig. 15 indicates that gasoline burns increasingly more strongly in a direct relation to the force of the applied electric field. As shown in Fig. 16, the combustion time was 62 seconds for 2cc of gasoline, ignited and burned in a normal atmosphere. However, in this experiment it was usually about 11 seconds with an induced electric field. For light oil the burning rates were reduced from 75 seconds to 17 seconds; for heavy oil it was 108 seconds reduced to 38 seconds; each type of hydrocarbon fuel was reduced in burning time in the proportions of 1/1.7 for gasoline, 1/4.4 for light oil and 1/2.8 for heavy oils respectively.

This indicates that combustion velocity was accelerated by the imposing of an electric field on the burning hydrocarbons. The principal reason for this acceleration must have been the strength of the given electric field. If the voltage is constant, it can be attributed to the distance relationship between the positive terminal and ground. This relationship is shown in Fig. 17 as a graph showing voltage (the distance between terminal and ground) to the combustion velocity cc/sec.

It must be pointed out, however, this result is not the combustion velocity which is simply measured as in Fig. 12 & 16. This is from the method whereby the combustion velocity is measured by an instrumentation setup, shown in Fig. 18, which is supplied a measured amount of hydrocarbon fuel.

Thereafter we assembled additional laboratory apparatus as shown in Fig. 19 to conduct an experiment for igniting and burning measured amounts of gasoline and air in the illustrated setup. In addition, temperature readings were taken during the experiment by placing a pyrometer (positioned 10mm inside the nozzle opening) and found the temperature increased by 30° to 40° C to a 700°-900°C range. The combustion velocity increased as expected in proportion to the increase in the voltages.

When a moderate magnetic field flux is induced at the outlet of the nozzle, the combustion amount of gasoline cc/sec decreased. This indicates that the burning gasoline was influenced and deflected by the magnetic field flux acting upon the ion current in the flame, which is very similar to the situation in which the resistance was caused at the outlet of the nozzle. Therefore, the temperature increase can be expected too, as shown in Fig. 20. It was obvious from close observation of the flame condition and characteristics that there was also a decrease in the unburnt fuel, i.e. more complete combustion being emitted from the nozzle outlet.

3.2 Experiments With An Internal Combustion Gasoline Engine

After the above phenomena was observed in these experiments it was decided to conduct a further series of experiments to determine the effect of using electrical fields by observing the conditions which could occur in a gasoline engine subjected to induced electrical fields while the engine was operated under controlled conditions in the laboratory. The basic setup was to attach a positive terminal connection from a high voltage terminal of a 200 watt neon lamp transformer to a terminal fixed to the rear of the cylinder cover of a 90cc 2 cycle gasoline engine.

While the engine was being operated various readings were taken during the experiments by a fan brake dynamometer and an electric tachometer. These are shown in Fig. 21. The readings show that beginning with the original 2300RPM throttle setting a 4KV electric field charge was induced which increased N = 2300RPM to N = 3200RPM. Subsequently various charges were induced at 5.4KV; 6.3KV; 7.2KV and 2.7KV which showed successive increases to between 3200RPM to 3300RPM except the 2.7KV induced voltage only increased the RPM from 2500 RPM to 2o00 RPM.

It was observed that beginning with the application of the 4.5KV charge and succeeding charges, the effects were similar in the internal combustion engine as in the former experiments (Fig. 15 & Fig. 16) in which combustion takes place at atmospheric pressure in contrast to the conventional compression pressures in a 2 cycle gasoline engine.

This relationship N/NO = 1.39 to 1.43 increase (average) but if we consider the generating power of the engine the reaction $(N/NO)^3$ is also a factor in the combustion experiment, or 2.63 to 2.92 - times increase as plotted on the ordinal scale. The indicated pressure diagram corresponds to the increase of the area of the diagram as shown in Fig. 22.

abstract

№ 1

講演要旨

414 燃焼に関する新見解 (第1報)

(物理学的手法による燃焼速度の促進とその作用研究)

日本大学 名誉教授 正 浅川 勇二
日本大学 正員 浅川 彦一
東京都立工業高等専門学校 正員 杉井 乾

緒言

著者の一人(1)はさきに燃焼性ガスの層流及びアルコールランプの火炎に高電場を附与することによって燃焼が強烈化し燃焼速度を計測すると相当変化が大きい事を、又これらの焔の流れが電荷を帯びている事実を指摘した。従って、この焔の外周にさらに逆の電場又は磁場を附与することで、さらに燃焼の強烈化、燃焼速度の増大がおこることが期待された。

これは、それらの追求が更に新らしき手法——焔中に電極を挿入し、他端をアースに繋ぐ——によって更に著しく燃焼速度の増加の起こること、並びに実際のエンジンへの応用(これを点火電極と称している)。更にはその燃焼速度の増大の原因を探求した。ここに特に指摘すべきは、燃焼速度の電場附与によって著しく大きい、燃焼速度の増大に比して数倍～数十倍にも達する事実である。

1. 燃焼に対する電場附与の文献

著者の一人(1)は古く昭和11年に流体の流出速度増加を試みての一環として電場附与の試みを例外として指摘しているが、それは今日まで(2)、Weinberg(3)等が第1図の如き試みを行った。それらの結果は、著者(浅川吉く)の得たものに比して何れも効果が少なかった。

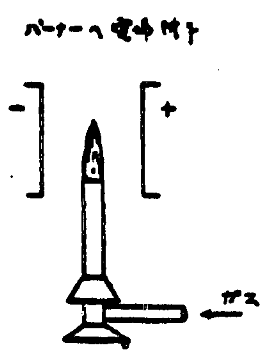

第1図

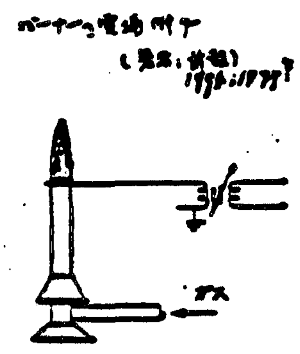

第2図

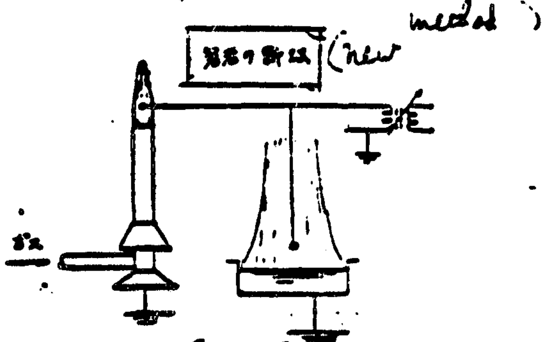

第3図

2. 実験結果

2.1 先ず第3図の如く四枚の容器に液体燃料を入れてこれに点火し焔中に電極を挿入する

* 本稿は一旦 詳細に記述したものであったが、今回の要旨の様式に詳細記述は省略。

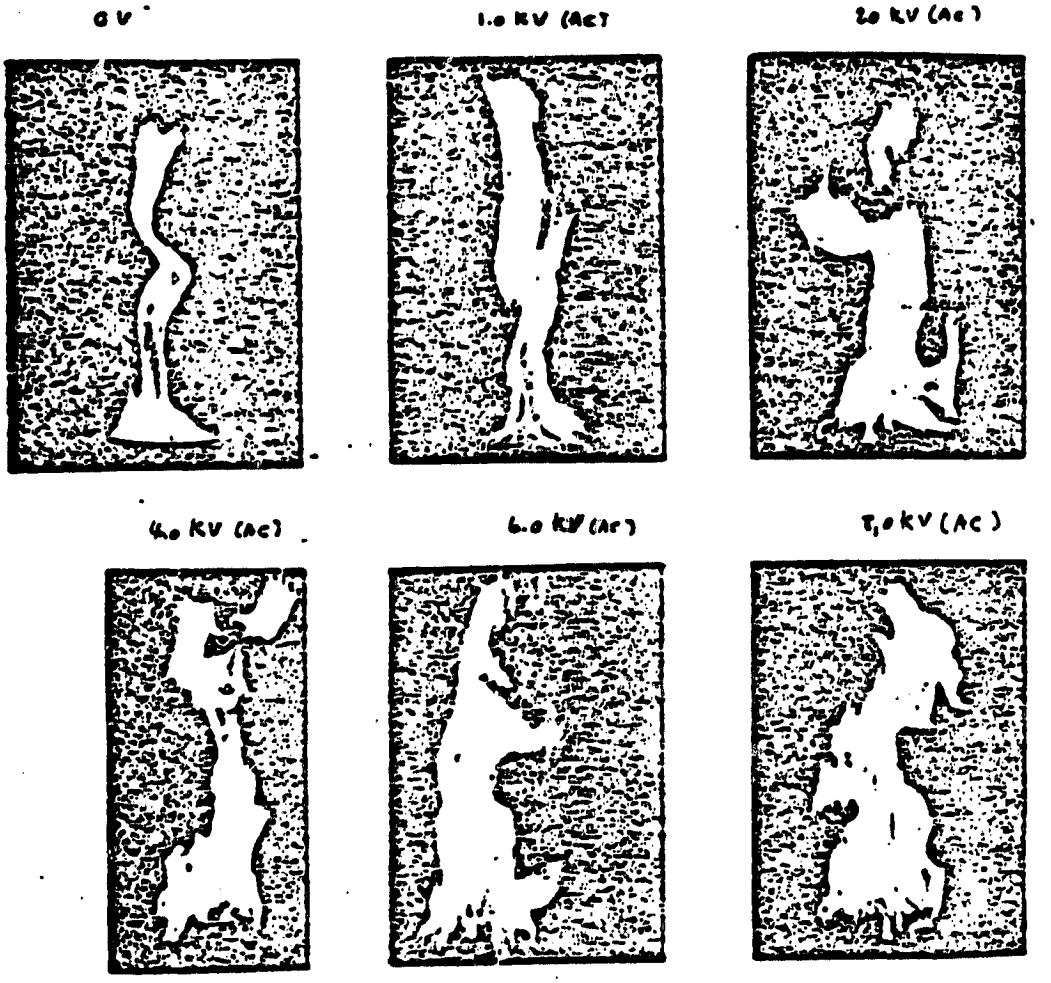

ORIGINAL PAGE IS
OF POOR QUALITY

第5図
種々の液体燃料の電場附加時の燃焼時間

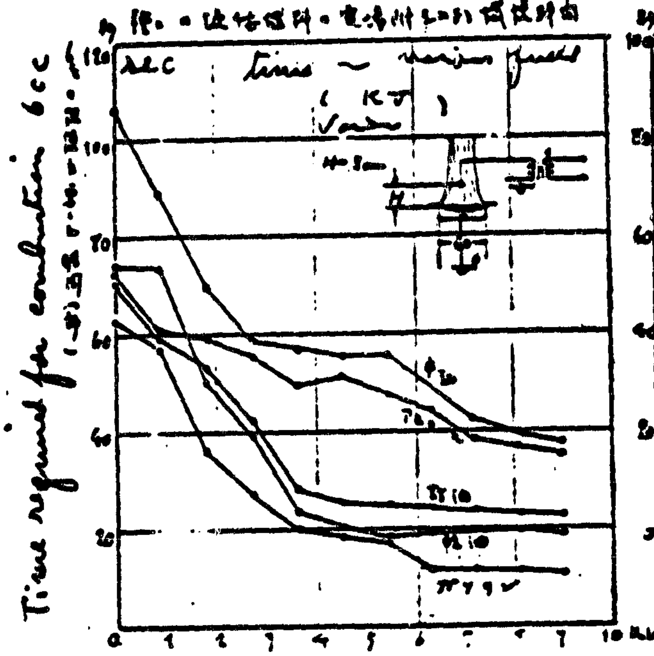

第6図
電極の液面からの距離(H)と燃焼時間

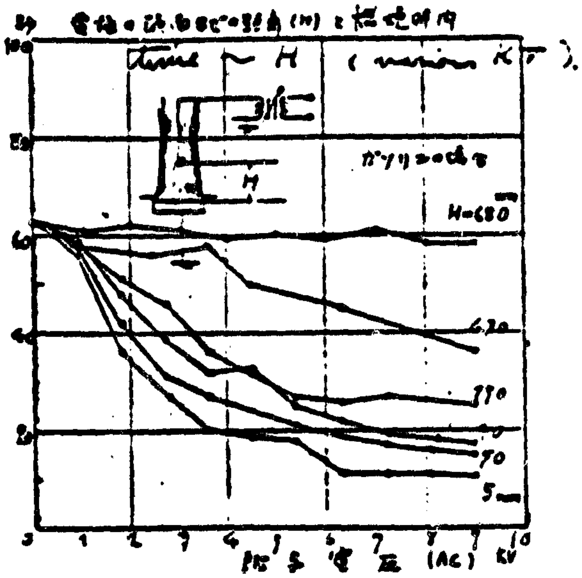

(2.2) エンジンへの応用。 I. C. ENGINE
エンジンへの応用の基礎実験(本稿では省略)にて[illegible]の如く燃焼促進が得られたので 90CC 2サイクルガソリンエンジンに応用し、その結果の一例を第7図に示す。ガソリン消費量の増加 12.5%—13.4% に対して出力は 7200r/(13700—14600)?, 1.78ps—1.97ps 位の増加するという注目すべき結果が得られた。

第7図 電極位置と燃焼完了時間

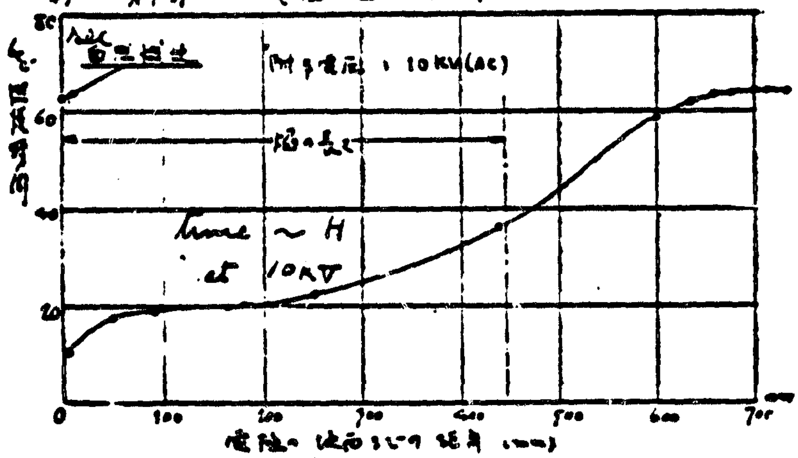

2.3. 電場下に於ける燃焼。 燃焼の促進に関して [illegible] 現象が大きく [illegible] 約10倍がそれである。液面の電極間隔が 60mm の場合 [illegible] 略直線的に増加する。しかしエンジンの場合 [illegible] 液面間隔 5mm [illegible] 100倍(速度の点で)に達する。しかも 10kV~ の印加電圧の場合であることが注目される。 [illegible]

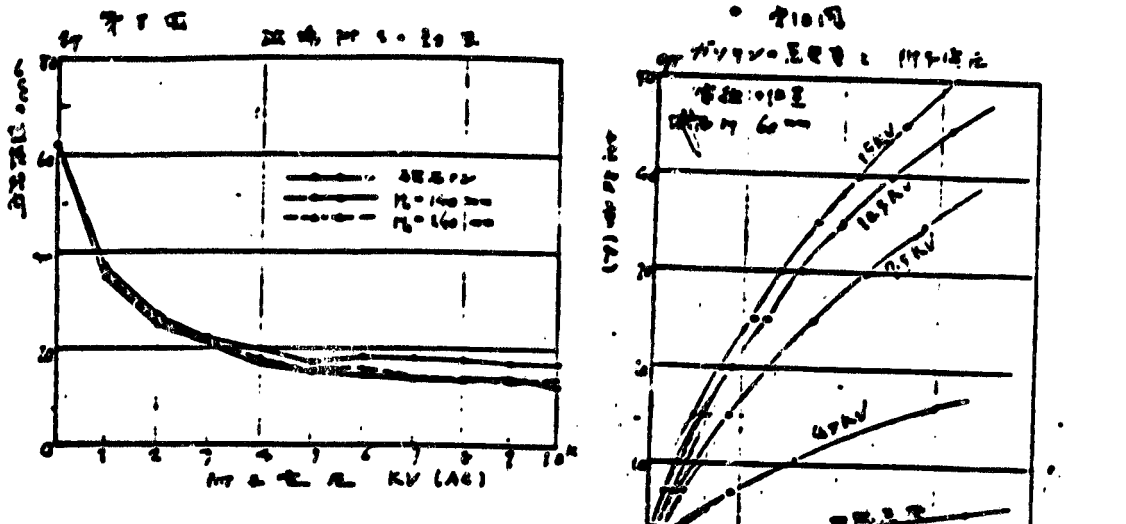

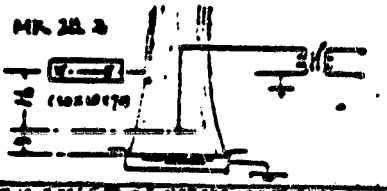

3.2 EXPERIMENTS WITH I.C. ENGINE

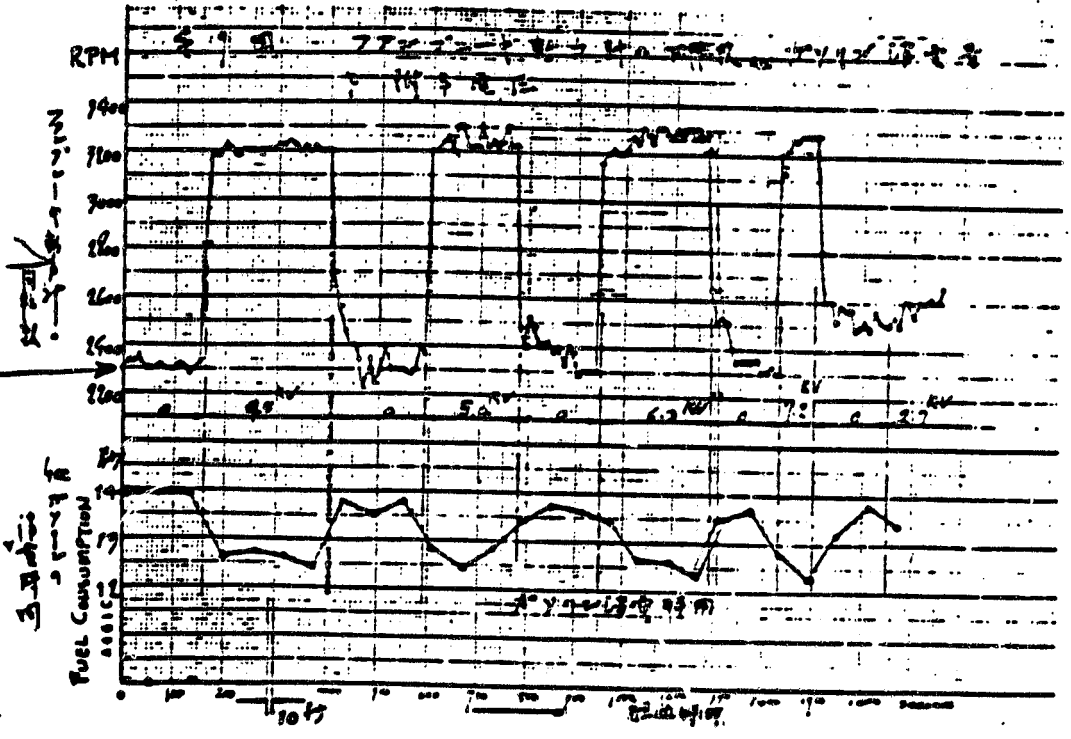

Promotion Of Vaporization By Means Of The Application Of An Electric Field

Prof. Dr. Yukichi Asakawa

Faculty of Technology
Nihon University
Koriyama, Japan

1. Introduction:

In 1956 the author had published several reports on "The Promotion of Combustion by the Application of an Electric Field".(1) The series of photographs in Fig. 1 definitely show that a burning gasoline flame is simultaneously lengthened and broadened by this electric field.

Fig. 2 shows the time required for burning time of 6 cc of gasoline is reduced from 62 seconds to 10 seconds, by the application of an electric field of 15 KV (AC).

Fig. 1 Combustion of Gasoline

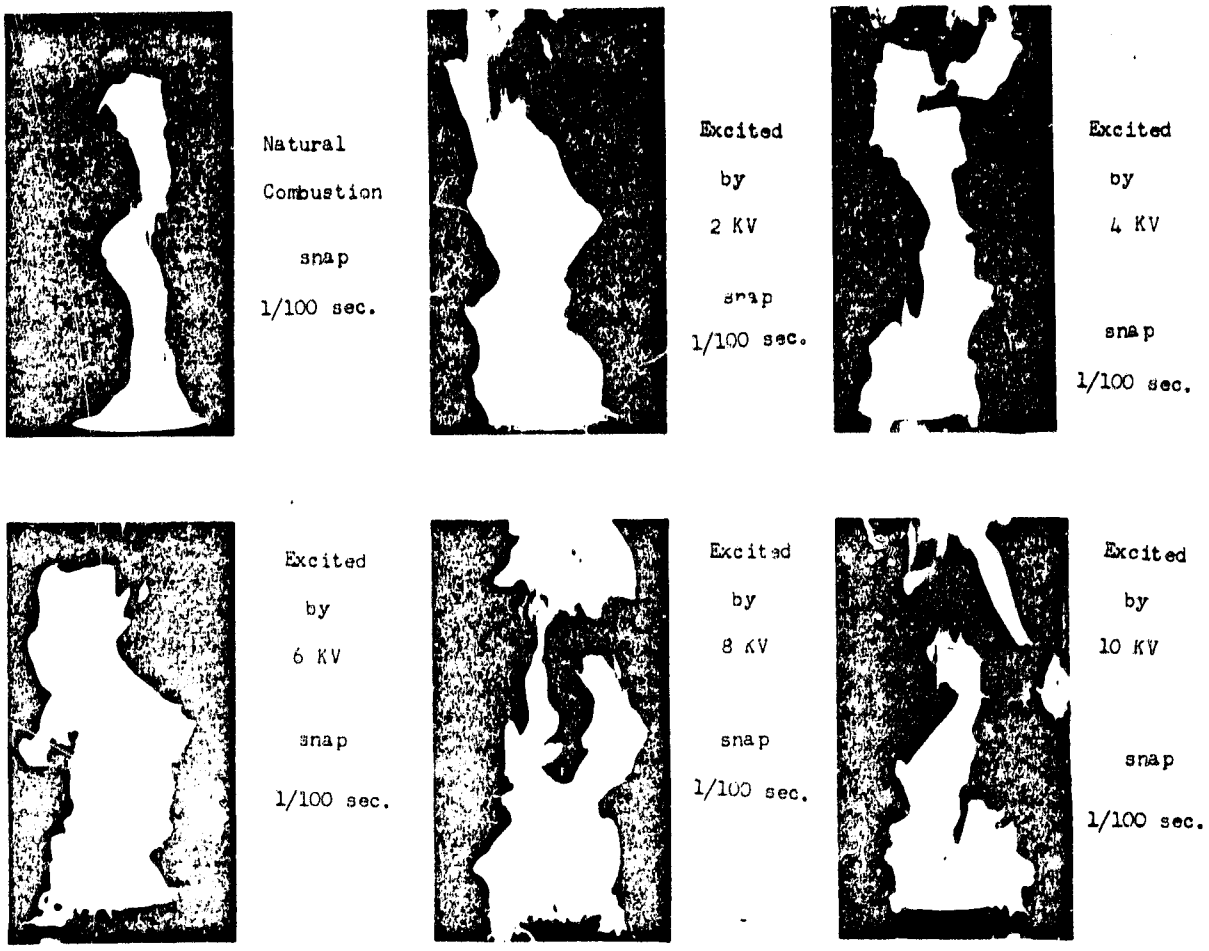

sTs
Ann Arbor, Michigan 48106

STS BIOMED
SCIENTIFIC TRANSLATION SERVICE

NEW METHOD FOR THE PROMOTION OF VAPORIZATION

By Y. Asakawa

General Meeting JSME No. 623 (1965-4), pp. 137-155

Translated from the Japanese
For Bendix Engineering Development Center
Ref. LR80-1085

STS Order No. 20507

NEW METHOD FOR THE PROMOTION OF VAPORIZATION

By Y. Asakawa

Physics and Engineering Department, Nippon University

1. Introduction

Based on the confirmation [1] of the promotion of the combustion rate by electrical field application, this author continued this line of thought as follows: In Fig. 1, (a) shows the natural combustion process, while in cases (b) and (c) a terminal from a high-voltage source placed into the flame applying an electrical field produces an intense effect on the flame with a decrease of the time required to burn a certain volume of fuel, i.e. an increase in combustion rate as shown in Fig. 2; the author postulated that a corresponding increase of vaporization (or evaporation) occurs prior to combustion.

To verify this, the terminal of a high-voltage source was used to measure the vaporization of a combustible fluid, such as gasoline, etc.

A marked increase of vaporization was observed as shown below. Moreover, the increase of vaporization was much greater than that of the combustion rate as seen in Fig. 2, which attained a few multiples of 10 sec. The figure shows that the ratio between the combustion and the vaporization rates is not 1:1; in other words, the increase of the vaporization rate is proportional to that of the combustion rate but not vice versa.

A similar test was applied to study the vaporation of water, salt water, etc. and it was found that the application of an electrical field had a marked influence with an increase of evaporation amounting to several multiples of 10 (at room temperature). In solids (camphor), a similar phenomenon was observed in the form of sublimation.

2. Test System

The system was simple as shown in Fig. 3. A neon-type 360 W transformer was used. The tested fluid was placed into a 200 cc container and a terminal was placed at a certain distance from the surface to measure the vaporization. As shown in the figures, the other terminal and the metal plate holding the container were grounded.

3. Test Results and Discussion

A. Gasoline

A-1 Influence of electrical field application. Commercial gasoline (150 cc) was placed into a 65 diam. x 70 mm iron vessel and the terminal was kept at a distance of 30 mm from the liquid surface; the vaporized volumes were measured at various voltages as shown in Fig. 3. It can be seen that a marked increase in vaporization occurred. Thus, compared to the test at 60 min, these increases were 4.2-fold at 4.5 kV, 8.4-fold at 7.5 kV, 10-fold at 10.5 kV and 11-fold at 15 kV.

A-2 Influence of terminal location. While maintaining the applied voltage at 15 kV, the terminal distance from the liquid surface was varied, producing the results shown in Fig. 4. The vaporization decreases with increasing distance. However, the increase still remains two-fold even at a distance of H = 105 mm.

In a logarithmic plot, the vaporization curve of Fig. 3 becomes a straight line as shown in Fig. 5, i.e.:

$$Q = At^n$$

where Q = vaporization

A = initial vaporization rate

t = elapsed time

The following equations can be obtained from the figure (Table 1).

Table 1

Applied volt.	Empirical equation
Natural vapor.	$Q = 0.1 t^{1.0}$
4.5 KV	$Q = 0.74 t^{0.78}$
7.5 KV	$Q = 1.48 t^{0.91}$
10.5 KV	$Q = 1.0 t^{0.78}$
15.0 KV	$Q = 1.9 t^{0.87}$

Since the lines in the figure are parallel, it is apparent that the value of the applied voltage is not related with the state of vaporization. Moreover, $Q = At^n$ [2] clearly defines A as the initial vaporization rate [3]. When the relation between A and the applied voltage kV was studied, it was found that the two values are related as shown in Fig. 6. Thus, the vaporization rate decreases with time but is proportional to the voltage when considered with respect to the initial rate.

We again studied the relationship between the initial vaporization rate A and the distance between terminal and liquid H. The result is shown in Fig. 7. Thus, the smaller the distance H, the higher the initial rate A in a nearly proportional relationship. This is to be expected, since the influence of the electrical field on the vaporizing liquid will increase with decreasing H.

A-3 Comments:

1) With regard to Fig. 4, the value of A should be studied for cases in which H is extremely small, such as $H \doteq 0$, i.e. with the terminal inserted in the liquid. Although the terminal in the test system was well insulated, no change in vaporization rate was observed. This means that when H decreases, A increases, but when $H \doteq 0$, the vaporization increase suddenly stops and A no longer changes. Consequently, in order to obtain an increase of vaporization, it is necessary for the liquid surface to be located between metal plates.

2) Color change of gasoline (to be explained later): During the test, we observed a change in color of the gasoline. The commercial fuel was pink but with increasing applied voltage and duration of application, this pink color gradually turned brown. Sometimes, the gasoline became milky white but this was explained by the entry of atmospheric moisture into the gasoline due to the marked temperature drop of the liquid to below the dew point caused by the strong vaporization. This was confirmed by the fact that the milky liquid became clear after removal of the electrical field when condensed water was found at the bottom of the container.

This phenomenon of a color change has not yet been studied sufficiently to offer a full explanation [5], but it should be added that a similar phenomenon, the formation of cloudiness, was observed also with water, alcohol, benzene, etc.

B. Alcohol

A similar test was run with alcohol. Fig. 8 shows an example with H = 10 mm.

It was found that when the applied voltage was 0-5.0 kV, no increase of vaporization occurred but as 5.5 kV is approached, the increase occurs suddenly and continues with increasing voltage.

As can be seen in the figure, the vaporization curve is a straight line contrary to that for gasoline. The rate of increase in vaporization (rate) is marked, attaining a 62-fold value with an applied voltage of 10 kV. Fig. 9 (a) shows the relationship between the rate of increase of the vaporization and the applied voltage. Fig. 9 (b) shows another test result. It is worthy of note that (b) is relatively higher than (a), presumably due to the lower temperature involved, but at any rate, the increase of vaporization by a factor of 60-plus with an application of 10 kV must be noted. Generally, in an atmosphere at room temperature, the vaporization process changes considerably as a function of temperature and humidity. Therefore, some discrepancies are inevitable in the vaporization measurements. In Fig. 10, H' = 10 and H' = 10 [sic], differ fairly significantly but compared to the above-mentioned H = 10, they are only 1/5-1/10 of that value.

sample temperature should be controlled

humidity control could be avoided by evaporation at reduced pressure? probably not!

dry air flowing over the surface?

C. Naphtha

Fig. 11 shows this test. It was carried out with H = 10 mm and the vaporization curve obtained is clearly a straight line as in the case of alcohol shown in Fig. 8. The temperature decreases due to vaporization were 5.5° and 10.5% for 8.1 and 10 kV, respectively. This temperature drop is considered to be due to insufficient heat absorption from the atmosphere over the latent heat as a result of the enhanced vaporization. Therefore, the measured increase of vaporization indicated that when the temperature decreased to below room level, the vaporization increase would become proportionally smaller; therefore, with a renewed temperature rise, the vaporization should also increase. At 10 kV, a 31-fold increase of vaporization was seen. Tests at other voltages and H = 5 also showed a marked increase of vaporization. Fig. 12 shows a proportional relationship between the increase of vaporization and the applied voltage both at H = 5 and H = 10 mm.

Returning to Fig. 11, a comparison of the temperature decrease and voltage shows 5.5° and 10.5° for 8.1 and 10 kV and a corresponding 18- and 31-fold increase of the vaporization rates. It is interesting to note that the ratio

between the temperature decreases of 5.5:10.5 is similar to that of the vaporization increase of 13:31.

D. Water

The influence on evaporation was also studied in tap water at various temperatures (7-10°). The results are shown in Fig. 13. In the figure (a) applies to H = 10 and (b) to H = 20; in both cases, the evaporation is linear as in the case of alcohol and naphtha.

The reason why the effect with water does not appear until the voltage attains 6.0 kV, in contrast to the case of gasoline, alcohol and naphtha, is that water has a lower electrical conductivity [7] and is more stable, making the occurrence of the evaporation effect more difficult. We then sought a relationship between the rate of increase of evaporation and the applied voltage, leading to the results shown in Figs. 13 and 14.

The general pattern of the evaporation increase is similar to that of alcohol shown in Fig. 9, but the actual values are 1/2.5 times those for alcohol. Fig. 15 shows the evaporation curves at 17-22°. The elapsed time was 72 h at the maximum and the curves are not straight but have a slope of $Q = At^n$ (n = 1.00-1.4%) which also applies to gasoline. Fig. 16 shows the relation between the rate of increase [8] and the applied voltage. When this is compared to the maximum increase of evaporation, the former is 18 times greater and the latter 28 times; this 1.6-fold difference is believed to be caused by the temperature differences in the tests [9]. When we examine Fig. 16, we find a step in the curve where the effect of increasing kV values stops; this can be recognized also in Fig. 14 and has been pointed out as being similar to an "electro-optical effect [10]."

We then investigated the considerable differences of these results even though the tests were conducted under similar conditions. Two groups of evaporation curves in Fig. 17 show that the variations with the applied voltage are not as different from each other as those for natural evaporation, with the following increases:

Solid lines: 14-fold (10 kV), 20 fold (12 kV);

Broken lines: 5.5-fold (10 kV), 8-fold (12 kV).

This was mentioned in connection with Fig. 10 for alcohol and is repeated here. Consequently, unless the temperature and moisture are well controlled in a long-term test of the influence on evaporation, a considerable scatter of the test results must be accepted. Fig. 18 shows a number of results of long-

term tests at 7-10° and at 17-25°. Based on a series of short-term tests, this figure indicates the increase of evaporation in proportion with the field strength as was seen in Fig. 12 for benzine, although those at 17-25° for the longer-term tests show a marked degree of scatter.

In summarizing all of these results, it can be concluded that a 9-28-fold increase can be expected with 15 kV at 7-25°. In the case of the tests at 7-10°, the temperature difference was only 3° and the moisture was maintained at 40-50%, i.e. the nearly constant conditions might have produced the regular test results.

E. Salt Water

Tests were run with 10% salt water using ordinary table salt. Fig. 19 shows the results indicating an increase of only 1/3.5 times compared to Fig. 14 at 15 kV. Here again phenomena similar to an electro-optical effect as in Fig. 14 can be seen and the effect ceases again with increasing voltage. Fig. 20 shows the evaporation curves used to plot Fig. 19. Fig. 20 shows three curves for 12 kV, zero kV and removal of the field. The following equations apply to these curves:

Applied field: $Q = 0.18\ t$

No field: $Q = 0.09\ t^{0.78}$

Evaporation after field removal: $Q = 0.004\ t^{1.15}$

It can be seen from this figure that the results of Fig. 19 apply to the evaporation increase after 150 h and reveal the increase of evaporation of salt water with application of an electrical field and the decrease of the process when the field is removed. In this case, the decrease of evaporation was interpreted as a dielectric after-effect [11]. It should also be noted that the evaporation of this 10% salt solution is 3-fold at 4 kV. This may be compared with the results of Figs. 13 and 14 which show that the first increase of evaporation occurs at 6-7 kV. This is attributed to the fact that salt water is an electrolyte and the effect therefore occurs at a lower field strength than with water, i.e. compared to a neutral electrolyte, it is affected more readily by static electricity, causing an increase of evaporation.

F. Benzene C_6H_6

The influence of an electrical field was also studied in benzene. The test temperature was 24-30° with a humidity in the range of 50-85% because of the summer season. Fig. 21 shows the results of a study with H = 10 mm for

the distance of the terminal to the liquid; the data show marked scatter. Despite this variation, we can summarize the results by the statement that at 15 kV, vaporization can be expected to increase 10-fold as a minimum to a maximum of 65-fold.

4. Test Results

A.1 The increase of the evaporation of water and influence of temperature were studied with the arrangement shown in Fig. 22; two 200 cc beakers were kept in a constant-temperature vessel and the evaporation from the two beakers was measured in order to determine the temperature effect. An opening was made in the top of the container to allow the vapors to escape. The applied voltage was kept at 15 kV and the temperature was varied from 15 to 90°. The result confirms the above formula: $Q = At^n$.

The A and n values at each temperature are listed in Table 2, showing that A increases markedly with the applied voltage, while n changes little, remaining approximately 1.0. The latter finding explains the approximately parallel logarithmic evaporation curves.

The increase in evaporation rate obtained from these logarithmic curves (not shown in this paper) is 50-fold at 15°, 24-fold at 25°, and 6.2-fold at 40°. The variation of the rates of increase are shown in Fig. 23 as a straight logarithmic line. With μ as the rate of increase [13], the following relationship is evident from this figure:

$$\mu = 95\ T^{-1.80}, \text{ where } T = \text{test temperature.}$$

For the A values, a logarithmic relationship as shown in Fig. 24 was found.

Therefore, we have:

For natural evaporation: $A = 0.000011\ T^{5.67}$

With electrical field (15 kV): $A = 0.0129\ T^{2.75}$

The finding that a certain relationship exists between the increase of evaporation with application of an electrical field, the initial evaporation rate and the temperature is important. For evaporation alone, a 1.6-fold increase can be expected at 100° which becomes 95 at 10°. Compared to the initial evaporation rate, it is a 1,100-fold increase at 10° but only 2.2-fold at 100°. In other words, compared to 100°, the initial evaporation increase is 2.2-fold greater, but after 150 min, the increase is 1.6-fold.

A.2 Increase of evaporation of water (continued) -- influence of electrical field: This subject was covered in Figs. 15 and 16, but some additional details follow.

In the logarithmic plot in Fig. 15, the evaporation curves were straight lines and are represented by the equation $Q = At^n$. As shown in Fig. 25, a linear relationship $A = B.V^{5.14}$ (B = constant) exists between A and the applied voltage.

By extrapolation, A = 1.3 with kV = 15 according to Fig. 25. When we convert g/h to g/min, A = 0.030. This result agrees well with the value A = 0.034 obtained by interpolation of Fig. 24.

This agreement of values obtained in two calculations confirms the reproducibility of the effect of the electrical field.

A.3 Example of boiling water: A similar test was run with boiling water. The same test system as above was used and the 200 cc beakers were heated on a Bunsen burner as shown in Fig. 26. The applied voltage was 9 kV and H was 15 mm.

In this figure, the dash-dot line applies to a small flame and the triangle-dash line to a relatively large flame; after 30 min, the latter showed a 23% increase, while the former shows a 63% decrease, contrary to expectation. Although these results are surprising, further study indicated that they were to be anticipated, i.e. in the latter case, the water temperature decreases instantaneously from 99.5° to 95° [14] and the evaporation process does not show an increase even under the influence of the electrical field. The enhancement of evaporation by application of an electrical field naturally needs an increase of the latent heat of evaporation but if the heat supply from the burner is not sufficient, the temperature of the liquid drops. When the temperature of the liquid decreases from 99.5° to 95°, even though the evaporation at this temperature increases with the field application, there is a decrease compared to 99.5°. Therefore, when the flame is made larger to produce sufficient heat to enhance evaporation, i.e. when there is no temperature drop, application of an electrical field allows us to expect an increase of evaporation and the triangle-dash line of the figure confirms this reasoning. Thus, the two lines of the figure seem to be contradictory, but essentially have a similar trend except that the experimental conditions are different.

In connection with the above phenomena, we need to recall the results for benzene in Fig. 10. Here, even with a 10° temperature decrease, the evaporation

increases 31-fold. Thus, even with this 10° temperature drop, which causes the vaporization to decrease, application of the electrical field enhanced the vaporization process 31-fold. The difference between the two tests is only that between water and benzene but the results are essentially the same. These two tests shown in Fig. 26 and Fig. 10 are representative in demonstrating the increase of vaporization by application of an electrical field.

B.1 Salt water in various concentrations at normal and constant temperature: We next investigated the effect on evaporation in salt water at normal temperature. An evaporation curve was plotted with an applied voltage of 15 kV. In each case, the results corresponded to the equation $Q = At^n$. When we look for the rate of increase after 1000 min, we find a linear decrease as shown in Fig. 27. When we compare this with Fig. 19 for salt water, we find an 8-fold increase in the latter, while it was 15-fold here; this is considered to be due to the temperature difference. In Fig. 27, the reason for the decrease in the rate of evaporation with increasing concentration is assumed to be the result of the gradual change in electrolyte strength with concentration.

B.2. Salt water, sugar solution, at boiling temperature: We now studied two solutions i.e. a 10% salt and a 10% sugar solution, for the effect of an electrical field application at boiling temperature. An example of the results is shown in Fig. 28. This was obtained with an applied voltage of 12 kV, showing the following increase of evaporation after 20 min:

Salt solution:	58% increase
Sugar solution:	20% increase

The increase for the salt water is approximately 3 times that of the sugar solution as a result of the electrolyte strength.

C. Camphor (Solid)

A test was run for a solid. Camphor plates of 5 x 30 x 30 size were used. The terminal-specimen distance was H = 30. In this case again, the increase in vaporization rate, i.e. the sublimation rate, was clearly evident. Fig. 29 shows the result with an applied voltage of 10 kV. The increase of vaporization with application of the field was approximately 8-fold.

This test confirmed the enhancement of vaporization (i.e., sublimation) by application of an electrical field in a solid. Since it is known that

solids have a vapor pressure, i.e. a vaporization capacity, this enhancement of vaporization in a solid is logical.

D. Summary of Tests

In the simple enumeration of the tests above it becomes clear that the enhancement of vaporization by application of an electrical field was confirmed in both liquids and solids. Under controlled test conditions, it will be possible to determine new methods for evaporation, vaporization, distillation, concentration, drying and dry distillation. It should be added that the method only represents one part of the enhancement of evaporation and vaporization, since an increase of heat capacity which allows this increase in evaporation rate must be supplied. The method does not directly attempt to obtain an improvement of heat economy. In summary, only an improvement of the efficiency of vaporization and evaporation equipment and an increase in production rate can be expected. The electrical current for application of the field is minimal.

5. Discussion of Tests and Related Phenomena

5.A Comments on Tests

1. Evaporation rate. Generally, the evaporation rate of a material is said to be proportional to the vapor pressure of the substance [19] but when the vaporization capacity itself is studied, its dependence on surface tension needs to be taken into account. Therefore, it can be reasoned that if a method to decrease the surface tension is obtained, it may be expected that evaporation will increase, although whether this can actually be accomplished is another matter.

2. Decrease of surface tension in an electrical field. Pohl [18] has represented the decrease of surface tension when a liquid is placed into an electrical field as follows:

$$p_e = \frac{\varepsilon_0}{2} \frac{V^2}{r^2} ,$$

should be possible to study surface tension

where p_e = pressure acting to decrease the surface tension,
ε_0 = dielectric factor,
V = voltage, V
r = distance

This equation indicates that when a liquid flows through a capillary it will form form droplets in the absence of an electrical field but flow in a stream under the influence of the field, and this should be a basis for an explanation of the enhancement of vaporization if the decrease of surface tension is confirmed for a liquid surface under the influence of vaporization.

3. Relation between enhancement of combustion and of evaporation. Some results were obtained from preliminary tests on the enhancement of combustion by application of an electrical field. Thus, with the use of the method [19] in which one terminal is inserted into the flame, a marked 4-5-fold increase of combustion rate was found as shown in Fig. 2 and the increase of vaporization preceding combustion was noted as the cause of this phenomenon. The present tests were run under the same conditions as the combustion test in order to study only the vaporization and evaporation process without ignition and they confirmed the enhancement of these processes, with an increase more than 10 times that of the combustion rate in the case of gasoline.

This great difference between the increase in rate of combustion and of evaporation leads us to conclude that the enhancement of vaporization is a prerequisite for that of combustion, but that an enhancement of combustion does not enhance the vaporization process. In other words, combustion can not follow vaporization, since the time needed for combustion is longer than for vaporization. Therefore, the combustion seen in Fig. 1 can be viewed as a continuation of the process while abnormally strong vaporizing effects induced on the liquid surface are suppressed.

B. Relative Phenomena

1. Application of magnetic field with electrical field - increase of vaporization. The results shown in Fig. 30 were obtained in a study of whether the simultaneous application of magnetic and electrical fields would enhance vaporization. The vaporization curves show a 4-8-fold increase with elapsed time with 8 kV applied voltage, while the application of a magnetic field at the same time added 11% to this increase. The effect of a magnetic field is much smaller than that of an electrical field.

However, since only a small-size 10 x 10 x 30 MK-type permanent magnet was used in this test, a more prominent influence can be expected with the use of a stronger magnetic field.

2. Decrease of vaporization - influence of residual electrical field. In connection with Fig. 30 we should also note the pattern of the vaporization

curve when the electrical field is removed. It is clear that vaporization after removal of the field is weaker than natural evaporation. Furthermore, the gradient of the curve, i.e. the vaporization rate, is considerable compared to that of natural evaporation. These phenomena may be considered to be the effect of a residual field. These results were also seen in a test with salt water shown in Fig. 20.

3. Color change of gasoline. As mentioned, in the test with commercial gasoline, the author observed a change from its pale pink color to brown. When the electrical field is relatively strong, i.e. above 8 kV, the pink color begins to darken with time. Fig. 31 shows a color reproduction. At 10 kV, the color turns brown in 30 min, while at a voltage below 5 kV, no color change occurs even after prolonged exposure. At times, the gasoline turned a milky white in a strong electrical field which was caused by mixing in of fine droplets of atmospheric moisture at the surface of the liquid where a marked temperature drop to below the dew point occurred with the enhanced vaporization; this was not identical to the color change noted above. This was confirmed when the liquid was allowed to stand for a period during which it recovered its transparency, while condensed water droplets could be observed on the bottom of the container.

4. Clouding of colorless transparent liquid. This phenomeonon was similar in gasoline, water, alcohol and benzene in which a certain clouding developed after prolonged electrical field application. This might be one of the effects of the electrical field [20] similar to the color change of gasoline which can be considered in relation with the decrease of evaporation.

5. Special location of terminal. As noted in connection with Figs. 4 and 7 relating to the location of the terminal for electrical field application, the effect on vaporization is greater with increasing proximity of the terminal to the evaporating liquid; a test was run to study this effect with the terminal inserted in the liquid. No influence on vaporization was seen and it may be assumed that the field effect on the process requires a liquid surface to be placed between 2 metal plates to form a capacitance. Insertion of the terminal into the liquid suppresses the electrical capacitance and the electrical field.

6. Conclusion

In summarizing the above discussion, we arrive at the following conclusions:

A. Information Related to a New Method for Increasing the Evaporation and Vaporization of Liquids in General

1. A relatively low voltage of 10-15 kV (ac) resulted in an increase of evaporation multiplying it by a few to several dozen times.

2. In general, the rate of increase of vaporization can be described by $\mu = \cdot V^n$, $\mu = \cdot T^{-n}$, where V is the applied voltage and T is the operating temperature.

3. In general, the vaporization curve is given by $Q = At^n$ regardless of the electrical field and the effect of the electrical field on A can be expressed by $A = o.V^n$.

4. Whenever vaporization increases by application of an electrical field, the degree of vaporization after removal of the field is smaller than the natural evaporation process. The influence of a residual electrical field on evaporation was demonstrated.

5. The influence of the field on liquids was verified in solids. The same effect was observed in coal at high temperature (above room temperature), i.e. as in dry distillation.

B. Expected Increase of Production in Evaporation, Distillation, Condensation, Drying and Dry-distillation of Liquids in General

In closing, the author wishes to express his gratefulness for the assistance of Nissan Auto Co., Aitoh Sharyo Co. and Teijin Co., for the counsel of Director T. Maeda, Nissan Auto Co. and Dr. M. Hotta, former head of Denki Shikenko and everyone at his laboratory engaged in this test and to Assist. Prof. K. Sugiura, Tokyo Toritsu Kogyo College.

Oct. 1964

References and Notes

[1] Preprint No. 302, 1964, Conference paper; Preprint No. 417 Sapporo National Conference, Oct. 1964.

[2] T. Kuwata: Solvents. Marusen Press, p. 30.

[3] In $Q = At^n$, $t = 1$, $A = Q/1$.

[4] From $Q = At^n$, $dQ/dt = An\ t^{n-1}$ $(n < 1)$.

[5] To be discussed elsewhere.

[6] By extrapolation of Fig. 7.

[7] The electrical conductivity coefficient of water is higher.

[8] Since $n = 1$, the increase of evaporation was calculated with respect to 6 h.

[9] 7-10° in Fig. 14, 17-22° in Fig. 16.

[10] See Physics textbook.

[11] Dielectric after-effect.

[12] This may be related with the slight clouding (see later).

[13] Obtained from a comparison of the amount evaporated at 150 min.

[14] Actually decreases from 99.5° to 95° in 10-20 sec.

[15] Enhancement of vaporization was observed already with naphthalene, benzoic acid and dry distillation of coal.

[16] Means coal of [15].

[17] Intern. Critical Tables, Vol. 5, p. 54.

[18] R. W. Pohl: Textbook of Electricity. Springer, 1957, p. 42.

[19] See [1].

[20] Currently under study.

Fig. 1. (a) Natural combustion (b) 4KV (c) 9KV

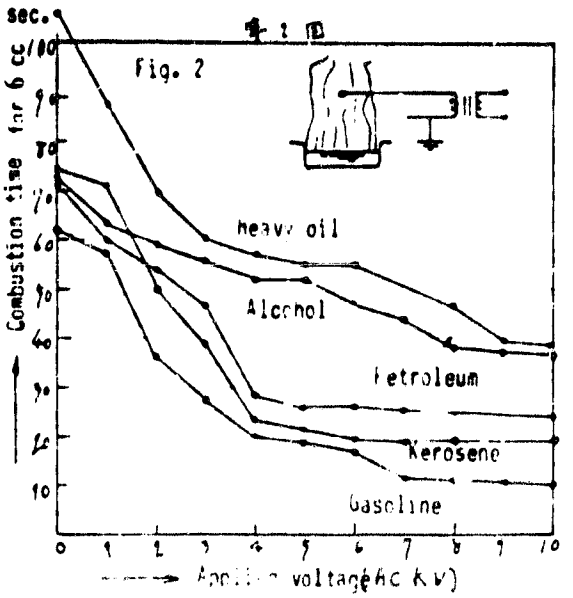

Fig. 3. Vaporization - elapsed time (influence of electrical field)

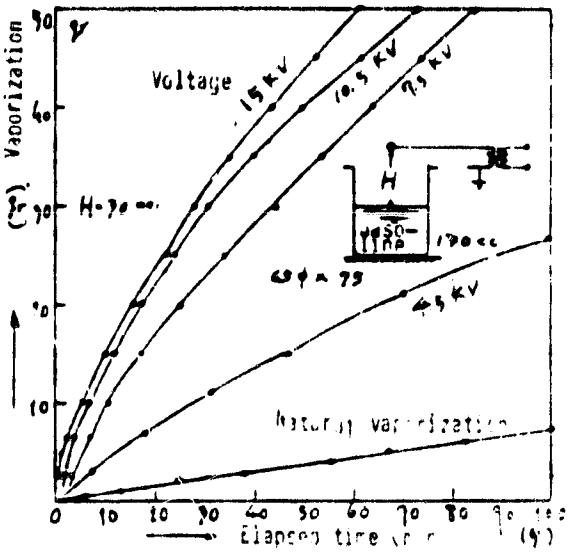

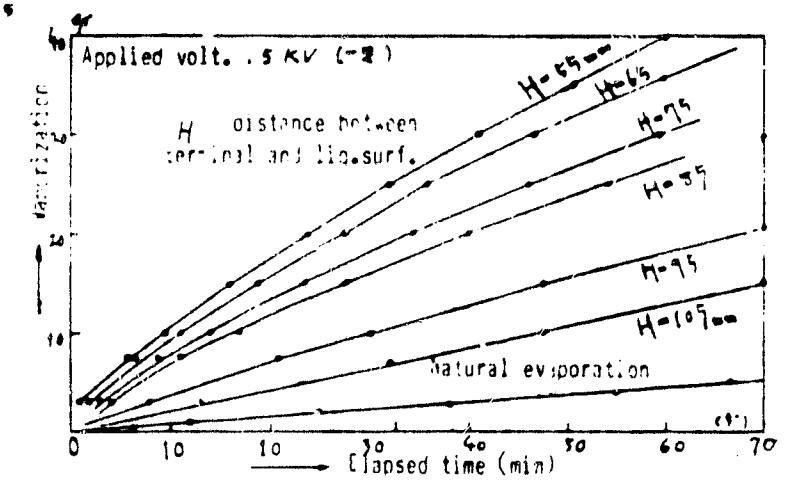

Fig. 4. Vaporization - elapsed time (influence of terminal location).

Fig. 5

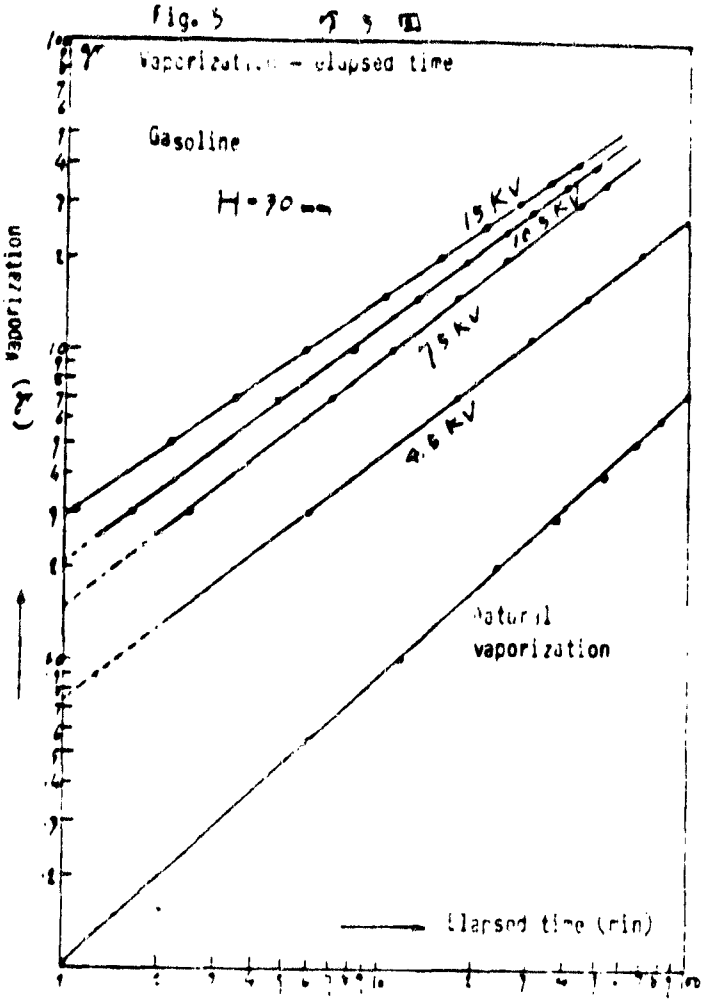

Fig. 6

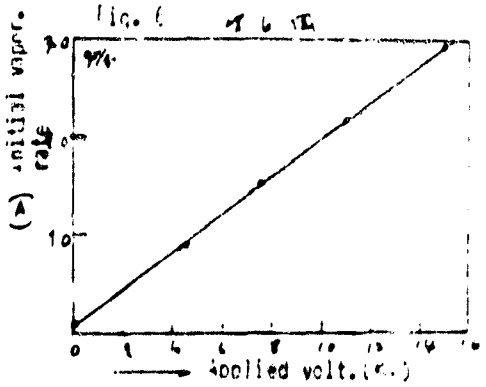

Fig. 7

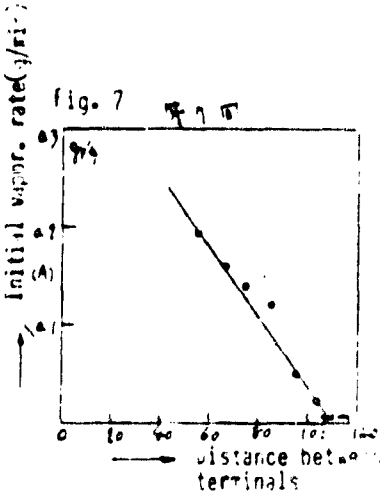

Fig. 8. Evaporation of alcohol.

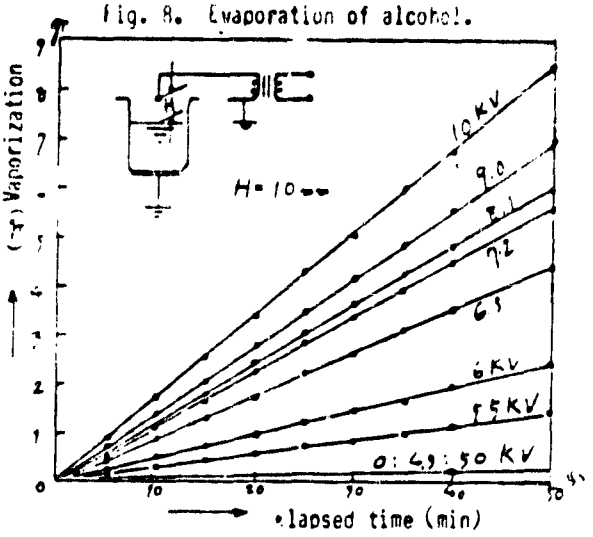

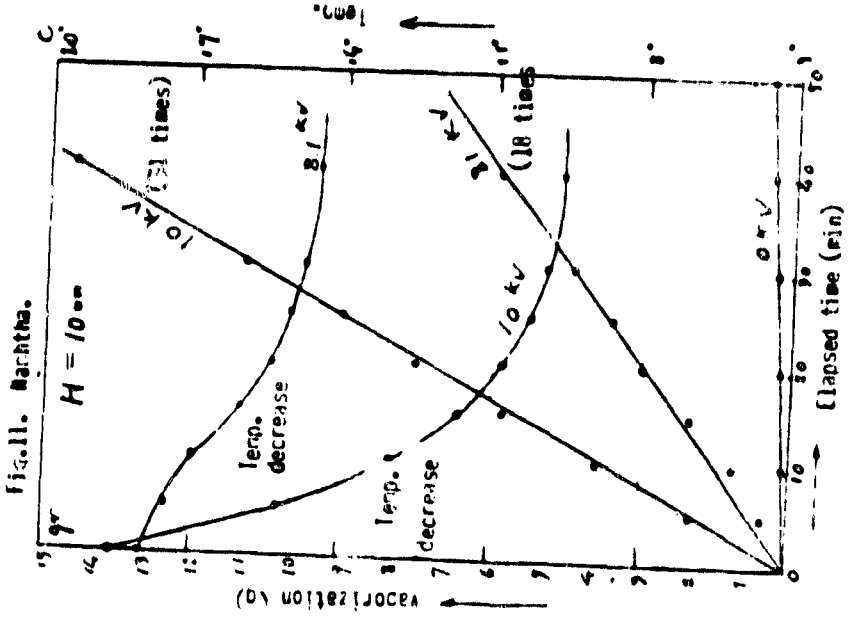

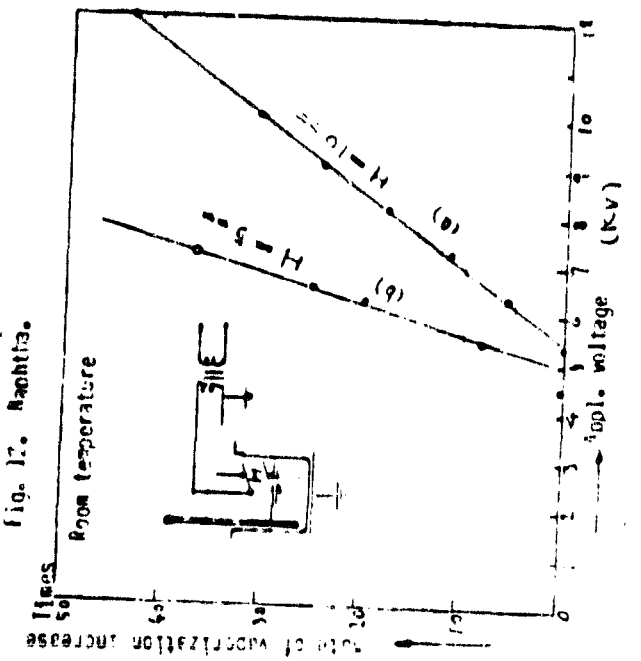

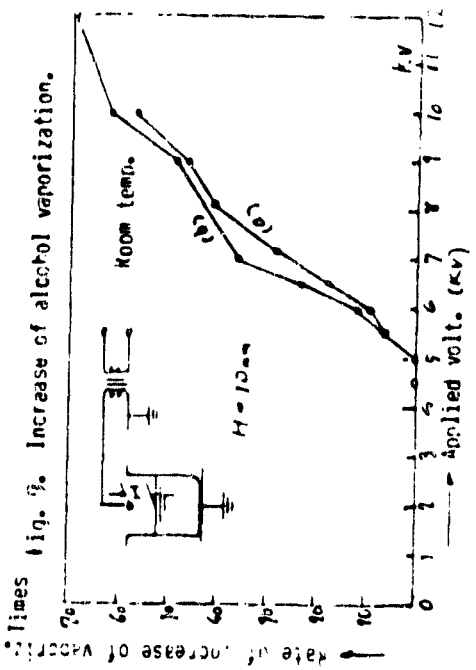

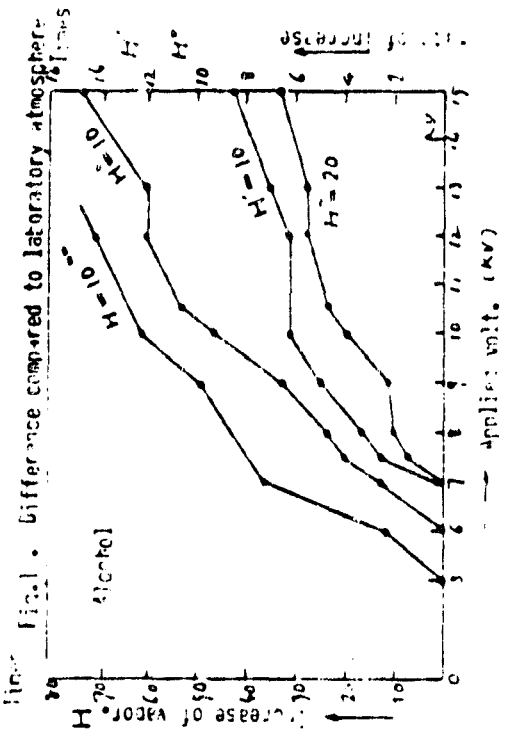

Fig. 13 (a) Evaporation of tap water

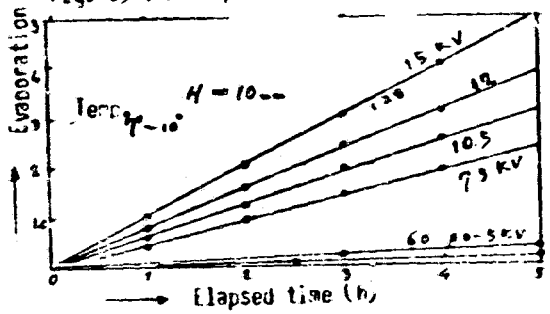

Fig. 13(b) Evaporation of tap water

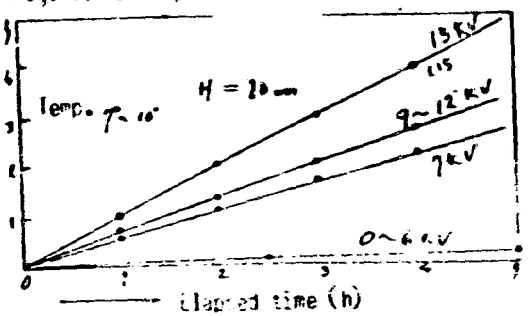

Fig. 14. Tap water

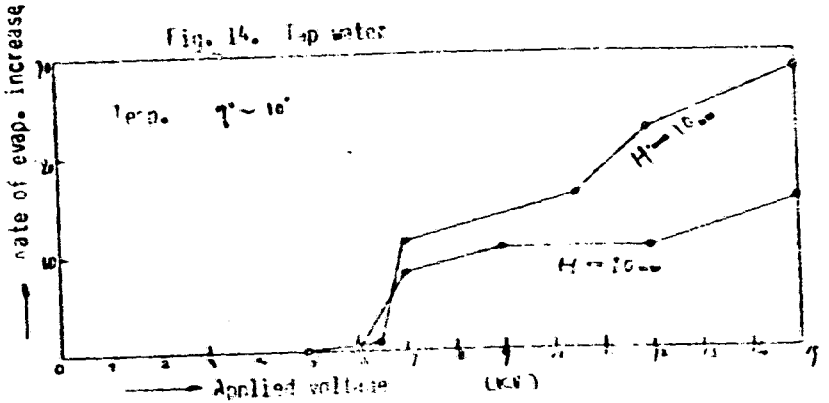

Fig. 15

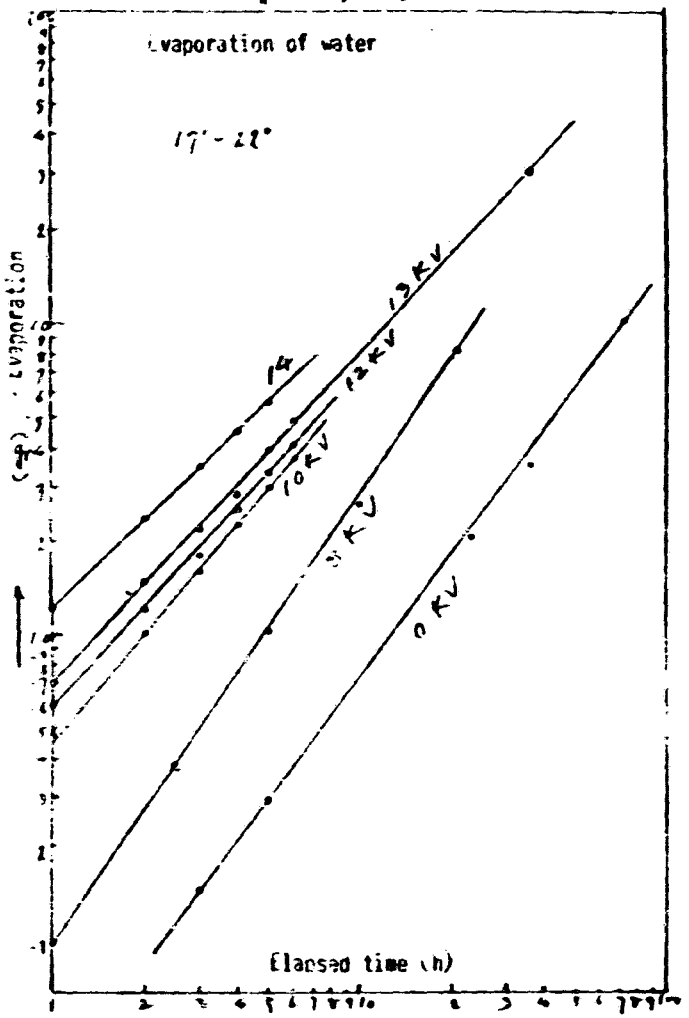

Fig. 16

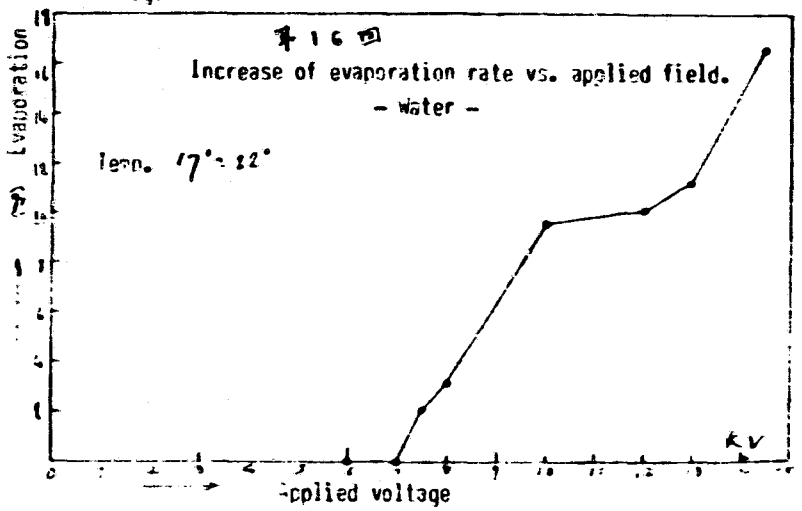

Fig. 17

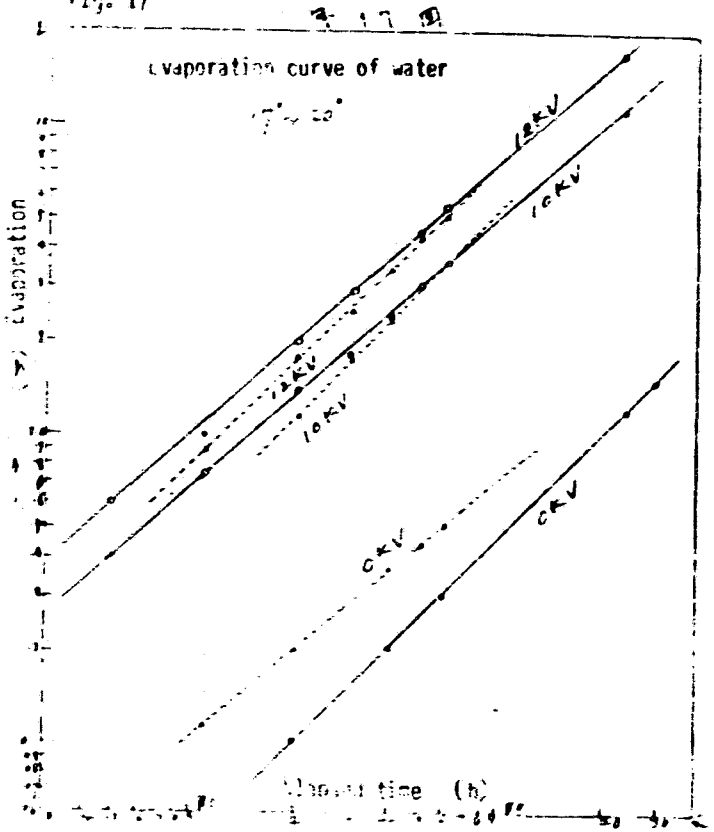

Fig. 18

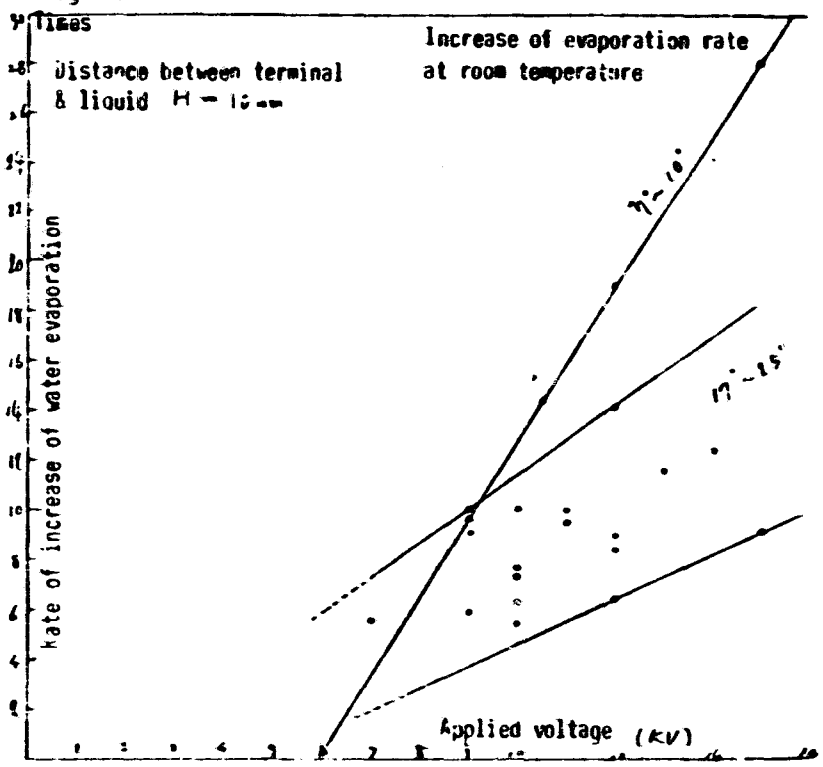

Fig. 19

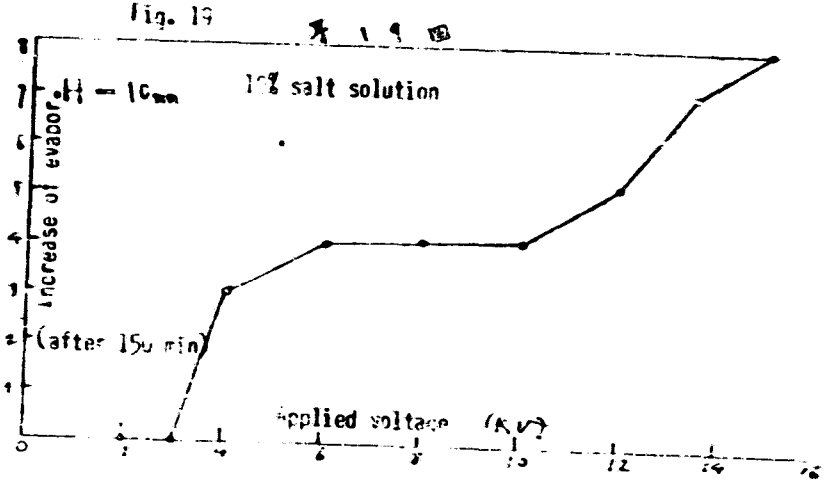

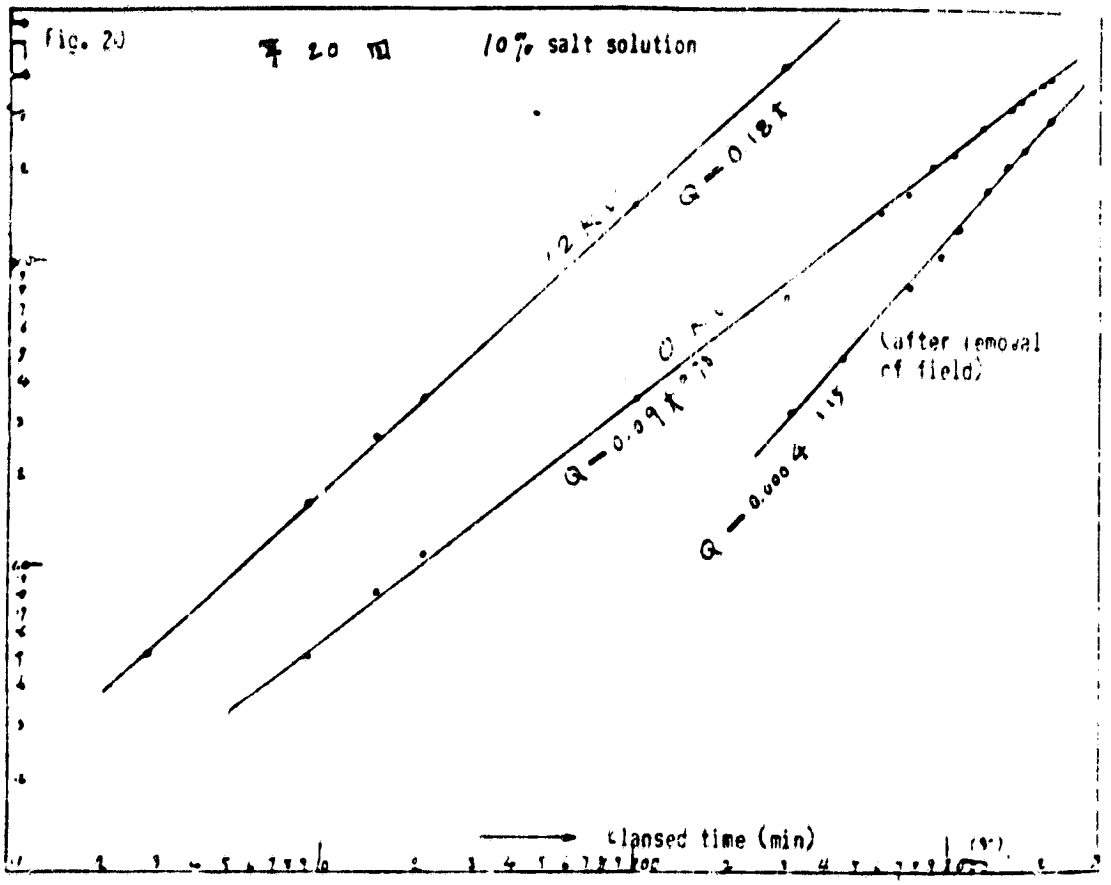

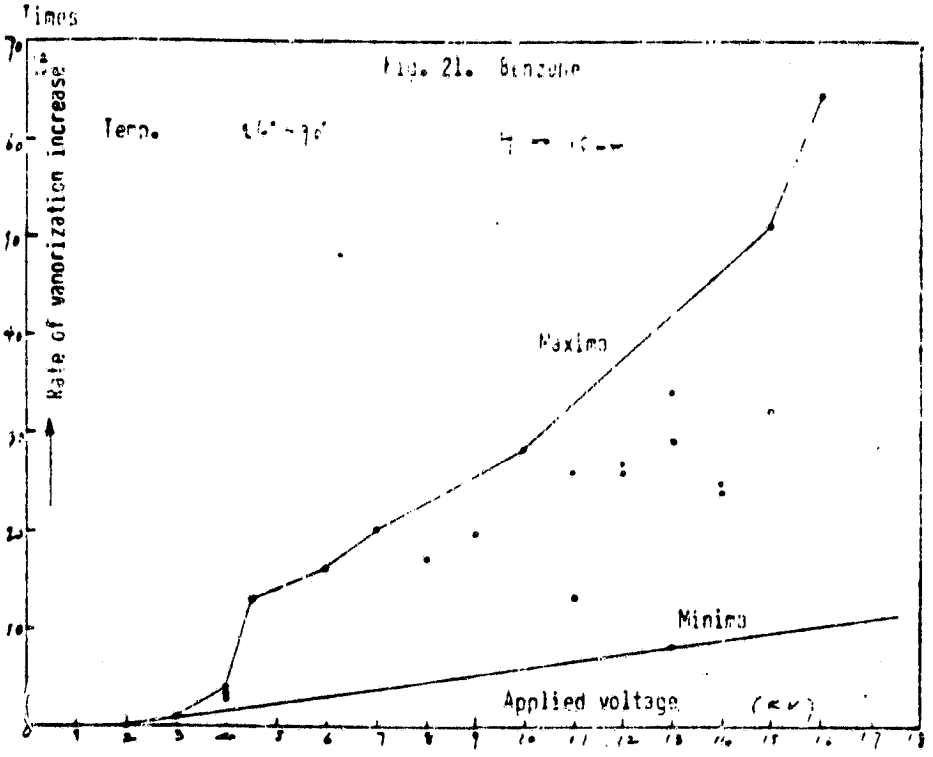

Fig. 22.

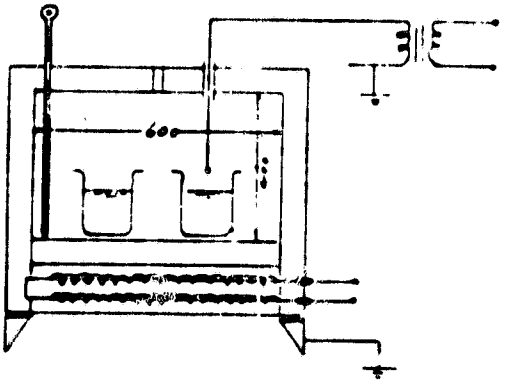

Fig. 23.

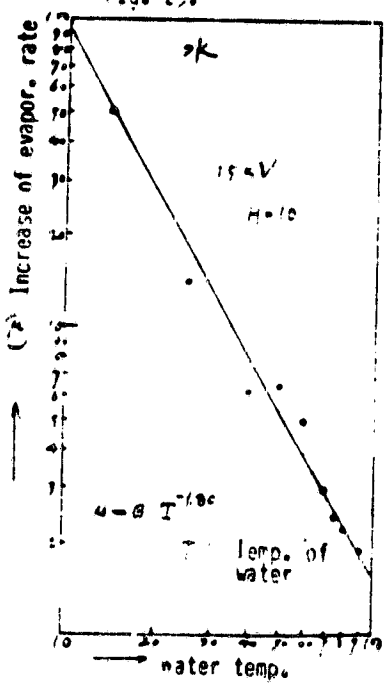

Table 2.

Test temp.	Natural evapor.		15 KV	
°C	A	n	A	n
15°	0.00019	1.48	10° 0.014 30° 0.106	0.93 1.19
30°	0.00040	1.19	0.62	0.70
40°	0.013	0.79	0.90	0.70
50°	0.10	1.00	2.82	0.93
60°	0.14	1.15	1.83	0.93
70°	0.36	1.19	3.10	0.81
80°	0.51	1.00	3.0	1.07
90°	1.19	1.00	4.1	0.74

Fig. 24

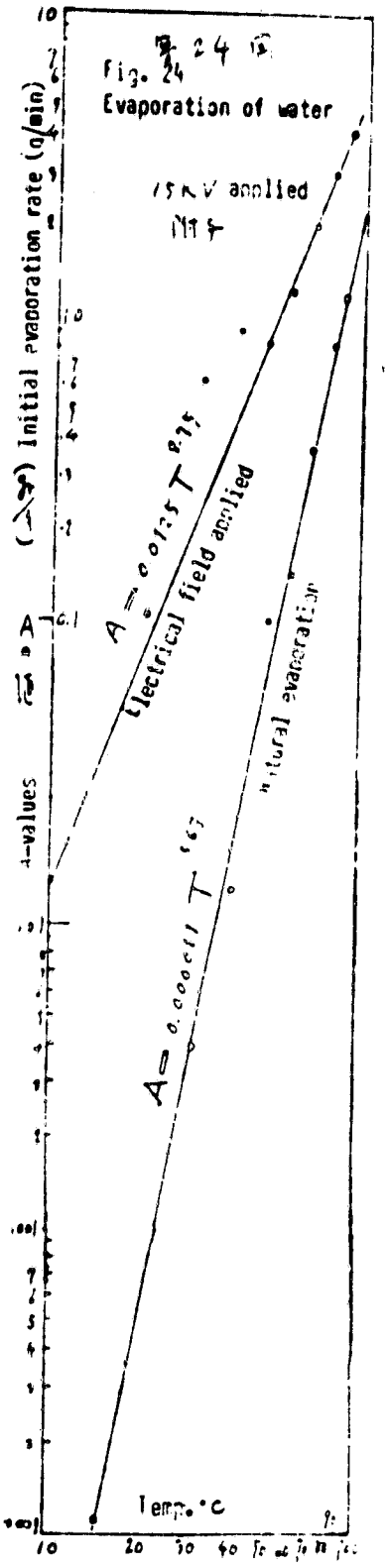

ORIGINAL PAGE IS
OF POOR QUALITY

Fig. 25.

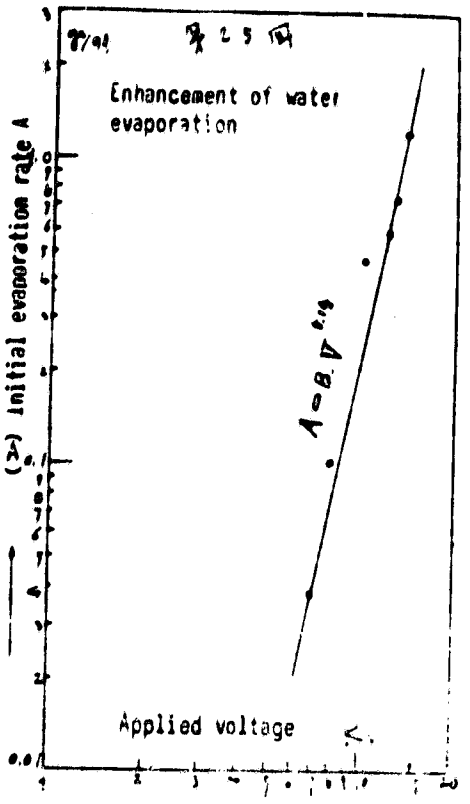

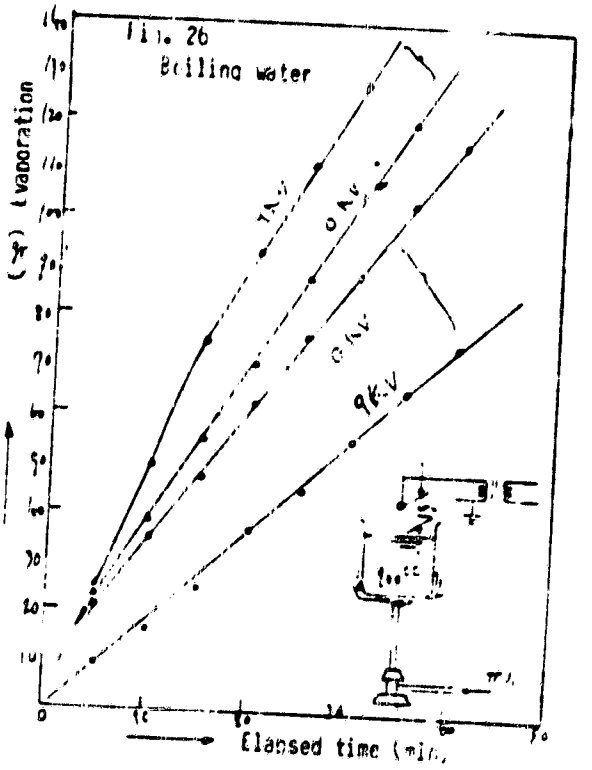

Fig. 27

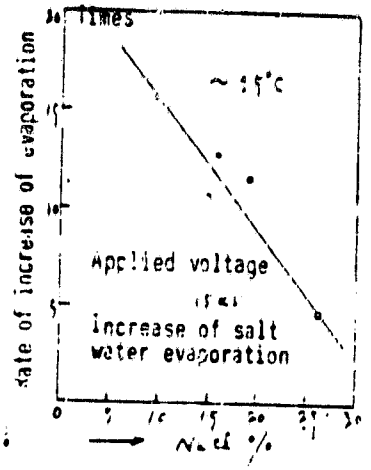

Fig. 29

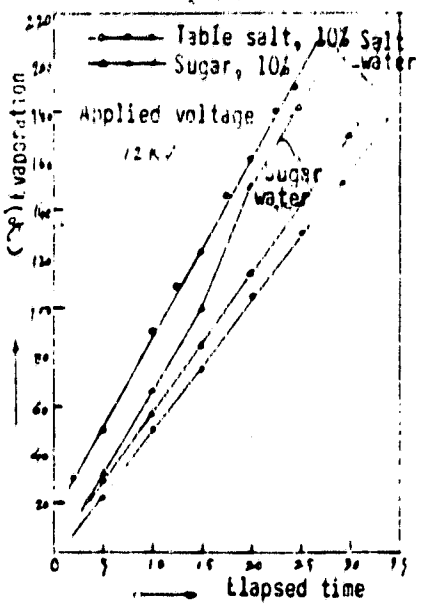

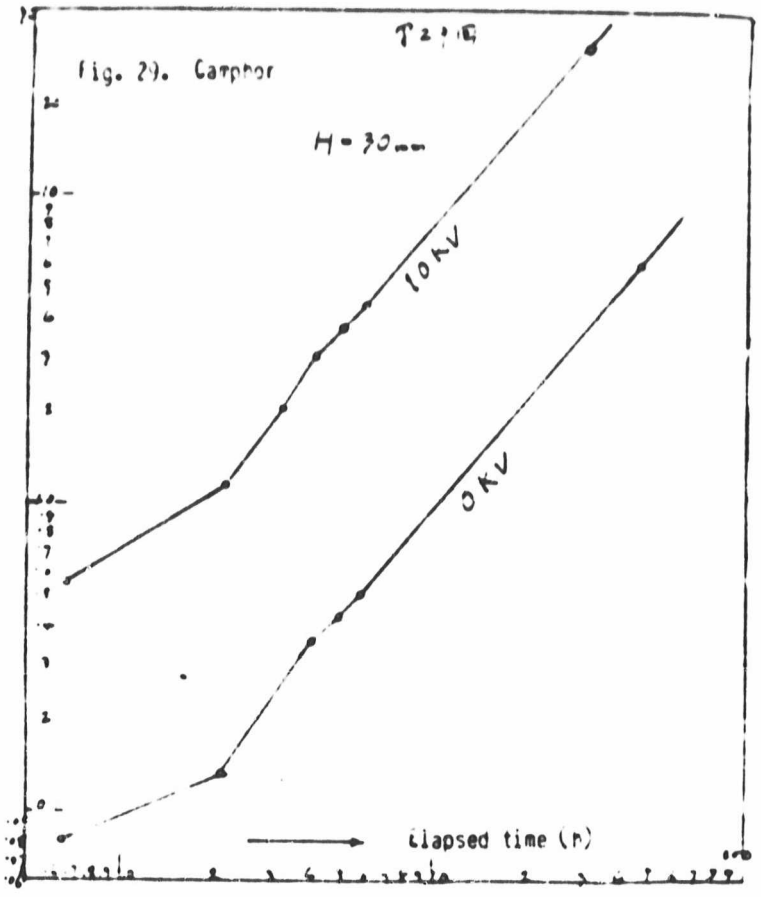

Fig. 29. Camphor

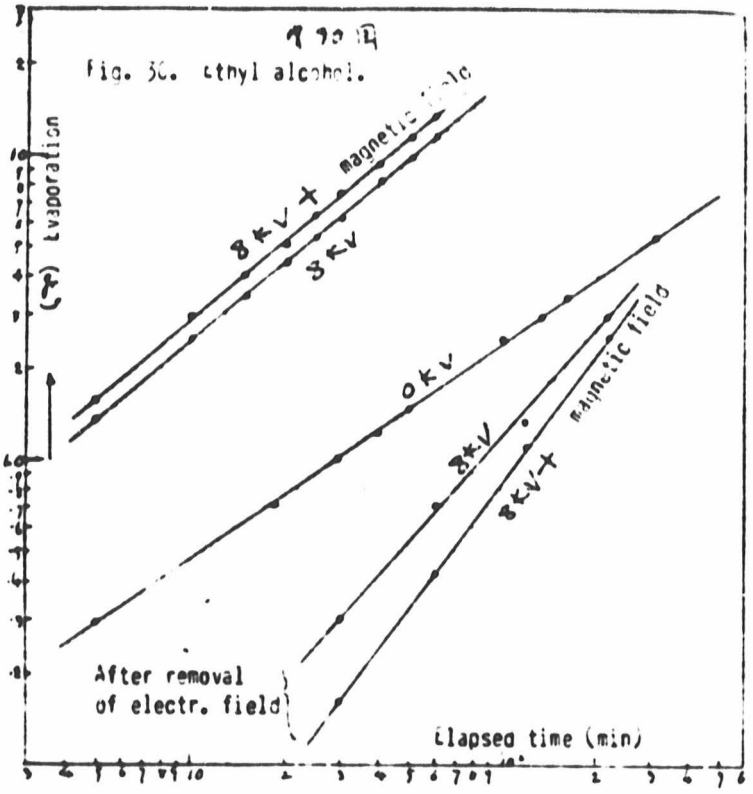

Fig. 30. Ethyl alcohol.

Color change of gasoline

A as received
B 10 KV
C
D
E 8 KV

STS
Ann Arbor, Michigan 48106

STS 80301D
SCIENTIFIC TRANSLATION SERVICE

IMPROVEMENT OF COMBUSTION IN INTERNAL COMBUSTION ENGINES BY APPLICATION OF AN ELECTRICAL FIELD

By Yukichi Asakawa and Setsuo Tomita

Japan Society of Mechanical Engineers (JSME),
Shimizu Meeting, No. 700-9, pp. 25-32 (1977-7)

Translated from the Japanese
For Bendix Engineering & Development Center
Ref. LR80-1085

STS Order No. 20506

IMPROVEMENT OF COMBUSTION IN INTERNAL COMBUSTION ENGINES BY APPLICATION OF AN ELECTRICAL FIELD

By Yukichi Asakawa and Setsuo Tomita*

1. Introduction

One of the authors reported previously that a marked improvement in the degree of combustion occurs when an electrical field is applied (voltages of less than 15 kV). However, recently it was discovered that the effect of this electrical field application differs greatly as a function of the interaction between the type of field application and the voltage, the frequency of the alternating current, etc. In the following, the authors present a brief overview of the subject and examples of the unusual increases in output of a small gasoline engine obtained by this method.

2. Test Method

2.1 Combustion in Air

Various methods of applying an electrical field on the propagating flame and a representative process are shown in Fig. 1. As to the method of combustion, we used one type in which a specific quantity of liquid fuel is ignited (types A, B of Fig. 1) and one in which a specific quantity of liquid fuel is kept in a vessel and is burnt on the surface (type C, Fig. 1).

The electrical field was applied to the flame by placing the body of the flame between high voltage terminals (Type A, Fig. 1) or by inserting one highvoltage terminal into the flame and grounding the other terminal (types B and C, Fig. 1). A version in which both of these types were combined (Fig. 2) was also considered and the effect obtained was vastly more marked than with the other two configurations.

We also observed that when a magnetic field is superimposed on the flame under the influence of an electrical field, the burning behavior of the flame is further enhanced and the combustion rate is increased.

The power consumed for the electrical field application as described above amounts to no more than a trickle current, so that only 150-150 μA and a few Watts are consumed in a high-voltage field of 20-30 kV.

2.2 Case of Internal Combustion Engine

Based on the observation of the great increase of the degree of combustion by application of an electrical field to combustion in air, one terminal of a high-voltage source (to be explained in the following) was connected to a dynamometer and the change in output of the engine was determined on the basis of the readings on an electrical tachometer (see below).

3. Test Results

3.1 Combustion in Air

The electrical field application in the configuration of Fig. 1 A is used most commonly; Prof. Kanehara [2] and Weinberg [3] explained this as follows: "shortening of the flame length under the influence of an electrical field" is due to a "decrease of vaporization by the electrical field" according to the former researcher, while the latter points out the phenomenon of the flame being pulled toward the outer terminal plate with a decrease of soot formation during combustion; however, neither mentioned the difference in combustion pattern and rate. In the following, we will discuss the change of flame geometry and the increase of the combustion rate, in other words, how the combustion phenomena are changed by application of an electrical field in the various configurations shown in Figs. 1 A to Fig. 3.

(a) Placing two terminal plates on the outside of the flame (type A, Fig. 1): We find that when terminal plates are placed outside of the flame, the flame length is short and wide and is pulled toward both plates. Fig. 4 shows the results of the combustion of city gas on a Bunsen burner. When a flame of 260 mm length is placed between thin iron terminals of 6 x 110 mm, the flame shortens and widens as in Figs. 4 and 5. With a distance of 100 or 130 mm between the plates, the flame length does not vary greatly but the width shows a 1.3-4.0 fold increase. When the spacing is 100 mm, the width becomes approximately twice that for the 130 mm spacing. The fact that the flame changes shape to a marked extent with changes in plate spacing indicates the influence of the density of the electrical field on the combustion process.

(b) Surrounding the flame with a cylindrical terminal: A thin iron cylinder of 74 diameter was used. In general, with increasing length of the

cylinder, the degree of shortening of the flame increased (illustration will be presented with the paper).

(c) One terminal in flame and the other grounded (Type B, Fig. 1): (c)-1: Direct current: An electrical field was applied on a city gas flame with a preadjusted length of 290 mm; Fig. 8 shows the logarithmic shortening of the flame. Moreover, a special reducing flame gradually changes into an oxidizing flame and at above 6 kV, the reducing flame disappears completely. The shortening in flame length and disappearance of the reducing flame indicate a promotion of the degree of combustion by a basic change of the combustion process under the influence of the electrical field.

(c)-2: Alternating current: Similarly, an ac field was applied to a city gas flame on a Bunsen burner. Again shortening of the flame was observed. The cycle of this shortening process corresponded to the frequency of the alternating current (illustration to be shown with presentation of the paper).

In the present case, a 10^{-4} amp current was present in the flame flux (with natural combustion, 10^{-8} to 10^{-9} amp). This indicates the influence of the application of a second field on the outer surface of the flame.

(c)-3: First field placed into flame and second field applied outside of flame: Fig. 11 shows the results with this configuration. The combustion rates of kerosine of 0.15, 0.23 g/min increased 3.5 and 2.9 times to 0.82 and 0.67 g/min, respectively, while a gasoline flame burning at 0.45 g/min increased 5 times to 2.25 g/min. In the absence of the outside field, the increases were 15-20% lower.

It was thus confirmed that an unusual increase of combustion rate results with the application of an electrical field on the combustion system. After searching for a practical method, the authors confirmed the effectiveness of the method shown in Fig. 1-C.

(d) One terminal in flame of fuels and the other grounded: (d)-1 Direct current: Fig. 12 shows an example using n-heptane in which the positive and negative terminal exhibit marked differences. In general, when the positive terminal is located in the flame, the flame pulses and shortens, while with the negative terminal in the flame, the flame is pulled out and lengthened. These phenomena are illustrated in Figs. 13 and 14.

Since the ion distribution of an electrical current in a natural flame gives a more positive current to the flame surface [4], it may be assumed that the flame undergoes corresponding retractions and extensions. The volume combustion per second was measured in these markedly different combustion

processes. Fig. 12 shows the results, i.e. the combustion rate in volume/sec increases with the applied voltage when the flame is shortened by the positive terminal, while it lengthens with the negative terminal (Fig. 14) and the combustion rate remains the same.

(d)-2: Alternating current: As shown in Figs. 1-C and 12, application of an alternating current within the flame results in an entirely different picture compared to Figs. 13 and 14. With increasing voltage, the flame increases in length and width and oscillates along with the number of cycles. Fig. 15 shows the strong combustion of gasoline according to the electrical field strength. Here and in Fig. 16, the combustion of 2 cc gasoline required 62 sec, kerosine 75 sec and heavy fuel oil 108 seconds under normal conditions, with a 1/6.7, 1/4.4, 1/2.8 fold change to 11 seconds, 17 seconds and 38 seconds, respectively, thus indicating the promotion of the combustion rate.

Since this phenomenon must depend on the applied field strength (on the gap between terminal and ground at constant voltage) [5], the relationship of the voltage/terminal-ground spacing - combustion rate (cc/sec) is as simple as that shown in Fig. 17. In this case, the combustion was not of a specific volume as shown in Fig. 16 but the fuel was supplied as shown in Fig. 18.

We then studied the influence of the electrical field during combustion of a specific volume of gasoline ejected from a nozzle.

Fig. 19 shows the configuration. As shown by Fig. 20, the temperature of the burning gas (10 mm from the discharge end) was 30-40° higher, amounting to 700-900°C. The combustion rate increases with the applied voltage (not shown) while the application of a magnetic field on the discharge point results in a decrease of the combustion rate in vol/sec. This is assumed to be due to the fact that the flame is pulled to the magnetic field by its interaction with the ionic current which is similar to the presence of a resistance at the discharge, causing a temperature rise as shown in Fig. 20. Actually, however, a decrease in unburnt gasoline was observed at the flame discharge point.

3.2 Application to Gasoline Engines

A site was provided for electrical field application on the back of the cylinder cover of an air-cooled 90 cc two-cycle engine and one terminal from the high-voltage side of a 200 W transformer was applied; the results read on a fan-brake dynamometer are shown in Fig. 21. The RPM N_o = 2300 rose to N = 3200-3300. When a voltage of more than 4.5 kV was applied, the effect remained the same, a finding which corresponds to combustion in air as shown in Figs.

15 and 16. This N/N_o = 1.39-1.43 means a 2.63-2.92-fold output which is proportional to $N/N_o)^3$. Fig. 22 shows the corresponding increase of the area under the pressure curve (the influence of the location of terminal insertion will be discussed in the lecture).

Notes

*Physics and Engineering Department, Nippon University and Suginira Tokyo Toritsu Kokyo Semmon Gakko.

1) Promotion of combustion by electrical field application. Regular Meeting, JAPPORO, 1964.

2) Kanehara, Nakamura: On liquid fuel flames in a longitudinal electrical field. University of Tokyo, Undergraduate Reports IV, No. 1.

3) R. G. Payne and F. J. Weinberg: A preliminary investigation of field-induced ion movement in flame gases and its applications. Proc. Roy.Soc. 316-36 (1959).

Fig. 1.
Electrical field application to the flame.

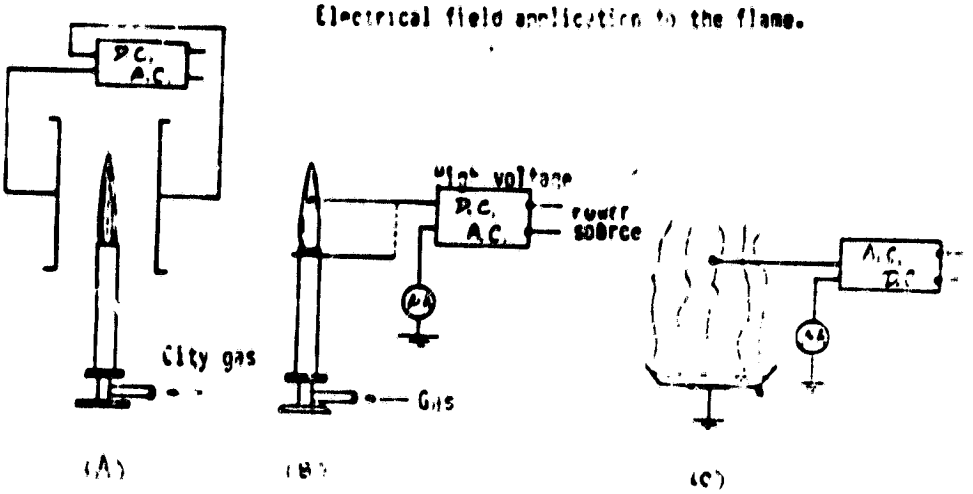

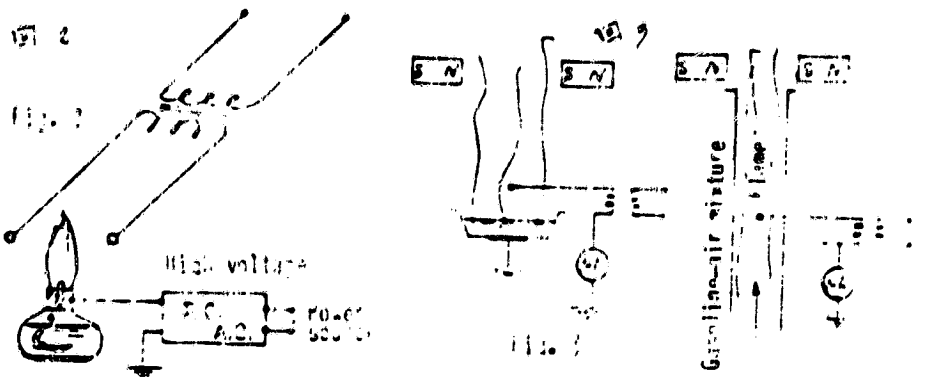

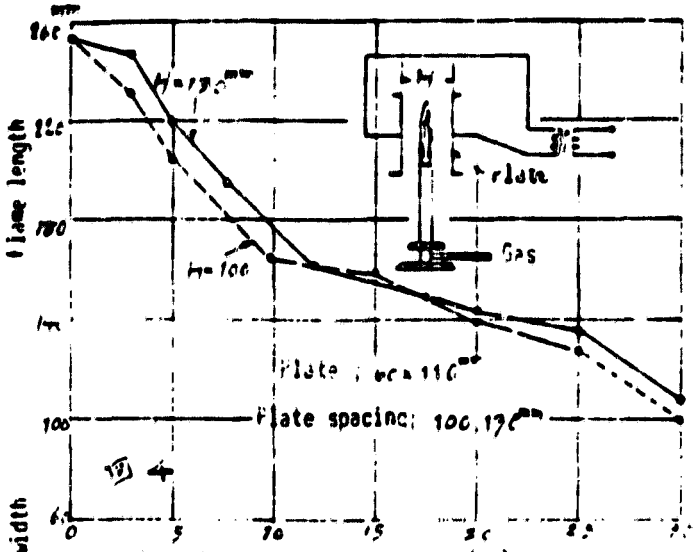

Fig. 4. Applied voltage (kV)

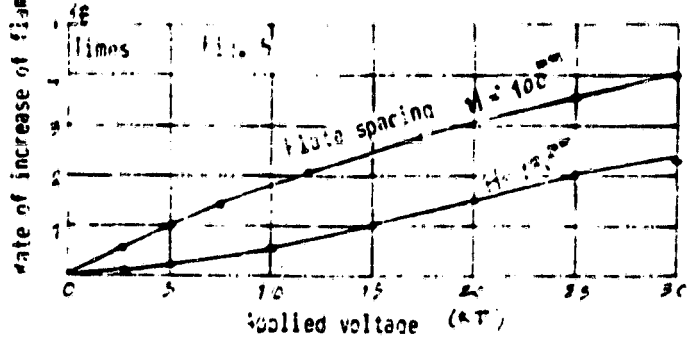

Fig. 5

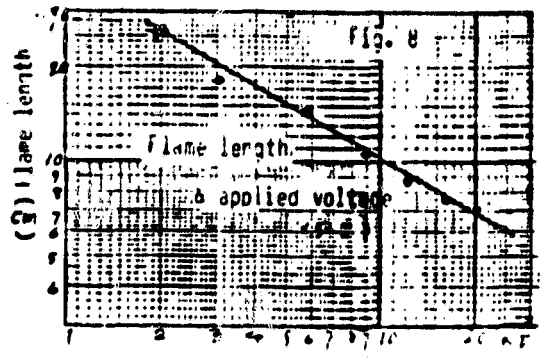

Fig. 6

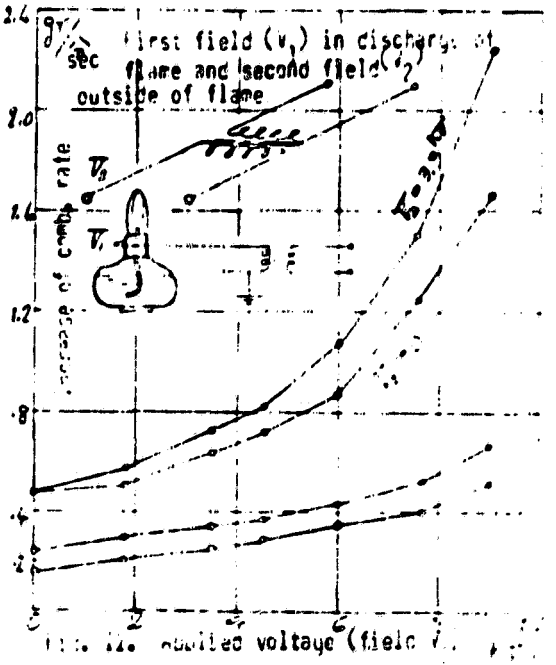

Fig. 12. Applied voltage (field

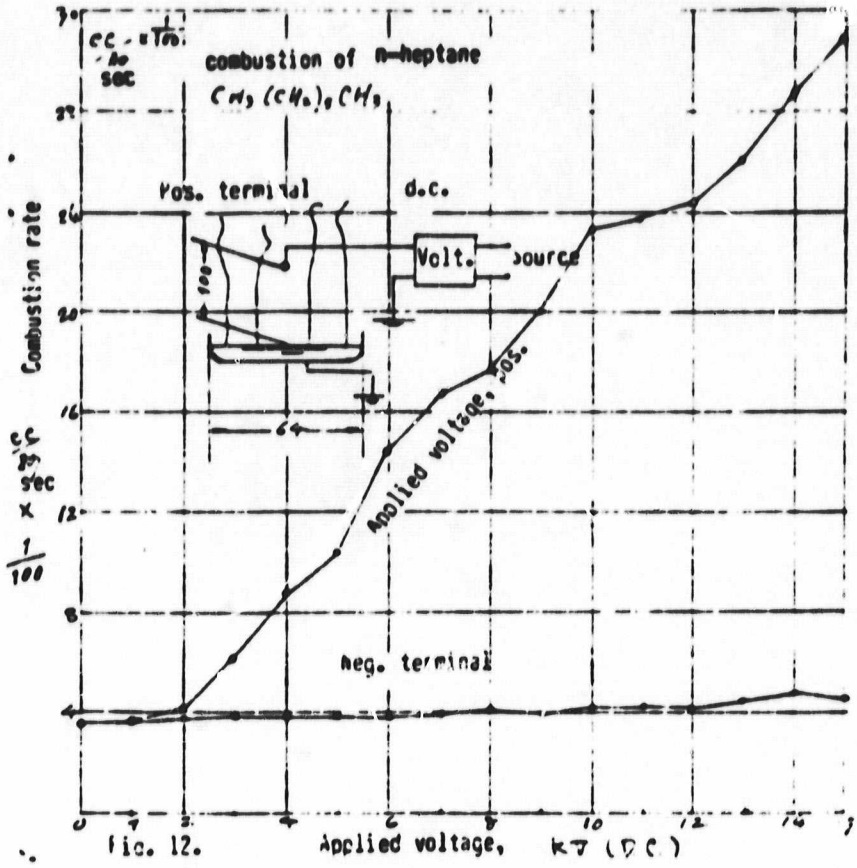

Fig. 12.

Fig. 13. Positive terminal is in flame.

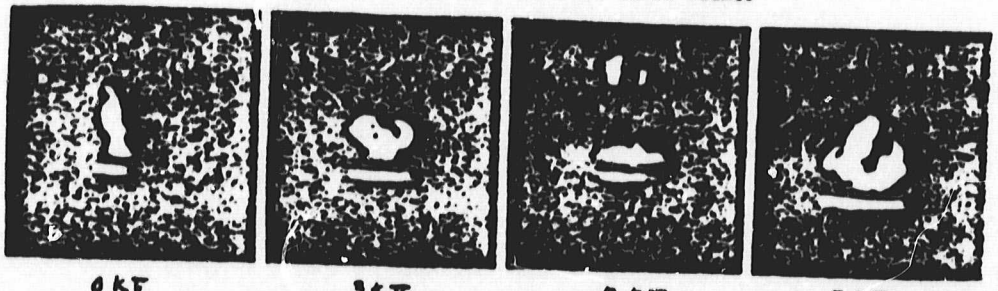

Fig. 14. Negative terminal is in flame.

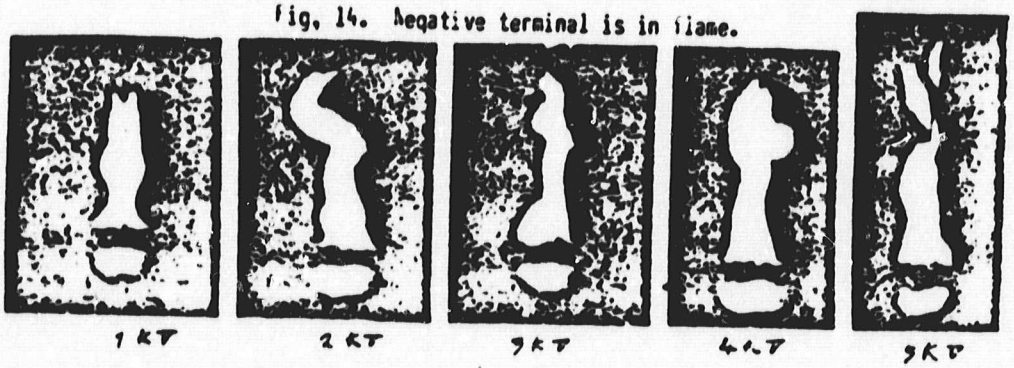

Fig. 15

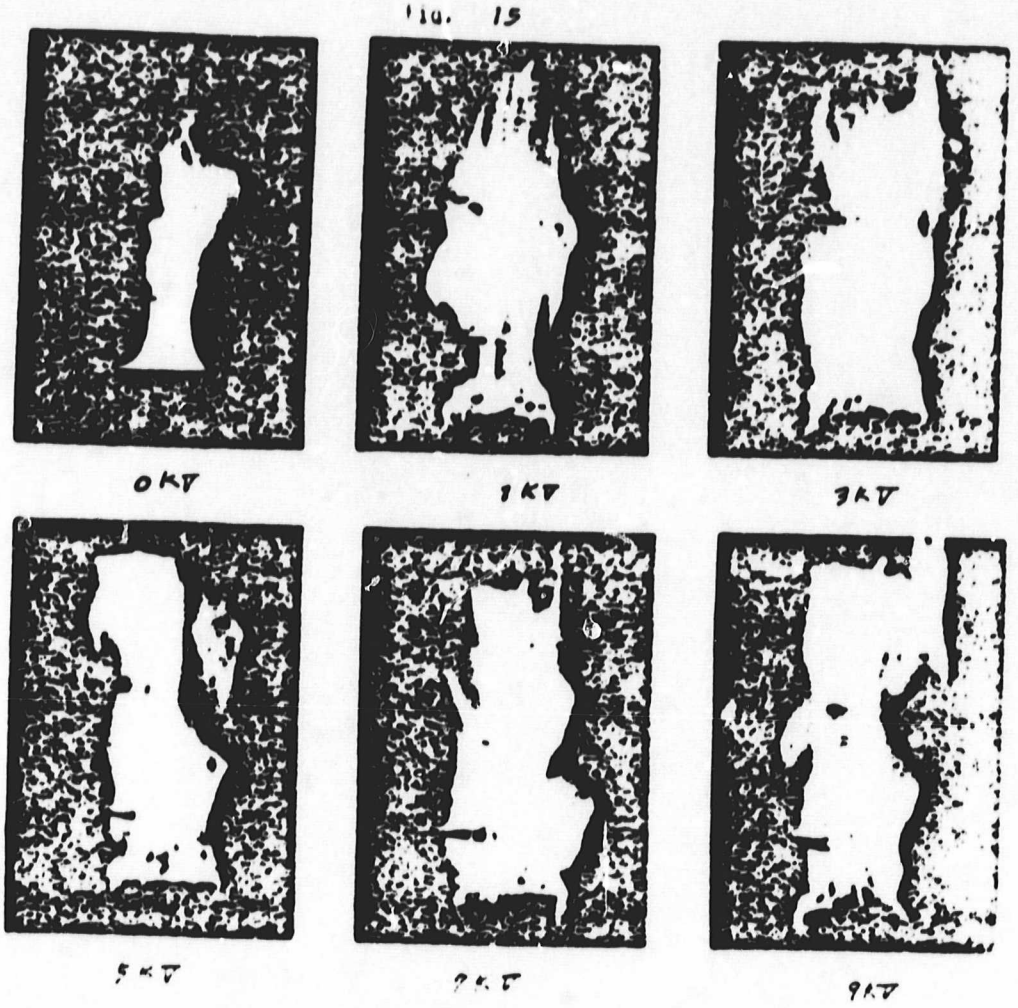

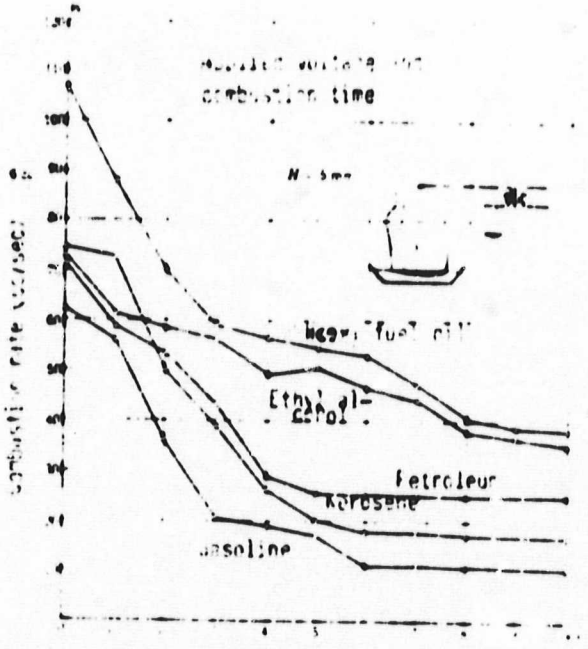

Fig. 16 Applied volta

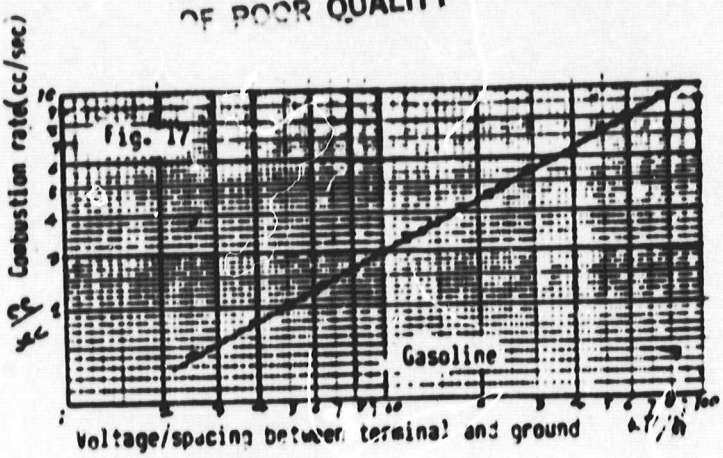

Measurement of combustion rate

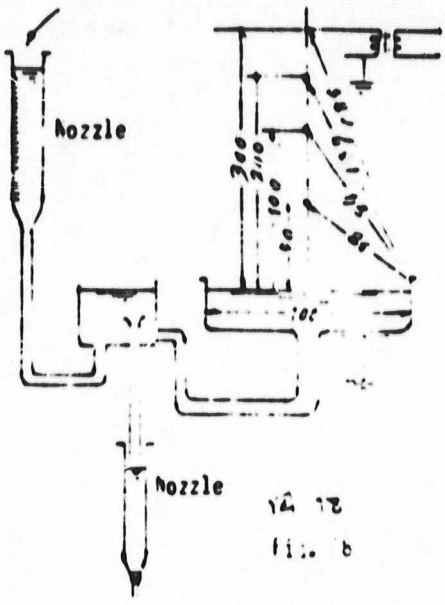

Fig. 6

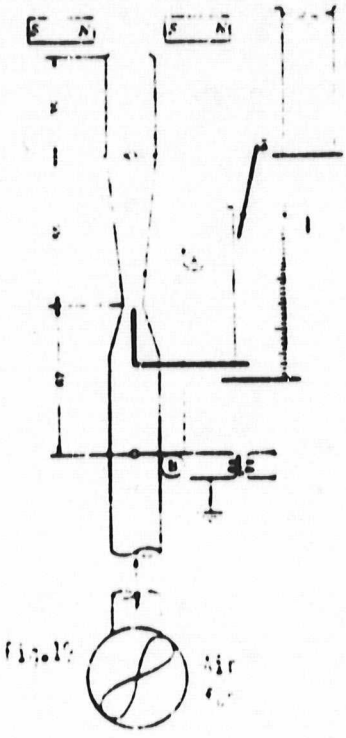

Fig. 8

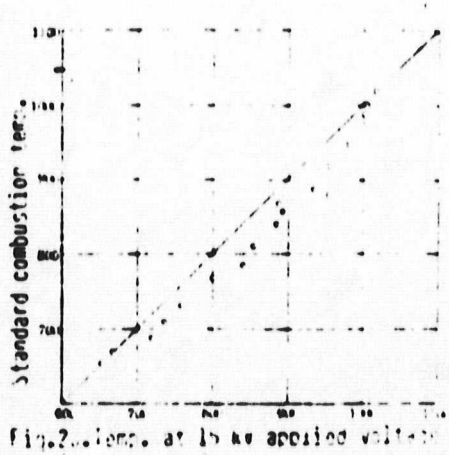

Fig. 2 ...temp. at 15 kv applied volta...

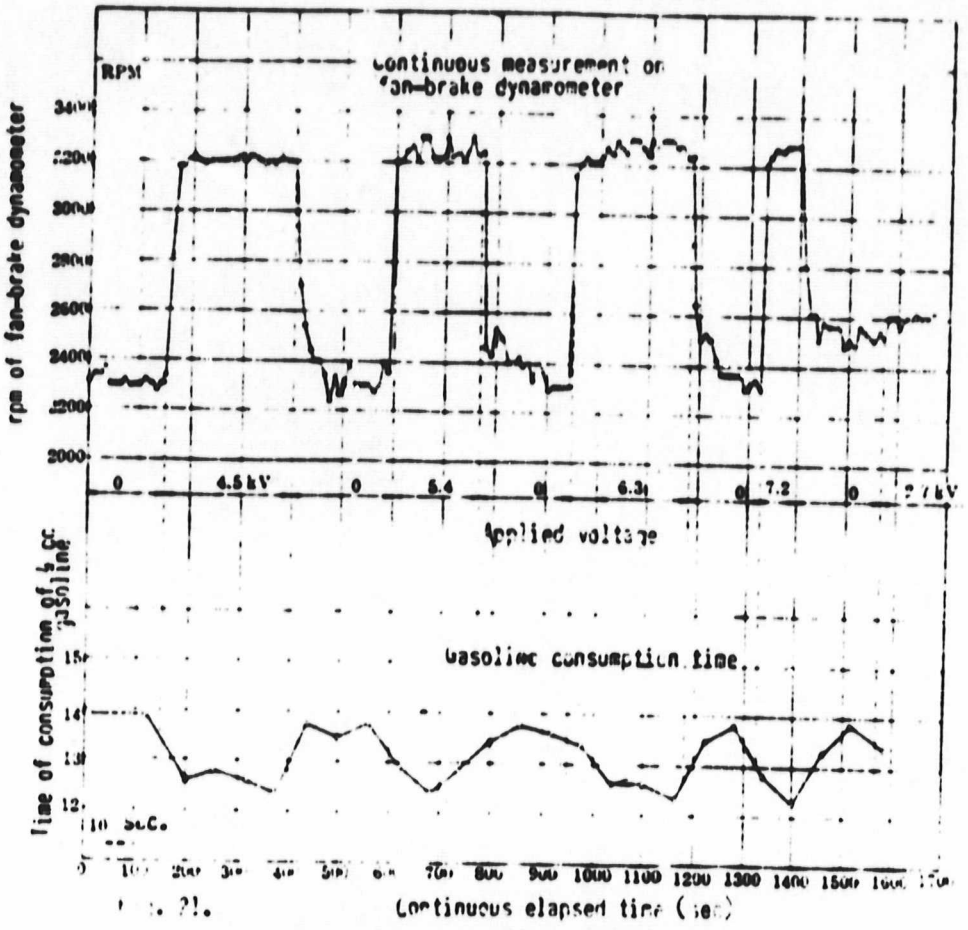

Fig. 21.

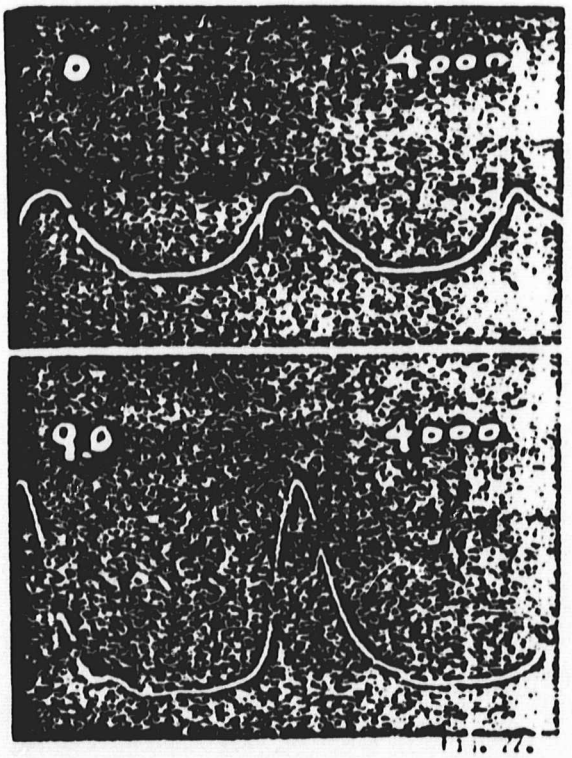

Fig. 22.